CFD MODEL OF FLOW THROUGH AIR FILTER PLEATS

By

CHARLES B. TEBBUTT

Bachelor of Arts

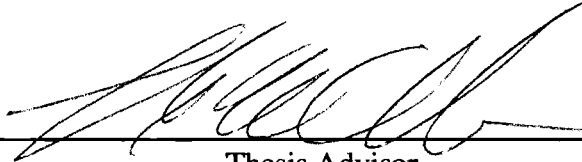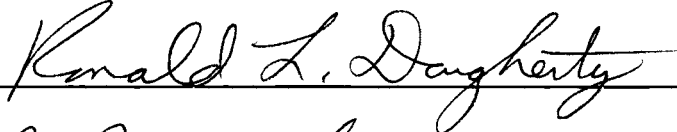Columbia College, Columbia University

New York

1988

Submitted to the Faculty of the
Graduate College of the
Oklahoma State University
in partial fulfillment of
the requirements for
the Degree of
MASTER OF SCIENCE
July 1995

CFD MODEL OF FLOW THROUGH
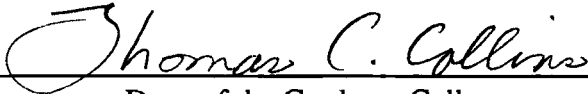# AIR FILTER PLEATS

Thesis approved:

_____
Thesis Advisor

_____
Ronald L. Dougherty

_____
A. J. Ghajar

_____
Thomas C. Collins
Dean of the Graduate College

ACKNOWLEDGMENTS

TABLE OF CONTENTS

LIST OF FIGURES

ix

LIST OF TABLES

NOMENCLATURE

b	inertial factor in filter momentum equation
c	packing factor, equal to $1/\delta$; dummy constant
cdown	in code, number of cells downstream relative to *ipleat*
cup	in code, number of cells upstream relative to *ipleat*
D	average diameter of fibers in media
d, d(x)	width of jet used in turbulence model, equal to the half-pleat width; called *wd* in code
delc	in code, cell dimension along pleat length (*i*-direction)
delx	in code, cell dimension (*i*-direction)
dely	in code, cell dimension (*j*-direction)
dnlgth	in code, total length downstream of filter
e	variable used in calculation of Darcy parameters, K and b
eta	in code, upstream expansion coefficient for grid
f	in code, x-momentum equation; also variable used in calculation of Darcy parameters, K and b
flgth	in code, total length of flowfield
freelength	number of flow-wise cells within pleat not directly influenced by pleat folds
g	in code, y-momentum equation; gravity
h	in code, continuity equation

ht	in code, pleat height
htdown	in code, length of downstream flowfield relative to pleat height
htup	in code, length of upstream flowfield relative to pleat height
i	in code, cell counter in x-direction
ibar	in code, number of cells within the flowfield in the x-direction
icell	in code, first *i* cell of pleat (x-direction)
idown	in code, number of cells downstream of filter relative to ipleat
im1	in code, imax - 1
imax	in code, number of cells flow-wise including boundaries
ipleat	in code, number of *i* cells within pleat
j	in code, cell counter in y-direction
$\bar{J}$	unit flow direction vector
jbar	in code, number of cells within the flowfield in the j-direction
jcell	in code, first *j* cell of pleat (y-direction)
jm1	in code, jmax - 1
jmax	in code, number of cells width-wise including boundaries
K	filter media permeability
l_{mfp}	molecular mean free path
l_{mix}	mixing length
L, l	descriptive length
nfil_c	in code, for square geometry, number of cells spanning length of pleat median
nfil_x	in code, for square geometry, number of cells spanning pleat section oriented normal to flow for triangular geometry, number of cells spanning pleat thickness
nfil_y	in code, for square geometry, number of cells spanning width of pleat median

P	mean pressure
p, p_{ij}	in code, mean pressure normalized for density
Q	volume flow rate
R	fiber radius
t	thickness of the filter media; time
tp	in code, pleat thickness
tx	in code, for triangular geometry, pleat thickness in i-direction
ty	in code, for triangular geometry, pleat thickness in j-direction
U	mean velocity in flow direction (x-direction)
$uplgth$	in code, length of flowfield upstream of filter
$\overline{uv}, \overline{u_i v_j}$	Reynold's averaged turbulent velocity fluctuations
u, u_{ij}	in code, mean velocity in flow direction (i-direction)
V	mean velocity in transverse direction (y-direction)
V_D	Darcian velocity (area-averaged velocity)
V_{mix}	mixing velocity
V_{pore}	pore velocity
V_{th}	molecular velocity
v, v_{ij}	in code, mean velocity in transverse direction (j-direction)
wd	in code, pleat width
x, x_i	flow direction
y, x_j	transverse direction
z	direction along pleat
$zeta$	in code, downstream expansion coefficient for grid

α	in code, upstream differencing coefficient
δ	porous media porosity, equals 1/c
γ	in code, constant to determine mixing length in turbulence model
μ_f	dynamic viscosity of fluid
μ_t	turbulent dynamic viscosity
ν_f	kinematic viscosity of fluid
ν_t	turbulent kinematic viscosity
θ	pleat angle
$\theta_\square$	pleat angle for square geometry
$\theta_\triangle$	pleat angle for triangular geometry
ρ	density
Ψ	dummy variable
∇	gradient
$\triangle$	represents triangular geometry
$\square$	represents square geometry

Chapter 1

Introduction

1.1 Function of the Air Filter

The combustion engine derives its energy from the exothermic reaction of fuel and air. As this reaction takes place within a collection of carefully gauged moving parts, it is important that the reactants are free from particulate matter that could damage the engine over time. Therefore filters are necessary to glean particles from the air and fuel as well as the lubricating oils used within the engine. Air filter systems are designed to rid the air of all particles larger than roughly 1 μm in diameter, as these exceed the oil film thickness between moving parts. Smaller particles can also cause problems, so their removal is sought as well [Jaroszczyk et al., 1993].

1.2 Filter Design and Pleating

Air filter design is guided by the sometimes opposing concerns of high efficiency and low cost. Thereby, the following conditions and requirements guide filter design:

- small space available within engine compartment;
- high required flow rate to fuel engine;
- low pressure drop across filter to reduce energy required to supply flow of air;
- high filtration efficiency for particles to sub-micron level;
- long filter lifetime, i.e. have large dust load capacity;
- low cost.

1

One of the key design features of air filters is *pleating* of the filter media. Pleating helps fulfill the above design specifications in several ways. It increases the effective area of filtration which immediately increases filter capacity and filter efficiency. Pleating also serves to reduce the flow velocity through the filter media for a given flow rate. This decreases the pressure drop across the filter, thus requiring less energy to supply a given flow rate to the engine.

A schematic of the effect of pleating on the pressure drop across a filter is shown in Fig. 1.1. This shows that the more compact the pleating, the lower the pressure drop, up to the point where the pleats begin creating a restriction in the flow, thereafter the pressure drop rises [Brown, 1993, p. 64].
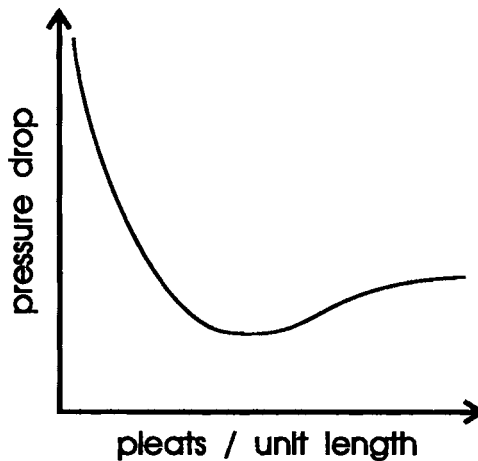
Fig. 1.1   Pressure drop vs. pleat density for given media type and pleat height, adapted from Brown [1993, p. 65].

The relationship between velocity and filtration efficiency is shown in Fig. 1.2. The velocity across the filter is slowed by pleating. So pleating can be manipulated to increase filter efficiency.
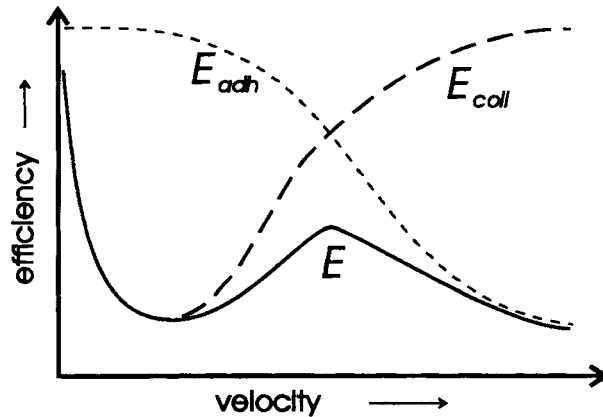
Fig. 1.2   Filtration efficiency vs. flow velocity, adapted from Stenhouse [1975].
The total efficiency E is the product of the efficiency via
separate mechanisms: adhesion E_{adh} and collection E_{coll}.

1.3 Motivation for Research

1.3.1 Applications of Simulated Pleat Flowfields

Some of the advantages of filter pleating mentioned above are based on certain

assumptions regarding flow through the pleats. Flow through pleats is assumed to be

oriented *normal* to the pleats, thus the effective area of the filter is presumed to be the

unpleated, flattened area of the filter. Also, the efficiency of a filter is a function of the

velocity; when calculating filter efficiency using a theoretical model, it is necessary to

know the velocity through the pleats. In addition, as the velocity will vary at different

points along the pleat, efficiency can be gauged on a local basis within the filter. A

flowfield model can also give a theoretical estimate of the pressure drop across a filter for

different pleat configurations.

1.3.2 Objective of this CFD Model

It is difficult to access the flow near and through a pleated filter with flow measuring

equipment. In this project, a flow simulation program called PLEATFLO is developed to

3

determine the actual path and magnitude of the flow through the pleats. This simulation program will allow the analysis of flow through pleats under varying conditions and varying geometries. It will also give a measure of the pressure drop across a filter.

1.4 Filter Geometry

The automobile air filter generally consists of the pleated filter media supported by a wire mesh encased in a rubberized frame. The media is machine pleated and attached to the base by glue. The actual shape of the pleats is between a square and triangular wave.

triangular wave

square wave

approximate pleat shape
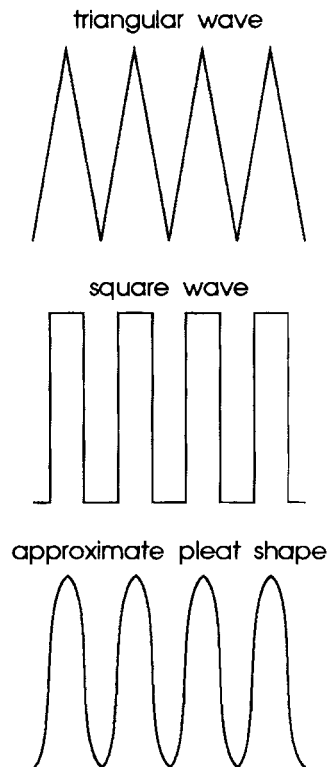
Fig. 1.3 Pleat shape.

The pleat angle of automobile engine air filters is generally near vertical. This serves to maximize filter area, reduce pressure drop, and lower intra-filter velocity. A schematic of

the Purolator AF3192 filter is shown below. The pleats are 3 cm high with a 3 mm pitch. The media is about 635 μm thick.

Bottom View

wire
mesh

Top View

rubberized
frame

Side View
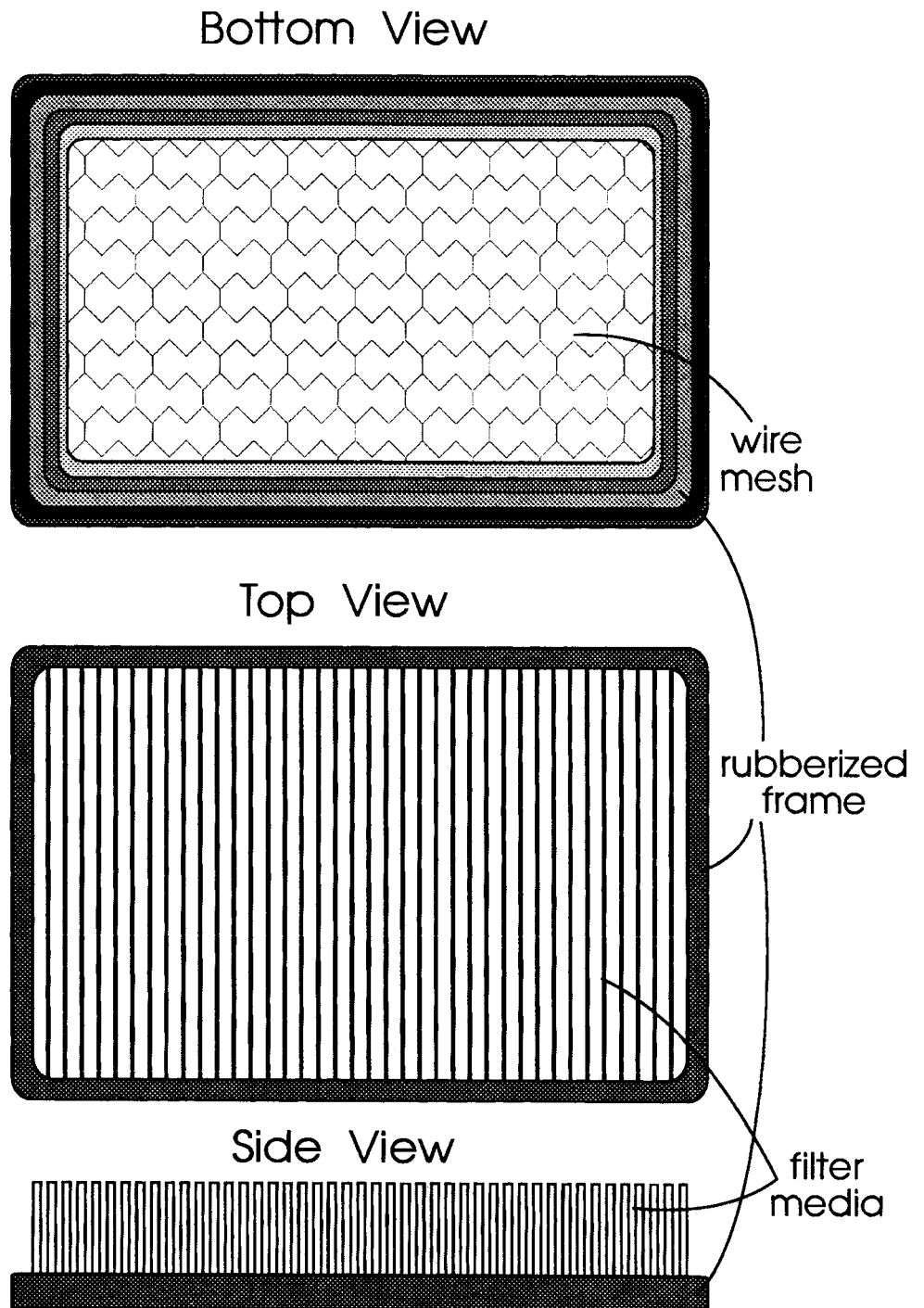
filter
media

Fig. 1.4 Schematic of filter

1.5.2 The Work of Gurumoothy

Gurumoothy [1990] modeled the flow through an entire air induction system (AIS),

including the filter. The flow was calculated with the PHOENICS code which solves fluid

flow using the transient viscous flow equations with a k-ε model for turbulence. The 3-

dimensional simulation included a boundary condition that accounted for the induction

system walls. The filter was treated as a separate *region* in the flow, solving the flow

according to the macroscopic qualities of the filter region.

The equation solved within the filter region was this extended form of the Darcy equation.

$$\frac{1}{\rho}\nabla P = -\frac{v_f}{K}\vec{V}_D - \frac{b}{2}(\vec{V}_D \bullet \vec{V}_D)\frac{\vec{V}_D}{|\vec{V}_D|} \qquad (1-2)$$

This includes the direct relation between pressure drop and velocity related by filter

resistance K which is the basic Darcy law. It also includes an account for pressure drop

due to flow inertia related by a factor b. The velocities are all macroscopic values.

An experimental method to calculate the parameters K and b for a specific media was

offered by Gurumoothy [1990]. The two parameters are related to pressure drop in 1-

dimensional form by

$$\frac{dP}{dx} = -\frac{\mu_f}{K}U_D - \frac{b}{2}\rho U_D^2 \qquad (1-3)$$

Integration of the equation over the filter width L and the substitution of Q/A for U yields

$$\Delta P = \frac{\mu_f L}{KA}Q + \frac{b\rho L}{2A^2}Q^2 \qquad (1-4)$$

This is of the form

$$\Delta P = eQ + fQ^2 \tag{1-5}$$

Using this relation K and b can be calculated experimentally. For the measurement of the width, L, the height of the entire pleated filter was used, thus the media region included a good deal of non-media space. The values Gurumoothy obtained were

$$K = 8.3561e - 09\,\text{m}^2 \quad b = 1.78759e + 03\,\text{m}^{-1} \tag{1-6}$$

Gurumoothy validated his program using comparison with experimentally determined wall and internal pressure values found within the AIS. The CFD prediction was generally within 10% of the experimental value. It is also notable that the CFD values were found to be grid dependent, although to a small extent.

1.5.3 The Work of Cai

Cai [1993] created a transient flow simulation program based on the SOLA program to analyze the detailed flow phenomena within the pleats. This program again applies the basic continuity and momentum equations of viscous flow over the region outside the filter; and turbulence was calculated with a k-ε model.

Within the filter a momentum equation that preserved the basic viscous flow formulation was introduced. The equation was adapted from Vafai & Tien [1981]. Vafai & Tien start with the Darcy law for pore velocity, which is the actual velocity within the media pore, as opposed to the "Darcian velocity" which is a macroscopic velocity for a given cell ($V_{darcy} = \delta \cdot V_{pore}$, $\delta \equiv$ media porosity). The coefficient function of the second term on the right is the equivalent of b used above.

$$\nabla P = -\frac{\mu \cdot \delta}{K}\vec{V}_p - \frac{F(K, \text{Re}_K, Geometry) \cdot \delta^2}{\sqrt{K}}\left(\vec{V}_p \bullet \vec{V}_p\right)\left(\frac{\vec{V}_p}{\left|\vec{V}_p\right|}\right) \tag{1-7}$$

This basic momentum equation is then reformulated for use within the porous media by volume averaging the variables to take into account pore space and media space. With V a small volume and V_f the part of the volume containing fluid, the volume average of a variable Ψ is

$$\langle \Psi \rangle = \frac{1}{V}\int_{V_f} \Psi d\,V.$$

This essentially re-establishes macroscopic variable values. Applying these to the Navier-Stokes formulation within the media yields

$$\rho\langle(\vec{V}\bullet\nabla)\vec{V}\rangle = -\nabla\langle P\rangle_f + \mu\nabla^2\langle\vec{V}\rangle + \text{filter resistance} \qquad (1\text{-}8)$$

The filter resistance is incorporated using the Darcy terms (Eq. 1-7) with the same volume-averaged velocity as introduced above.

$$\rho\frac{D\langle\vec{V}\rangle}{Dt} = -\nabla\langle P\rangle^f + g + \mu\nabla^2\langle\vec{V}\rangle - \frac{\mu}{K}\delta\cdot\langle\vec{V}\rangle - \frac{F}{\sqrt{K}}\rho_f\delta^2\cdot\left(\langle\vec{V}\rangle\bullet\langle\vec{V}\rangle\right)\frac{\langle\vec{V}\rangle}{|\langle\vec{V}\rangle|}$$

$$(1\text{-}9)$$

Cai used this equation to represent momentum within the filter.

The main difficulties in doing a transient analysis of detailed flow through a pleat are the large gradients encountered and the draconian stability criteria required as a consequence of these gradients. A transient analysis requires a sufficient number of time steps to reach a steady state flow condition. Cai's results seem to be limited by an exceedingly small time forwarding criterion required for stability.

1.5.4 The Work of Chen, Pui, and Liu

Chen, Pui, & Liu [1993] created a finite element method to solve for flow through pleated media. For flow within the media, an expression that combines the basic laminar momentum equation with Darcy's law is used.

$$\frac{\rho}{\delta^2}(\vec{V}_D \bullet \nabla)\vec{V}_D = -\nabla P - \frac{\mu}{K}\vec{V}_D + \frac{\mu}{\delta}\nabla^2\vec{V}_D \qquad (1\text{-}10)$$

This is similar to the previous formulation except that it is steady-state and does not include an inertial resistance term, as their research involved only low flow velocities. The authors examined a square pleat geometry.
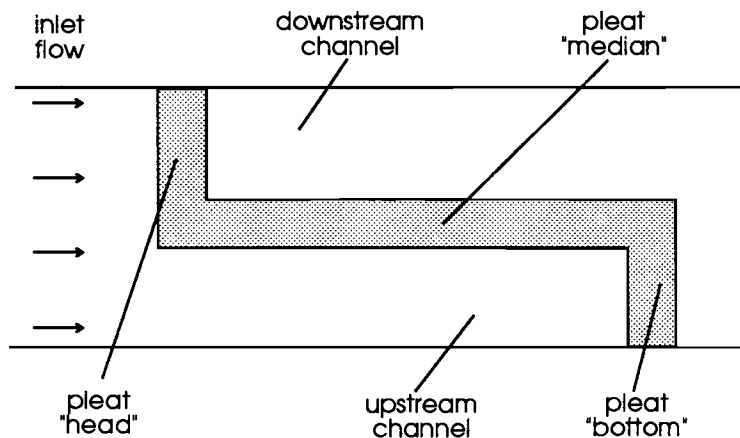
Fig. 1.5 Square pleat geometry used by Chen et al. [1993].

A description of their findings for the velocity flowfield follows. At the entrance of the pleat a portion of the flow passes through the pleat head, but the bulk of the flow enters the pleat channel. In the channel they found the tangential velocity at the pleat median to be near zero, there is very little horizontal flow. In the downstream channel the flow

exhibits similar characteristics. The flow emits from the downstream channel in a jet-like manner.

The authors found the pressure drop to be linearly related to velocity. This suggests the dominance of the Darcy term. Pressure drop over a pleat geometry is dominated by media resistance at low pleat count (pleats per unit length) and viscous drag at high pleat count. An optimal pleat count (i.e. that which yields minimal pressure drop) was found where the combined effects of media resistance and viscous drag were minimized. Data were non-dimensionalized to create a correlation curve for normalized pressure drop as a function of various filter parameters for various media types. This results in curves similar to that of Fig 1.2.

1.6 Description of this CFD Model

1.6.1 General Method

In this CFD code, the steady state equations are solved directly. Three partial differential equations (PDEs) are used. These are the two-dimensional continuity equation and the x- and y-components of the momentum equation. The latter equation has two forms, one for extra-filter flow, one for intra-filter flow. The extra-filter form of the momentum equation is for viscous flow and includes a simple algebraic model for turbulent flow. The intra-filter equation includes the Darcy law modified to include the effects of flow inertia.

The PDEs are translated into finite difference equations (FDEs) to be solved for a grid covering the flow region. The non-linear FDE matrix is solved iteratively. The grid is sized based on given filter geometry and dimensions. The grid cells can expand up and downstream of the filter. The modeled filter can have either triangular or square pleats

(see Fig. 1.4). The results are written to files that can be viewed or further analyzed with vector plotting software.

1.6.2 Key Assumptions

As filter systems are generally given rather cramped spaces, the flow entering the filter chamber is not generally normal to the filter. In addition, the flow entering the filter comes down piping, so pipe geometry shapes the flow profile entering the filter. However, in this simulation we assume the flow enters the filter chamber normal to the filter. The inlet flow is assumed to be uniform flow with free slip at the boundaries (i.e. no normal flow component). The pleating is assumed to run infinitely. The permeability is assumed constant even though a reduction might occur at the corners due to glue and folding. Finally the fluid is taken to be clean single phase air.
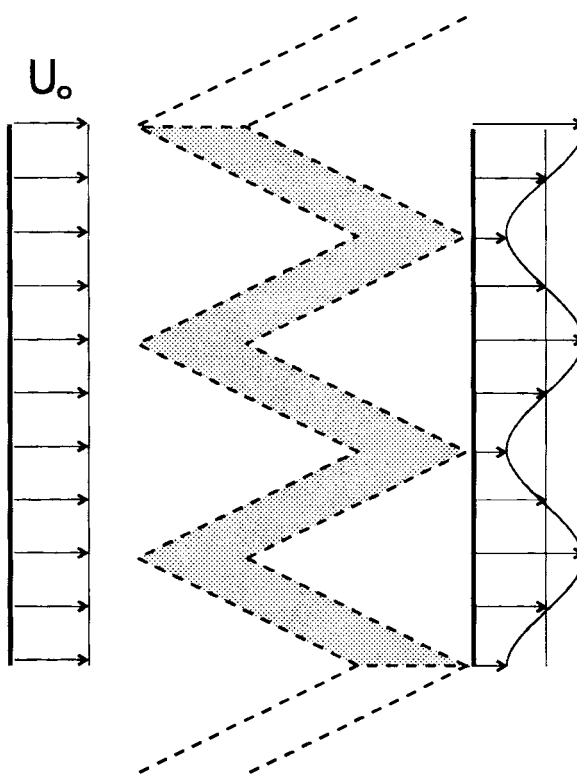
Fig. 1.6 Assumed flow through pleats.

Chapter 2

Derivation of Numerical Method

2.1 Overview of Method

For the present study, a numerical solution is to provide velocity and pressure throughout the flowfield upstream, within, and downstream of a pleated filter. To arrive at a solution, the differential equation forms of the fundamental viscous flow equations are translated into finite difference equations (FDEs). The FDEs are then fit to a grid representing the flowfield, and they are solved for each gridpoint in the field. This method is contained in a FORTRAN code program called PLEATFLO.

2.2 Flow Outside of the Filter

2.2.1 Viscous Flow Equations

Fluid flow is governed by the laws of conservation of mass, momentum, and energy. Air flow at low Mach numbers can be considered an incompressible Newtonian flow. The viscosity can be assumed constant because the temperature varies insignificantly. Thus velocity and pressure can be found without the energy equation.

Conservation of mass is expressed in the continuity equation.

$$\nabla \bullet \vec{V} = 0 \qquad (2\text{-}1)$$

Conservation of momentum takes the form of the Navier-Stokes equations.

$$\frac{D\vec{V}}{Dt} = -\frac{1}{\rho}\nabla P + \vec{g} + \nu_f \nabla^2 \vec{V} \qquad\qquad (2\text{-}2)$$

Certain assumptions about the flowfield affect the final appearance of the FDEs.

- Flow is sought in its steady-state condition. Time is not a factor.

- Gravity plays an insignificant role.

- Flow is considered to be two dimensional. The velocity component along the pleat (z) is considered constant or zero, so the Navier-Stokes equation will have only two plane component directions (x and y).

Fig. 2.1 Coordinate orientation with reference to filter.

- As seen in the direction of the expected flow streamlines of Fig. 2.2, the velocity gradients around the pleat will be large, so turbulent effects can be expected to be significant. This will affect the mean flow parameters, so it must be considered. Thus the fundamental equations are taken in their turbulent form. This is accomplished by splitting the
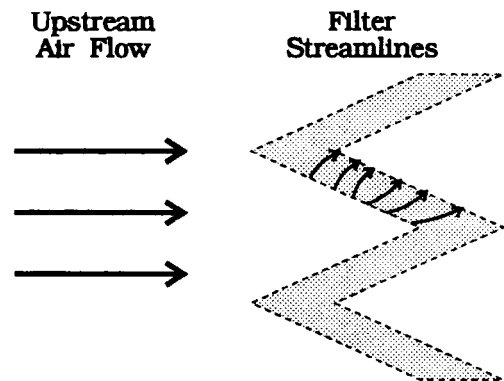
Fig. 2.2 Expected flow streamlines through pleat, adapted from Brown [1993, p. 65].

14

equation variables into mean (capital letters) and fluctuating (small letters) components, then time-averaging the equations. This adds turbulent stresses $(\overline{u_i u_j})$ to the momentum formulation:

$$\frac{D\vec{V}}{Dt} = -\nabla p + \mu \nabla^2 \vec{V} - \frac{\partial}{\partial x_j}\left(\overline{u_i u_j}\right) \qquad (2\text{-}3)$$

Taking into account these four assumptions, the fluid dynamic equations are represented with these three component equations:

continuity: $\quad \dfrac{\partial U}{\partial x} + \dfrac{\partial V}{\partial y} = 0$ $\qquad\qquad\qquad (2\text{-}4)$

x-momentum:

$$U\frac{\partial U}{\partial x} + V\frac{\partial U}{\partial y} =$$
$$-\frac{1}{\rho}\frac{\partial P}{\partial x} + \nu_f\left(\frac{\partial^2 U}{\partial x^2} + \frac{\partial^2 U}{\partial y^2}\right) - \left(\frac{\partial \overline{(uu)}}{\partial x} + \frac{\partial \overline{(uv)}}{\partial y}\right) \qquad (2\text{-}5)$$

y-momentum:

$$U\frac{\partial V}{\partial x} + V\frac{\partial V}{\partial y} =$$
$$-\frac{1}{\rho}\frac{\partial P}{\partial y} + \nu_f\left(\frac{\partial^2 V}{\partial x^2} + \frac{\partial^2 V}{\partial y^2}\right) - \left(\frac{\partial \overline{(vu)}}{\partial x} + \frac{\partial \overline{(vv)}}{\partial y}\right) \qquad (2\text{-}6)$$

These three equations contain six unknowns:

- the mean velocity terms, U, V;
- the mean pressure, P;
- the turbulent fluctuations of velocity, $\overline{uu}, \overline{uv}, \overline{vv}$.

15

So their solution requires further information.

2.2.2 Turbulence Considerations

Turbulent fluctuations cannot be calculated directly, short of direct numerical simulation.

However, they can be modeled fairly successfully. Models up to recent times have been

based on the Boussinesq eddy-viscosity approximation. This assumes a turbulence

viscosity (μ_t or ν_t) that is analogous to molecular viscosity, except that it is based on the

scale of the local turbulence rather than molecular scales. Similar to molecular viscosity's

role in relating shear stress to the velocity gradient ($\tau_{xy} = \mu \cdot dU/dy$), turbulent viscosity is

used to relate the turbulent shear stress $\left(-\overline{u_i u_j} \right)$ to the velocity gradient.

$$-\overline{uv} = \nu_t \frac{dU}{dy} \qquad (2\text{-}7)$$

However, unlike molecular viscosity, turbulent viscosity is not a constant property of the

fluid. It varies with the flow; its value is a function of the flow. Various models of

turbulence have been devised to solve for μ_t. Some of the more accurate models involve

the addition of partial differential equations (PDEs) to the solution set, such as the k-ε

model which adds the turbulent kinetic energy (TKE) equation and the turbulent

dissipation (TD) equation to the three conservation equations already given above, and

solves for μ_t as a function of TKE and TD locally. These additional PDEs complicate the

solution matrix and increase computation time for solution. Moreover, Cai's [1993]

computations made with the k-ε model showed turbulence to have little effect on the flow

distribution through the filter. For these reasons, the use of extra PDEs was avoided.

The "algebraic" models of turbulence are so called because they are based on geometric

approximations of turbulence. They add no PDEs to the solution. Turbulent viscosity is

modeled by analogy to molecular viscosity for a dilute gas following Wilcox [1993, p. 27-

16

30]. Just as molecular viscosity is a product of the mean free path and an average molecular velocity,

$$\mu = \frac{1}{2}\rho v_{th} l_{mfp} \qquad v_{th} \equiv \text{molecular velocity} \quad l_{mfp} \equiv \text{mean free path} \qquad (2\text{-}8)$$

so the turbulent viscosity is calculated as an analogous function of a length and a velocity.

$$\mu_t = \frac{1}{2}\rho v_{mix} l_{mix} \qquad (2\text{-}9)$$

The mixing length (l_{mix}) is an estimate of the distance over which an eddy maintains its directional momentum. The mixing velocity (v_{mix}) is the product of the mixing length and the velocity gradient.

$$v_{mix} = c \cdot l_{mix} \left| \frac{dU}{dy} \right| \qquad (2\text{-}10)$$

so

$$\mu_t = \frac{1}{2}c \cdot \rho \cdot l_{mix}^2 \left| \frac{dU}{dy} \right| \quad \text{or} \quad v_t = \frac{1}{2}c \cdot l_{mix}^2 \left| \frac{dU}{dy} \right| \qquad (2\text{-}11)$$

The constant and the ½ are absorbed in the mixing length. The turbulent viscosity is then substituted in Eq. (2-7) to give the formulation of the shear stress.

$$-\overline{uv} = l_{mix}^2 \left| \frac{dU}{dy} \right| \frac{dU}{dy} \qquad (2\text{-}12)$$

This yields a formulation for turbulent shear stress as a function of the mean flow variables. As velocity *along* the pleat length is considered to be zero or constant ($dU/dz = 0$), the shear stresses in the z-direction ($-\overline{uw}$) are insignificant [Townsend,

1976, p.196]. Turbulent normal stresses $(-\overline{u_i u_i})$ are also less significant [ibid, p. 190] so that in the fluid momentum equations,

$$\overline{uv} >> \overline{uu}, \overline{vv}, \overline{uw}, \overline{vw} \qquad (2\text{-}13)$$

It remains for the mixing length (l_{mix}) to be determined. Wilcox [1993] has reviewed mixing length models calibrated for specific empirical models of self-similar turbulent flows. For self-preserving free shear flows the mixing length is calculated as a product of a constant (γ) and the width of the flow phenomenon $(d(x))$.

$$l_{mix} = \gamma \cdot d(x) \qquad (2\text{-}14)$$

Free shear flows are qualified as turbulent flows not bounded by walls but bounded by a non-turbulent ambient fluid. The general classifications of these consist of wake, jet, and mixing layer flows.
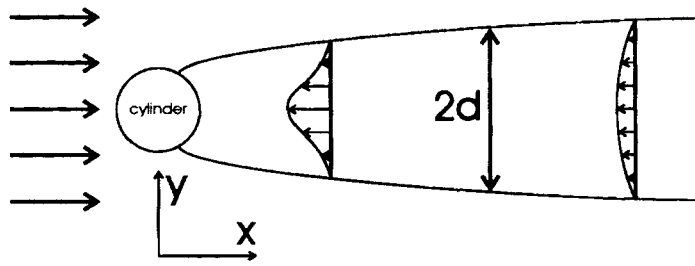
Fig. 2.3   Wake flow.
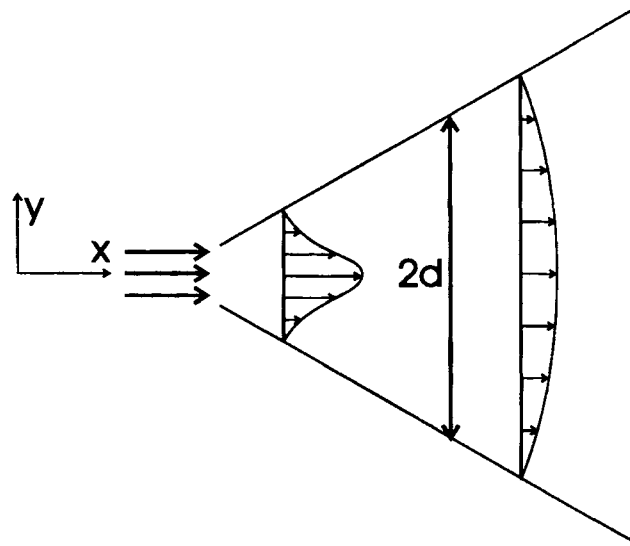
Fig. 2.4   Jet flow.
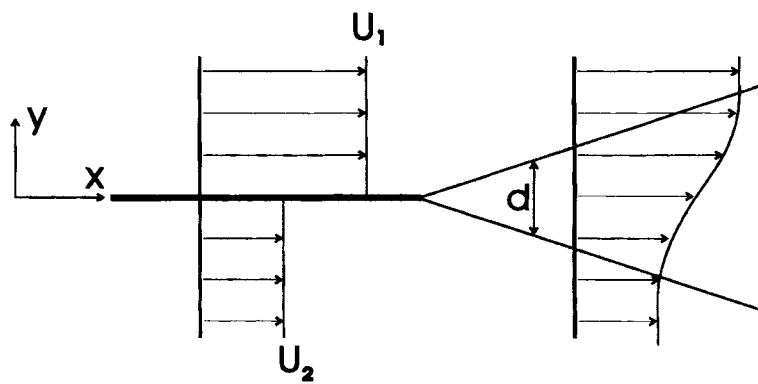
Fig. 2.5   Mixing layer flow.

19

Execution of the numerical method using the laminar equations showed that the flow

emanating downstream from the filter has a profile similar to that shown in Fig. 2.6. The

square pleat produces a similar, even stronger gradient.
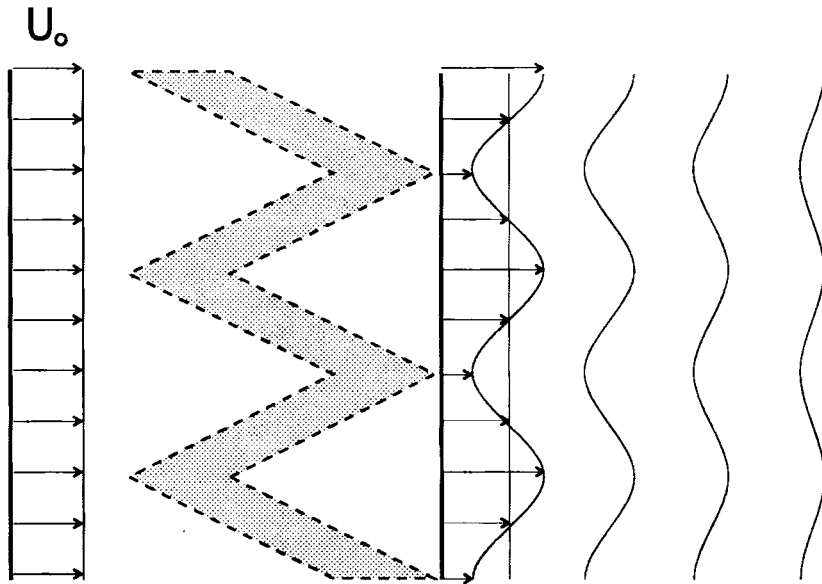
Fig. 2.6   Flow profiles downstream of filter.

A series of strong and weak flow sections can be seen. The flow does not qualify as a

mixing layer because the initial "ambient" velocities (U_1 and U_2) would change moving

downstream. The wake model cannot be applied because the magnitude of the "defect" in

the downstream flow is too large to be considered a wake [White, 1991, p. 259]. The flow

is, however, similar to the general shape of a jet profile. It is strong in the middle and

tapers off toward the sides, and the relative strength of the middle compared to the sides

weakens as the flow moves downstream.

There are several aspects in which the downstream filter flow is not analogous to the jet

model. Each section is *not* bounded by a non-turbulent ambient fluid; it is bounded by an

identical flow. Also, the flows spread into one another, so the profiles are unable to spread

20

out moving downstream. Moreover, a self-preserving shape does not develop until about 20 diameters downstream [White, 1991, p. 471], farther than we wish to consider; however this "jet" does have a somewhat developed profile to begin with.

Even with these shortcomings, the magnitude of the turbulent stresses should be reasonably gauged by the jet model. The main divergence with the archetype is that the flow width is constant rather than continually spreading. The practical result of this is that the scale of the turbulent stress will shrink moving downstream. This would be expected to occur as the velocity gradient decreases downstream, and the flow profile flattens out.

So, to apply the jet model, a flow half-width (d) must be specified. The choice is either (a) to consider the flow as a positive jet stretching between low velocity points or (b) to view the flow as a set of positive and negative jets relative to the inlet flow. The former is chosen because that profile is truer to a jet profile, i.e. the velocity gradient inverts at the edges. Moreover, with this model the filter is considered to stretch infinitely, so the outflow need not be related to the magnitude of the inlet flow.
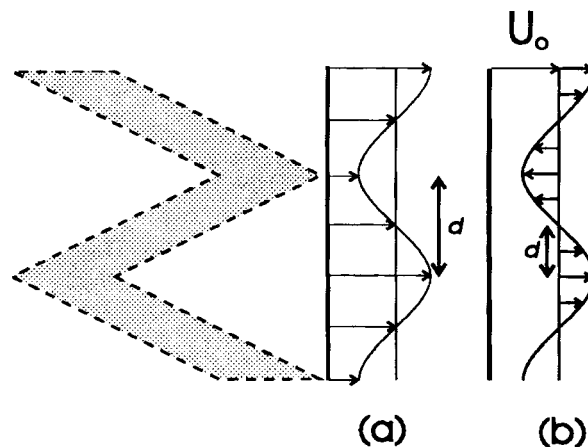
Fig. 2.7   Choosing a characteristic width for the jet model.

21

Wilcox's value of γ for a plane jet (0.098) is applied to the flow simulation. Since the flow width does not expand downstream, $d(x)$ is considered a constant equal to half the width of a jet which equals the width of a *half-pleat*. A half-pleat is one half of the "V" that makes up the pleat.

$$d(x) = d = \text{halfpleat width} \qquad (2\text{-}15)$$

So the mixing length approximation is

$$l_{mix} = 0.098 * d \qquad (2\text{-}16)$$

and the turbulent shear stress is

$$-\left(\overline{uv}\right) = \left(0.098 * d\right)^2 \left|\frac{dU}{dy}\right| \frac{dU}{dy} \qquad (2\text{-}17)$$

2.3 Flow Within the Filter

2.3.1 Development of the Intra-Filter Momentum Equation

Within the filter, the flow obeys the same physical rules as outside the filter. Continuity still holds in the same form, but the momentum equation must be reformulated to take into account the fibrous media as well. Instead of entering the fibers into the flowfield, a macroscopic model of flow through a porous media can be applied. For a flow where viscous effects far outweigh inertial effects, known as Stokes flow, dimensional analysis of such a flow through porous media shows that the pressure drop across the media is directly proportional to the macroscopic velocity. The filter variables involved are media thickness (t), average fiber radius (R), and packing factor (c) (the proportion of media / space) [Brown, 1993, p. 33].

$$\nabla P = \frac{\mu t \vec{V} f(c)}{R^2} \qquad (2\text{-}18)$$

The filter variables are grouped inversely under one variable K that represents the *permeability* of the filter media. The result is Darcy's law for Stokes flow which shows the pressure drop to be a direct function of velocity (Darcian velocity).

$$\nabla P = -\frac{\mu}{K} \bar{V}_D \qquad (2\text{-}19)$$

When the velocities are higher, inertia becomes appreciable and must be considered in a model of fluid momentum. A Reynolds number for flow through a filter can be calculated using fiber diameter (D) or the square root of permeability ($\sqrt{K}$).

$$\text{Re}_D = \frac{VD}{v_f} \qquad \text{Re}_{\sqrt{K}} = \frac{V\sqrt{K}}{v_f} \qquad (2\text{-}20)$$

If Re is less than one, a condition of Stokes flow exists, and inertia is insignificant. As our work on this project has shown, actual inlet velocity over an air filter can vary significantly, from the Stokes flow range to the inertial range (see Sabnis [1993] and Newman [1994] for experimental flow regimes). From this, it can be assumed that the maximum velocity would be on the order of 10 m/s. The fibers in the AF3192 filter media average approximately 40 μm in diameter [Sabnis, 1993]. The permeability for the media is $7.8e - 11$ m^2. Thus the expected maximum Re_D and $\text{Re}_{\sqrt{K}}$ are 27 and 6 respectively. This is beyond the realm of Stokes flow, thus inertia can be expected to be significant and will be considered. However, with pleating effects, intra-filter velocities are often less than 1 m/s, so in practice a condition near to Stokes flow will often exist.

Vafai & Tien [1981] show inertia in porous media flow to be affected by permeability and a function based on permeability, a permeability-based Reynolds number (Re_K), and the media geometry relating the layout of the fibers.

$$\nabla P = -\frac{f(K, \text{Re}_K, Geometry)}{\sqrt{K}} \cdot \frac{1}{2}\rho(\bar{V}_D \bullet \bar{V}_D)\bar{J} \qquad (2\text{-}21)$$

with $\vec{J} = \vec{V}_D / |\vec{V}_D|$, a unit direction vector.

These filter-based coefficients in front of inertia can be grouped together under one inertial coefficient, b.

$$\nabla P = -\frac{b}{2} \rho (\vec{V}_D \bullet \vec{V}_D) \vec{J} \qquad (2\text{-}22)$$

Note that the flow velocities found through the filter are area averaged, that is they represent the velocity in the cell assuming the media resistance exists but the fibers do not. Vafai & Tien term this the "Darcian fluid velocity". The actual velocities through the filter would be a function of the porosity, δ. Thus, following continuity, the actual "pore" velocity would be

$$\vec{V}_{pore} = \frac{\vec{V}_D}{\delta} \qquad (2\text{-}23)$$

However, Darcian velocities are used throughout this analysis.

Clearly, flow through the filter is laminar (Re ~ 10). So by including the Darcy terms, the momentum equation for flow within the filter becomes

$$\frac{\rho}{\delta^2} (\vec{V}_D \bullet \nabla) \vec{V}_D = -\nabla P + \frac{\mu}{\delta} \nabla^2 \vec{V}_D - \frac{\mu}{K} \vec{V}_D - \rho \frac{b}{2} (\vec{V}_D \bullet \vec{V}_D) J \qquad (2\text{-}24)$$

An analysis of the magnitude of the various terms allows for some pruning of this equation.

Katto and Masuoka [1966] devised a criterion for the onset of convective flow within a porous medium. The criterion is a function of the Rayleigh number Ra, media permeability K, and media thickness L.
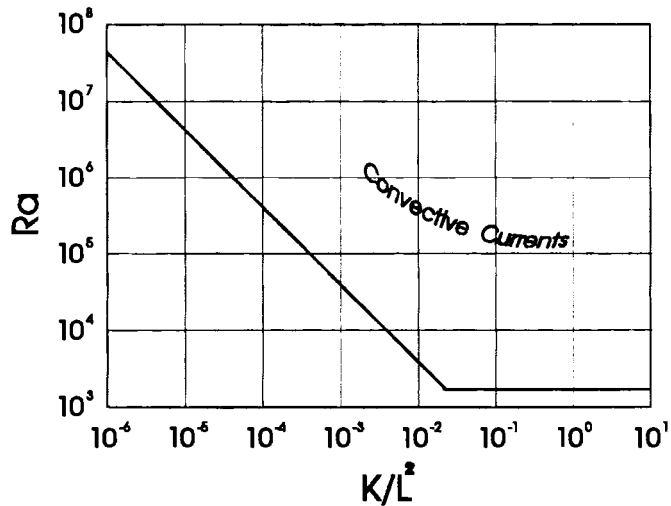
Fig. 2.8 Critical Rayleigh number vs. K/L^2,
adapted from Katto & Masuoka [1966].

Obviously, as the temperature gradient is assumed to be slight across the flowfield,

$Ra \approx 0$. However, to get an idea of the particular magnitude of the Rayleigh number for

this problem, a ΔT of 1°C is assumed and the thermal diffusivity of the saturated media

k_{media} is assumed equal to that of air. From this we get $K/L^2 \approx 2.0e - 04$ and

$Ra \approx 2.5e - 02$, well under the limit even if a significant discrepancy exists in the

assumptions.

Although flow within the media pores is certainly in the low Reynolds number regime, the

magnitude of the viscous term in relation to the Darcy terms is minimal. Assuming *extreme*

gradients $(U \sim 1 \quad dU \sim 1 \quad d^2U \sim 1 \quad dx \sim 1.0e - 04)$, the magnitude of the viscous term is

still well below those of the Darcy terms[**] .

$$\frac{\mu}{\delta}\frac{d^2U}{dx^2} \approx 2400 \qquad \frac{\mu}{K}U \approx 300,000 \qquad \rho\frac{b}{2}U^2 \approx 42,000$$

Viscous diffusion   Darcy resistance   Inertial Resistance

[**] Values of Darcy parameters to be derived below.

25

Thus the final momentum equation includes the pressure as a function of the Darcy resistance and flow inertia. This is referred to as the extended Darcy equation.

$$\frac{1}{\rho}\nabla P = -\frac{\nu_f}{K}\vec{V}_D - \frac{b}{2}\left(\vec{V}_D \bullet \vec{V}_D\right)\vec{J} \qquad (2\text{-}25)$$

This is a macroscopic momentum equation for flow through porous media. The terms are negative because the pressure drops moving downstream in a flow.

2.3.2 Calculation of Darcy Parameters

It remains for the Darcy parameters for particular media to be determined. Gurumoothy [1990] has demonstrated how to organize the Darcy equation as a function of pressure drop and flow rate. The Darcy equation is integrated over the media thickness (t), then velocity is replaced with the flow rate divided by the flow normal area (Q/A). This yields

$$\Delta P = \frac{\mu t}{KA}Q + \frac{b\rho t}{2A^2}Q^2 \qquad (2\text{-}26)$$

This equation is of the form

$$\Delta P = eQ + fQ^2 \qquad (2\text{-}27)$$

This is a 2nd degree polynomial. An experiment to measure pressure drop across a filter media versus flow rate was completed to derive e and f and thus K and b. The experiment was done using the media from the AF3192 filter. The values for K and b found from the experiment were

$$K = 7.8e - 11 \text{ m}^2 \qquad b = 6.8e + 04 \text{ m}^{-1} \qquad (2\text{-}28)$$

The experimental method is detailed in the appendix. These values differ considerably from those of Gurumoothy (Eq. 1-6) as that integration was carried over the whole *height* of the filter, while here the integration was done over the thickness of the media.

26

2.4 Grid Development

2.4.1 Range of Coverage

Grid generation algorithms are created for both triangular and square pleats. The scope of the flowfield needs to be minimized as much as possible in order to permit as detailed an analysis as possible. The inlet flow is uniform, so, because of the symmetry of the geometry, coverage can be limited to a half pleat width.
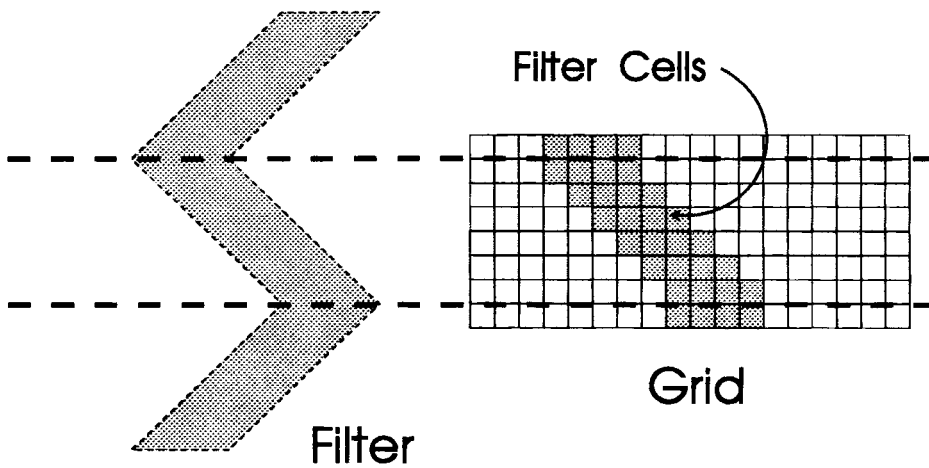
Fig. 2.9(a)   Grid simulation (triangular pleat).
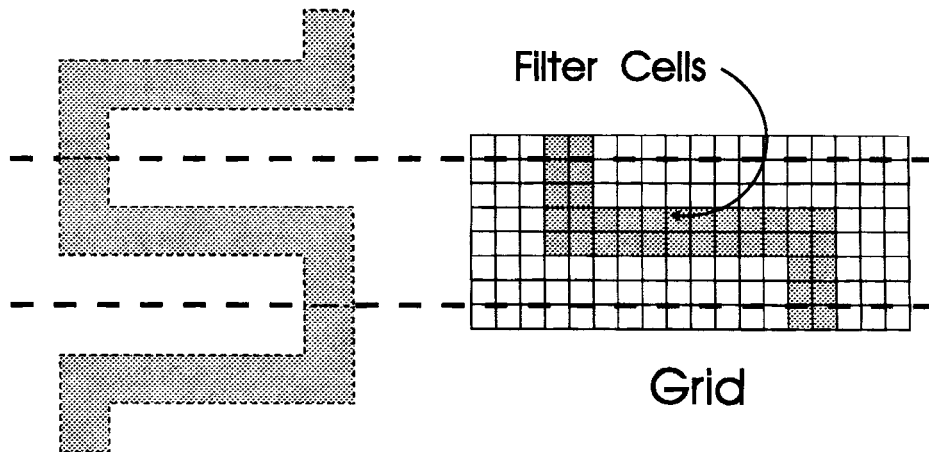
Fig. 2.9(b)   Grid simulation (square pleat).

27

To set positioning points for the finite difference equations, a grid is set up. A rectangular grid cell is used with pressure in the center, u-velocity on the front wall and v-velocity on the top wall.
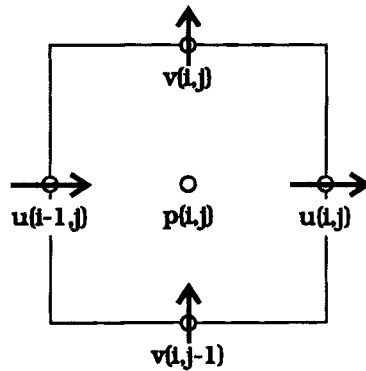
Fig. 2.10   Variable location in cell.

The key control parameters and grid are shown for each geometry below. The parameters are defined in Table 2.1.
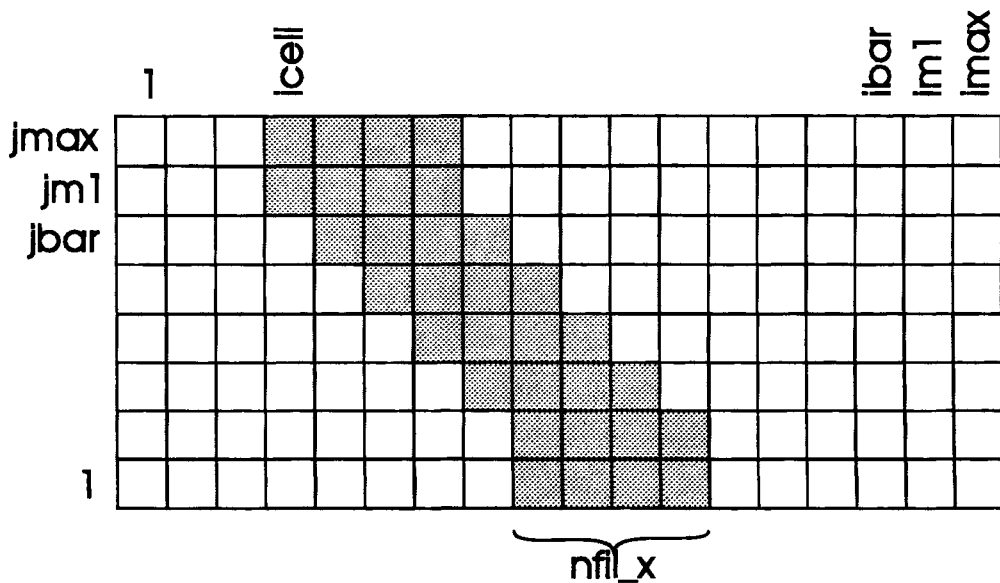
Fig. 2.11(a)   Grid showing key parameters (triangular pleat).

28
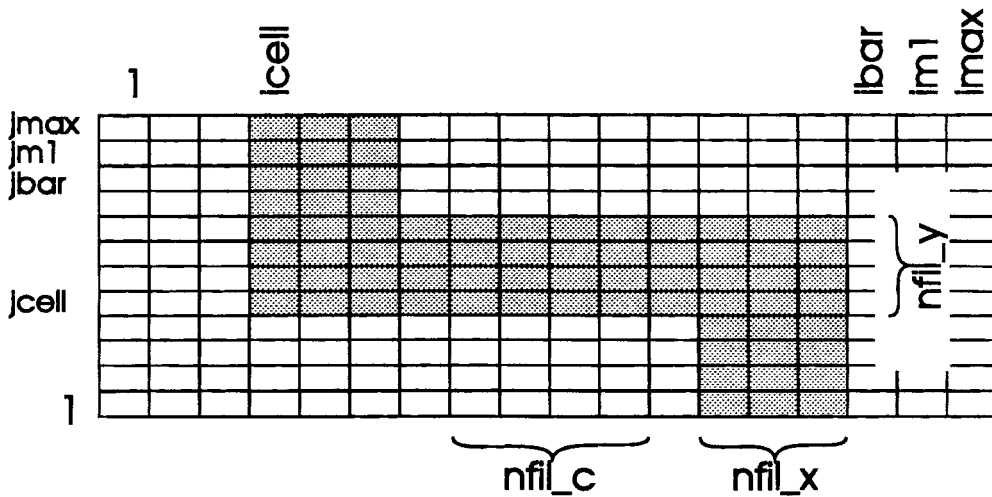
Fig. 2.11(b)   Grid showing key parameters (square pleat).

Using this grid the modeled filter / air interface would seem to be a jagged line for the triangular pleat and a smooth interface for the square pleat. However the actual interface is more closely related to a line connecting the pressure points at the cell centers, as the velocities on the left and lower sides of the cell have the characteristic (air or filter region) of the previous cell. So the grid of the square pleat lacks the consistent cell symmetry of the grid of the triangular pleat.
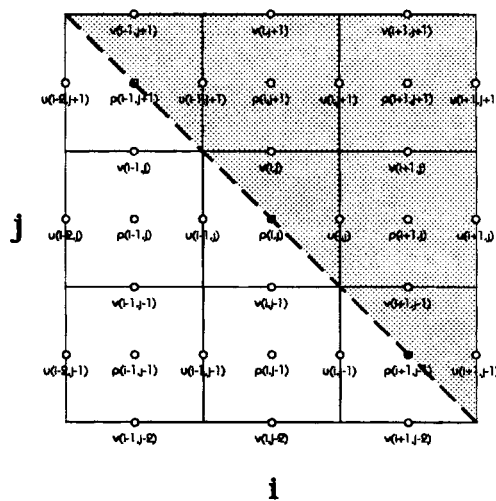
Fig. 2.12(a)   Actual air / filter interface (triangular pleat).

29
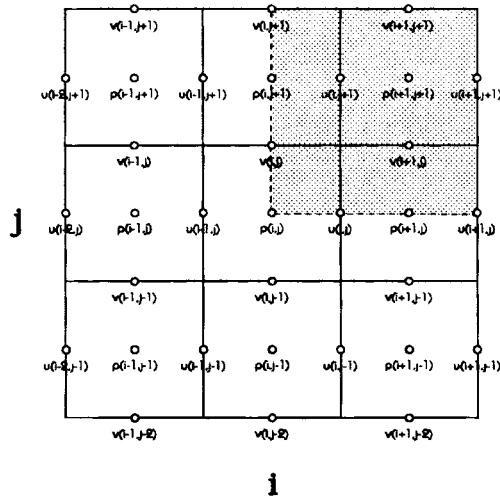
Fig. 2.12(b) Actual air / filter interface (square pleat at corner).

2.4.2 Calculation of Grid Geometry

The key criteria for setting up grids for each geometry are the angle of the pleating (θ), the height of the pleating (*ht*), and the thickness of the pleat media (*tp*). The fineness of the grid is determined by the number of cells across the pleat. There are three fineness parameters for the square pleat (*nfil_x, nfil_y, nfil_c*), and only one for the triangular pleat (*nfil_x*). The number of cells width-wise (*jbar*) and the number of cells along the pleat (*ipleat*) as well as the cell dimensions are determined using this data (see Table 2.1 below).

A key difference between the two geometries is what the angle θ represents. For the triangular pleat, the angle θ_Δ represents the slope of the media face versus the freestream. For the square pleat, the angle $\theta_\square$ is the tangent of the half-pleat width over the height. These are not the same; the difference is intensified for shorter pleats.

30
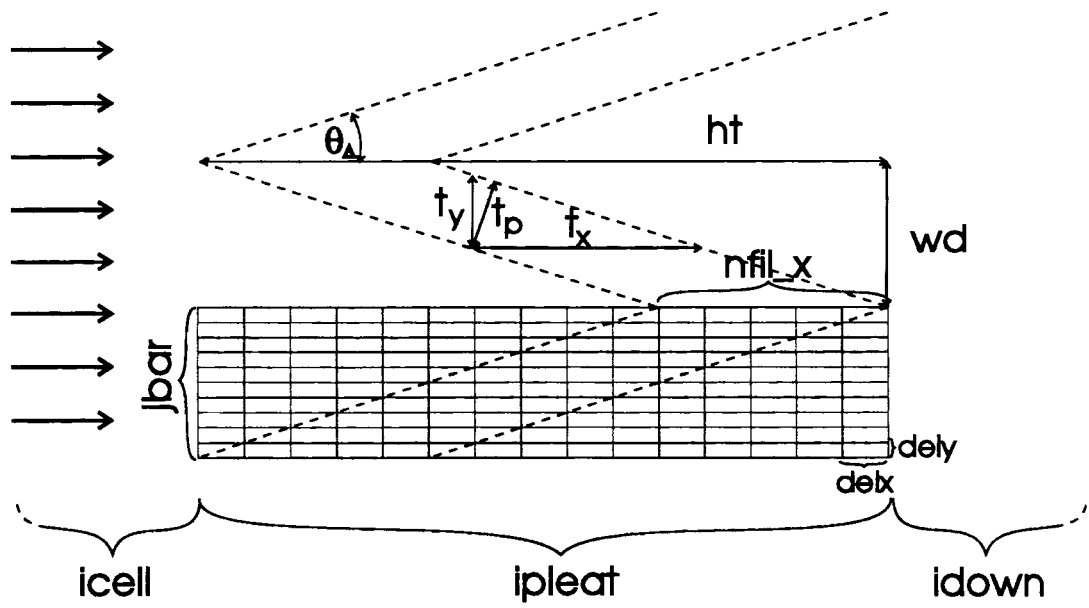
Fig. 2.13(a)   Schematic showing geometric parameters (triangular pleat).
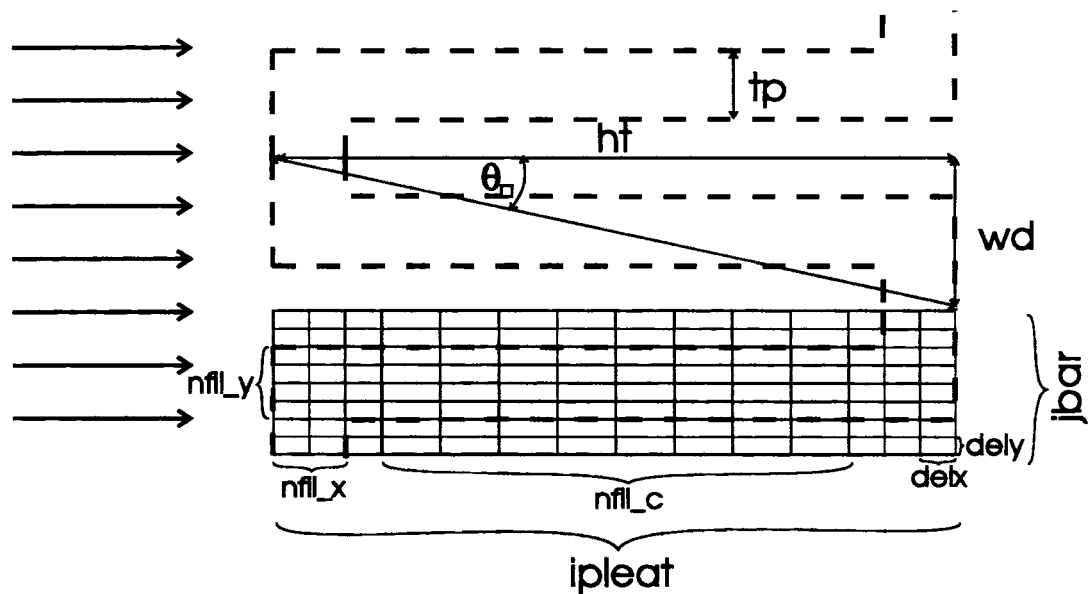
Fig. 2.13(b)   Schematic showing geometric parameters (square pleat).

31

The number of cells up and downstream of the pleat are calculated relative to the number cells along the pleat (*ipleat*) using the multipliers *cup* and *cdown* respectively. The grid is expanded up and downstream using the expansion coefficients *eta* and *zeta* respectively.
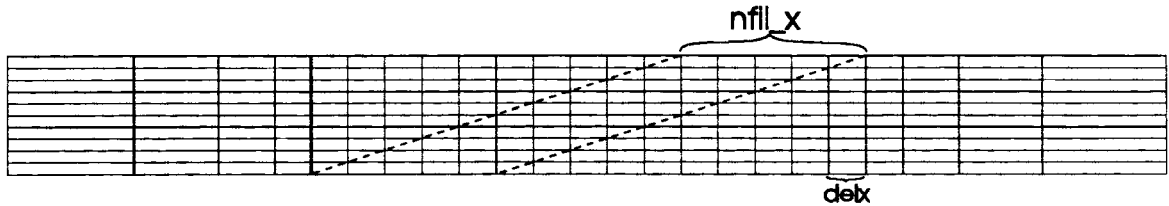
Fig. 2.14(a)   Schematic showing expanded grid (triangular pleat).
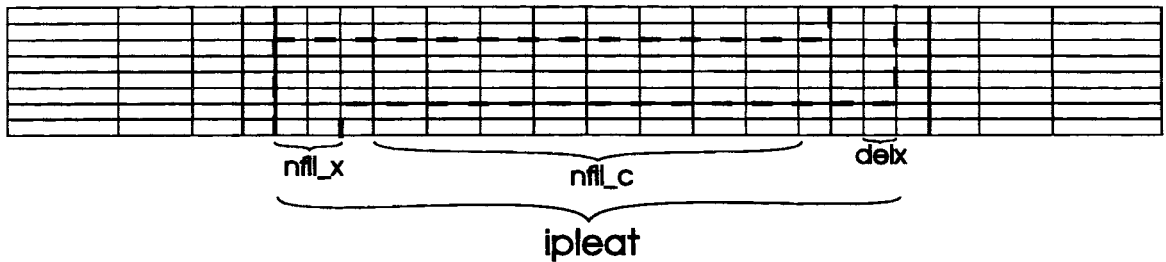
Fig. 2.14(b)   Schematic showing expanded grid (square pleat).

The table on the following page shows the derivation of all the geometric parameters.

The user-defined media thickness (*tp*) and pleat angle (θ) are always maintained. However, as the precision of the settings is limited by the fineness of the grid, the pleat height (*ht*) can only be as precise as the grid dimension *delx*. If *delx* equals 1.0, then *ht* cannot equal 8.5, it can only be 8.0 or 9.0.

Also note that the width of the flowfield is *jbar* * *dely*, this will be used as the jet width in the formulation for the mixing length *lmix*.

Parameter Summary

PARAMETER	SYMBOL	SHAPE	DERIVATION
pleat angle	θ	$\triangle$, $\square$	
pleat thickness	*tp*	$\triangle$, $\square$	
pleat height	*ht*	$\triangle$, $\square$	
cells across media (x-dir.)	*nfil_x*	$\triangle$, $\square$	
cells across media (y-dir.)	*nfil_y*	$\square$	
cells along media (x-dir.)	*nfil_c*	$\square$	
relative # cells upstream	*cup*	$\triangle$, $\square$	
relative # cells downstream	*cdown*	$\triangle$, $\square$	
cell width across filt. (x-dir.)	*delx*	$\triangle$	$tp \: / \: sin(\theta \:\:) \: / \: nfil\_x$
		$\square$	$tp \: / \: nfil\_x$
cell width along filt. length (x-dir.)	*delc*	$\square$	$(ht - 2tp - 2delx) \: / \: nfil\_c$
cell width (y-dir.)	*dely*	$\triangle$	$delx * tan(\theta \:\:)$
		$\square$	$tp \: / \: nfil\_y$
upstream expansion coeff.	*eta*	$\triangle$, $\square$	
downstream expansion coeff.	*zeta*	$\triangle$, $\square$	
length upstream of filt.	*uplgth*	$\triangle$, $\square$	$delx \cdot \sum\limits_{k=0}^{icell-2} eta^k$
length downstream of filt.	*dnlgth*	$\triangle$, $\square$	$delx \cdot \sum\limits_{k=0}^{idown-1} zeta^k$
pleat heights upstream	*htup*	$\triangle$, $\square$	$uplgth/ht$
pleat heights downstream	*htdown*	$\triangle$, $\square$	$dnlgth/ht$
total length of flowfield	*flgth*	$\triangle$, $\square$	$ht + uplgth + dnlgth$
pleat width	*wd*	$\triangle$	$ht * tan(\theta \:\:) - tp \: / \: cos(\theta \:\:)$
		$\square$	$ht * tan(\theta \:\:)$

Table 2.1 Program parameters (continued on next page).

first cell of pleat (y-dir.)	*jcell*	□	*((jbar+2) / 2) - (nfil_y / 2) + 1*
# cells width-wise	*jbar*	Δ, □	*wd / dely*
# cells in pleat flow-wise	*ipleat*	Δ	*nfil_x + jbar*
		□	*2 * nfil_x + 2 + nfil_c*
first cell of pleat (x-dir.)	*icell*	Δ, □	*cup * ipleat + 1 + 0.5*
# cells downstream of filter	*idown*	Δ, □	*cdown * ipleat + 0.5*
# cells flow-wise	*ibar*	Δ, □	*icell - 2 + ipleat + idown*
# cells width-wise inc. boundaries	*jmax*	Δ, □	*jbar + 2*
# cells flow-wise inc. boundaries	*imax*	Δ, □	*ibar + 2*

Table 2.1 Program parameters (continued from previous page).

2.5 Finite Difference Equations

2.5.1 Overview

The PDEs to be solved are as follows.

Continuity

$$\frac{\partial U}{\partial x} + \frac{\partial V}{\partial y} = 0 \tag{2-29}$$

Momentum outside the filter including turbulence model, conservative form

$$\frac{\partial(U^2)}{\partial x} + \frac{\partial(UV)}{\partial y} + \frac{1}{\rho}\frac{\partial P}{\partial x} - \nu_f(\frac{\partial^2 U}{\partial x^2} + \frac{\partial^2 U}{\partial y^2}) - \frac{\partial}{\partial y}(l_{mix})^2\left|\frac{\partial U}{\partial y}\right|\frac{\partial U}{\partial y} = 0$$

$$\frac{\partial(UV)}{\partial x} + \frac{\partial(V^2)}{\partial y} + \frac{1}{\rho}\frac{\partial P}{\partial y} - \nu_f(\frac{\partial^2 V}{\partial x^2} + \frac{\partial^2 V}{\partial y^2}) - \frac{\partial}{\partial x}(l_{mix})^2\left|\frac{\partial U}{\partial y}\right|\frac{\partial U}{\partial y} = 0 \tag{2-30, 2-31}$$

34

Momentum inside the filter

$$\frac{1}{\rho}\frac{\partial P}{\partial x}+\frac{v_f}{K}U_D+\frac{b}{2}(\vec{V}_D \bullet U_D)=0$$

$$\frac{1}{\rho}\frac{\partial P}{\partial y}+\frac{v_f}{K}V_D+\frac{b}{2}(\vec{V}_D \bullet V_D)=0$$

(2-32, 2-33)

Each grid point has the continuity equation and the two components of the particular momentum equation to solve for three unknowns. These equations must be translated into finite difference equations based on grid location. A location within the cell was chosen as the central point for finite difference approximation for each equation. The x-momentum equations (f) were centered about the u-velocity at the front wall; the y-momentum equations (g) were centered about the v-velocity at the top wall; and the continuity equation (h) was centered about the pressure variable location at the center of the cell. Finite difference approximations were made with central differencing and simple forward differencing. However, for the convective terms in the fluid momentum equations ($d(U_iU_j)/dx_j$), some amount of upstream differencing is necessary in order to maintain stability. The following diagram is a reference for orientation.
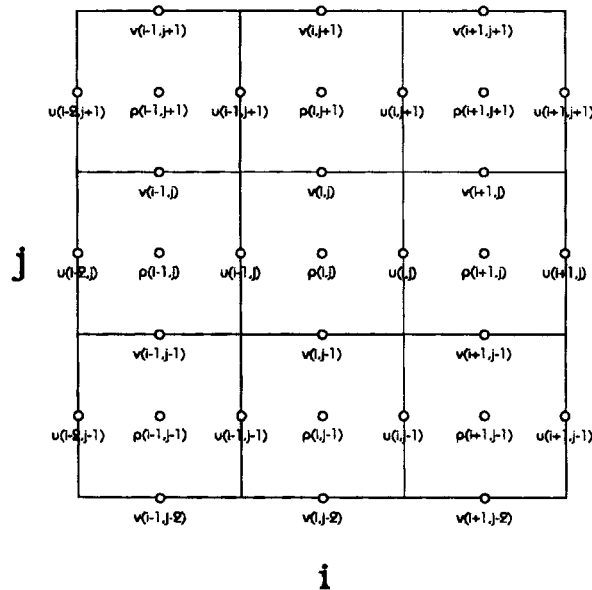
Fig. 2.15   Local cell orientation.

35

2.5.2 Finite Difference Formulations for Convective Terms

For higher Reynolds number flows, a central difference representation of convection yields an unstable result. A way to ensure stability is to use upstream differencing -- derivatives made with upstream and center stream grid points only. Physically, a central difference representation of convection is inappropriate, because, in fact, convection is really "received" from upstream and "transmitted" downstream [White, 1991, p. 199]. However, although sole use of upstream differencing ensures stability, it can lead to "an unnecessary amount of numerical smoothing" [Hirt et al., 1975]. So a combination of upstream and central differencing is used. The proportion of upstream differencing is specified by the parameter α. The FDEs for the convection terms are as follows [ibid].

$$\frac{d(UU)}{dx} = \frac{1}{4\Delta x}\{(u_{i,j}+u_{i+1,j})^2 + \alpha*|u_{i,j}+u_{i+1,j}|(u_{i,j}-u_{i+1,j})$$
$$-(u_{i-1,j}+u_{i,j})^2 - \alpha*|u_{i-1,j}+u_{i,j}|(u_{i-1,j}-u_{i,j})\} \tag{2-34}$$

$$\frac{d(UV)}{dy} = \frac{1}{4\Delta y}\{(v_{i,j}+v_{i+1,j})(u_{i,j}+u_{i,j+1}) + \alpha|v_{i,j}+v_{i+1,j}|(u_{i,j}-u_{i,j+1})$$
$$-(v_{i,j-1}+v_{i+1,j-1})(u_{i,j-1}+u_{i,j}) - \alpha|v_{i,j-1}+v_{i+1,j-1}|(u_{i,j-1}-u_{i,j})\} \tag{2-35}$$

$$\frac{d(UV)}{dx} = \frac{1}{4\Delta x}\{(u_{i,j}+u_{i,j+1})(v_{i,j}+v_{i+1,j}) + \alpha|u_{i,j}+u_{i,j+1}|(v_{i,j}-v_{i+1,j})$$
$$-(u_{i,j-1}+u_{i,j+1})(v_{i-1,j}+v_{i,j}) - \alpha|u_{i,j-1}+u_{i,j+1}|(v_{i-1,j}-v_{i,j})\} \tag{2-36}$$

$$\frac{d(VV)}{dy} = \frac{1}{4\Delta y}\{(v_{i,j}+v_{i,j+1})^2 + \alpha|v_{i,j}+v_{i,j+1}|(v_{i,j}-v_{i,j+1})$$
$$-(v_{i,j-1}+v_{i,j})^2 - \alpha|v_{i,j-1}+v_{i,j}|(v_{i,j-1}-v_{i,j})\} \tag{2-37}$$

Analysis of these equations shows that the α terms serve to cancel out the downstream $(i+1)$ terms in the central difference approximations.

2.5.3 Finite Difference Approximations for Other Terms

The remaining terms in the Navier-Stokes equations are centered on the particular variable within the cell as stated earlier.

The pressure terms are represented with forward differencing. Pressure in the program is normalized with density, so $p = \frac{1}{\rho} p$.

$$\frac{1}{\rho}\frac{\partial P}{\partial x} = \frac{(p_{i+1,j} - p_{i,j})}{\Delta x} \qquad \frac{1}{\rho}\frac{\partial P}{\partial y} = \frac{(p_{i,j+1} - p_{i,j})}{\Delta y} \qquad (2\text{-}38)$$

The diffusion terms use central differencing.

$$\nu_f\left(\frac{\partial^2 U}{\partial x^2} + \frac{\partial^2 U}{\partial y^2}\right) = \nu_f\left(\frac{u_{i+1,j} - 2u_{i,j} + u_{i-1,j}}{(\Delta x)^2} + \frac{u_{i,j+1} - 2u_{i,j} + u_{i,j-1}}{(\Delta y)^2}\right)$$

$$\nu_f\left(\frac{\partial^2 V}{\partial x^2} + \frac{\partial^2 V}{\partial y^2}\right) = \nu_f\left(\frac{v_{i+1,j} - 2v_{i,j} + v_{i-1,j}}{(\Delta x)^2} + \frac{v_{i,j+1} - 2v_{i,j} + v_{i,j-1}}{(\Delta y)^2}\right) \qquad (2\text{-}39, 2\text{-}40)$$

The turbulent shear stress formulations were also represented with central differencing.

$$-\frac{d}{dy}\overline{uv} = \frac{d}{dy}\left(l_{mix}^2 \left|\frac{dU}{dy}\right|\frac{dU}{dy}\right) =$$

$$(\gamma \cdot jbar \cdot \Delta y)^2 \cdot \frac{|u_{i,j+1} - u_{i,j}|(u_{i,j+1} - u_{i,j}) - |u_{i,j} - u_{i,j-1}|(u_{i,j} - u_{i,j-1})}{(\Delta y)^3} \qquad (2\text{-}41)$$

$$-\frac{d}{dx}\overline{uv} = \frac{d}{dx}\left(l_{mix}^2 \left|\frac{dU}{dy}\right|\frac{dU}{dy}\right) =$$

$$(\gamma \cdot jbar \cdot \Delta y)^2 \cdot \frac{|u_{i,j+1} - u_{i,j}|(u_{i,j+1} - u_{i,j}) - |u_{i-1,j+1} - u_{i-1,j}|(u_{i-1,j+1} - u_{i-1,j})}{\Delta x \cdot (\Delta y)^2} \qquad (2\text{-}42)$$

In the Darcy equation, the inertia term requires a calculation of total velocity $\bar{V}_D$; of course $\bar{V}_D = \sqrt{U_D^2 + V_D^2}$. The x-Darcy equation is centered at the u-velocity variable position in the cell (refer to Fig. 2.10). So it is necessary to create a formulation for the v-velocity component at the *front* of the cell. So V is taken as an average of the v's to the northwest and southeast of the u-point, as these points run parallel to the filter face.

$$v(\text{at } u_{ij}) = \frac{v_{i,j} + v_{i+1,j-1}}{2}$$

Likewise,

$$u(\text{at } v_{ij}) = \frac{u_{i-1,j+1} + u_{i,j}}{2}$$

This formulation is better suited for the triangular pleat, as there is no mixing of filter and non-filter cells.

The inertia terms in the Darcy equation are thus:

$$\frac{b}{2}(\bar{V}_D \bullet U_D) = \frac{b}{2} u_{i,j} \sqrt{\left(\frac{v_{i,j} + v_{i+1,j-1}}{2}\right)^2 + (u_{i,j})^2}$$

$$\frac{b}{2}(\bar{V}_D \bullet V_D) = \frac{b}{2} v_{i,j} \sqrt{\left(\frac{u_{i-1,j+1} + u_{i,j}}{2}\right)^2 + (v_{i,j})^2}$$

(2-43, 2-44)

2.5.4 Complete Form of the Finite Difference Equations

Taking all components together, the full FDEs are as follows.

Equation "f" outside of filter (fluid momentum x-component) $\qquad$ (2-45)

$$\frac{(u_{i,j}+u_{i+1,j})^2+\alpha|u_{i,j}+u_{i+1,j}|(u_{i,j}-u_{i+1,j})-(u_{i-1,j}+u_{i,j})^2-\alpha|u_{i-1,j}+u_{i,j}|(u_{i-1,j}-u_{i,j})}{4\Delta x}$$

$$+\frac{\left\{\begin{array}{l}(v_{i,j}+v_{i+1,j})(u_{i,j}+u_{i,j+1})+\alpha|v_{i,j}+v_{i+1,j}|(u_{i,j}-u_{i,j+1})\\ -(v_{i,j-1}+v_{i+1,j-1})(u_{i,j-1}+u_{i,j})-\alpha|v_{i,j-1}+v_{i+1,j-1}|(u_{i,j-1}-u_{i,j})\end{array}\right\}}{4\Delta y}$$

$$+\frac{(p_{i+1,j}-p_{i,j})}{\Delta x}-v_f\left(\frac{u_{i+1,j}-2u_{i,j}+u_{i-1,j}}{(\Delta x)^2}+\frac{u_{i,j+1}-2u_{i,j}+u_{i,j-1}}{(\Delta y)^2}\right)$$

$$-(\alpha\cdot jbar\cdot\Delta y)^2\cdot\frac{|u_{i,j+1}-u_{i,j}|(u_{i,j+1}-u_{i,j})-|u_{i,j}-u_{i,j-1}|(u_{i,j}-u_{i,j-1})}{(\Delta y)^3}=0$$

Equation "g" outside of filter (fluid momentum y-component) $\qquad$ (2-46)

$$\frac{\left\{\begin{array}{l}(u_{i,j}+u_{i,j+1})(v_{i,j}+v_{i+1,j})+\alpha|u_{i,j}+u_{i,j+1}|(v_{i,j}-v_{i+1,j})\\ -(u_{i,j-1}+u_{i,j+1})(v_{i-1,j}+v_{i,j})-\alpha|u_{i,j-1}+u_{i,j+1}|(v_{i-1,j}-v_{i,j})\end{array}\right\}}{4\Delta x}$$

$$+\frac{(v_{i,j}+v_{i,j+1})^2+\alpha|v_{i,j}+v_{i,j+1}|(v_{i,j}-v_{i,j+1})-(v_{i,j-1}+v_{i,j})^2-\alpha|v_{i,j-1}+v_{i,j}|(v_{i,j-1}-v_{i,j})}{4\Delta y}$$

$$+\frac{(p_{i,j+1}-p_{i,j})}{\Delta y}-v_f\left(\frac{v_{i+1,j}-2v_{i,j}+v_{i-1,j}}{(\Delta x)^2}+\frac{v_{i,j+1}-2v_{i,j}+v_{i,j-1}}{(\Delta y)^2}\right)$$

$$-(\alpha\cdot jbar\cdot\Delta y)^2\cdot\frac{|u_{i,j+1}-u_{i,j}|(u_{i,j+1}-u_{i,j})-|u_{i-1,j+1}-u_{i-1,j}|(u_{i-1,j+1}-u_{i-1,j})}{\Delta x\cdot(\Delta y)^2}=0$$

Equation "f" in filter (Extended Darcy x-component)

$$(p_{i+1,j} - p_{i,j}) + \Delta x \frac{v_f}{K} u_{i,j} + \Delta x \frac{b}{2} u_{i,j} \sqrt{\left(\frac{v_{i+1,j-1} + v_{i,j}}{2}\right)^2 + u_{i,j}^2} = 0 \quad (2\text{-}47)$$

Equation "g" in filter (Extended Darcy y-component)

$$(p_{i,j+1} - p_{i,j}) + \Delta y \frac{v_f}{K} v_{i,j} + \Delta y \frac{b}{2} v_{i,j} \sqrt{\left(\frac{u_{i-1,j+1} + u_{i,j}}{2}\right)^2 + v_{i,j}^2} = 0 \quad (2\text{-}48)$$

Equation "h" (continuity inside and outside of filter)

$$\frac{u_{i,j} - u_{i-1,j}}{\Delta x} + \frac{v_{i,j} - v_{i,j-1}}{\Delta y} = 0 \quad (2\text{-}49)$$

2.6 Boundary Conditions

At the upstream position of the flow, the uniform inlet velocity is imposed. At the final downstream column, a boundary condition of continuitive flow is assumed. This assumes the velocity gradient over the exit boundary is zero. The length of the grid should be sufficient so that these conditions do not influence the flow immediately near the boundary, i.e. the velocity gradients should be zero at the upstream and downstream boundaries. However, as it worthwhile to reduce the grid size as much as possible to thereby reduce run time, the effects of imposing these upstream and downstream boundary conditions over too tight a grid are analyzed in the next chapter to see the effect over the area of importance, *viz.* the pleat. If the effect is minimal, the smaller number of grid cells could be used.

At the downstream boundary, a pressure reading of zero is prescribed to provide a reference to flow pressure upstream.

Along the sides of the flow, free slip symmetry is assumed. So at the edges of the half-pleat, crosswise velocity is assumed to be zero, and velocities on either side of the pleat are assumed to be reflective. This symmetry condition requires that the inlet velocity have no cross-flow component.
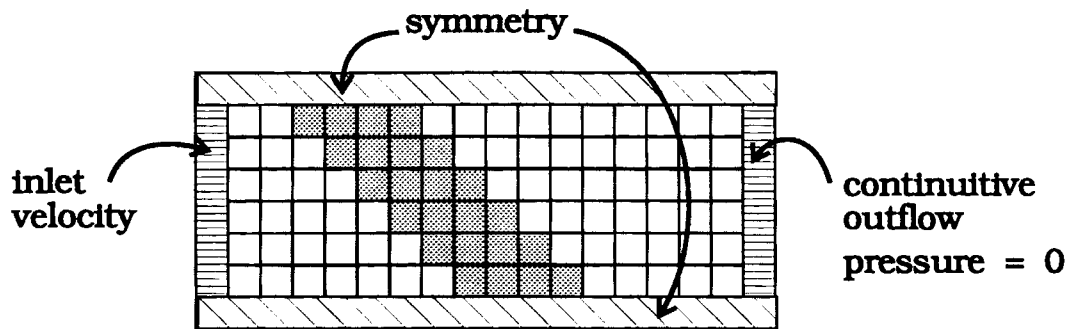
Fig. 2.16   Boundary conditions.

Lastly, it is noted that at the air / filter interface there is no boundary condition to prevent variables on either side from being included in both the viscous flow and filter momentum equations. This betrays itself in certain aspects of the solution.

2.7 Solution Method

Solving for the FDEs is somewhat complicated by the non-linearity of the equations. The following summary of the solution method is from Gerald & Wheatly [1994] pp. 165-7.

There are three equations to solve for three unknowns per cell.

$$f(u,v,p) = x\text{-momentum} = 0$$

$$g(u,v,p) = y\text{-momentum} = 0$$

$$h(u,v) = \text{continuity} = 0$$

The solution to the equations is (u_r, v_r, p_r). With an initial guess of the solution (u_i, v_i, p_i), the functions can be expanded to a truncated Taylor series.

$$f(u_r, v_r, p_r) = 0 = f(u_i, v_i, p_i) + f_u(u_i, v_i, p_i)(u_r - u_i) + f_v(u_i, v_i, p_i)(v_r - v_i) + f_p(u_i, v_i, p_i)(p_r - p_i)$$
$$g(u_r, v_r, p_r) = 0 = g(u_i, v_i, p_i) + g_u(u_i, v_i, p_i)(u_r - u_i) + g_v(u_i, v_i, p_i)(v_r - v_i) + g_p(u_i, v_i, p_i)(p_r - p_i)$$
$$h(u_r, v_r, p_r) = 0 = h(u_i, v_i, p_i) + h_u(u_i, v_i, p_i)(u_r - u_i) + h_v(u_i, v_i, p_i)(v_r - v_i) + h_p(u_i, v_i, p_i)(p_r - p_i)$$

$$(2\text{-}50)$$

Here $f_x \equiv \dfrac{df}{dx}$, etc. These equations can thus be solved for the difference between the solution and the estimate.

$$
\begin{bmatrix}
f_u(u_i, v_i, p_i) & f_v(u_i, v_i, p_i) & f_p(u_i, v_i, p_i) \\
g_u(u_i, v_i, p_i) & g_v(u_i, v_i, p_i) & g_p(u_i, v_i, p_i) \\
h_u(u_i, v_i, p_i) & h_v(u_i, v_i, p_i) & h_p(u_i, v_i, p_i)
\end{bmatrix}
\begin{bmatrix}
\Delta u_i \\
\Delta v_i \\
\Delta p_i
\end{bmatrix}
= -
\begin{bmatrix}
f(u_i, v_i, p_i) \\
g(u_i, v_i, p_i) \\
h(u_i, v_i, p_i)
\end{bmatrix}
\qquad (2\text{-}51)
$$

where

$$\Delta u_i = u_r - u_i \quad \Delta v_i = v_r - v_i \quad \Delta p_i = p_r - p_i$$

The Δ terms are solved by Gaussian elimination and added to the original estimate of the solution.

$$
\begin{bmatrix}
u_{i+1} \\
v_{i+1} \\
p_{i+1}
\end{bmatrix}
=
\begin{bmatrix}
u_i \\
v_i \\
p_i
\end{bmatrix}
+
\begin{bmatrix}
\Delta u_i \\
\Delta v_i \\
\Delta p_i
\end{bmatrix}
\qquad (2\text{-}52)
$$

Then equation (2-51) is solved again using the new estimates. This iteration is continued until convergence. Convergence is obtained when the difference between two iterations reaches an arbitrarily small value. This criterion is discussed in Chapter 3.

2.8 Output of Program

The program outputs data to two files. The file OUTPUT.DAT has the final values displayed for each gridpoint, including:

- u and v velocities,
- angle of flow,
- pressure,
- and continuity.

The file VELOCITY.DAT and other variants contain columnated position and velocity data to be output to a vector plotting utility.

Chapter 3

Investigation of Parameters

3.1 Introduction

The following section examines some of the parameters used in the PLEATFLO program with the triangle-shaped pleat geometry. Parameters are examined in two categories: parameters directly affecting program output and parameters affecting program run time. Lastly, the square-wave pleat geometry is examined separately.

As one of the difficulties in implementing a CFD method for viscous fluid flow is program stability, the key parameter in maintaining stability, the upstream differencing proportion α, is studied to find the best value. Also, as the applied turbulence model is not tailored for the particular flow in this study, the effect of the turbulence parameter that determines the mixing length (γ) is discussed.

The area of the flow that is of particular interest is the entrance and exit to the pleat. In order to have a more detailed and faithful simulation of the flow, a fine grid is desired. However, the greater the number of grid points, the more computer resources required. So this part of the parameter analysis examines ways to minimize coverage of the less crucial areas of the flowfield, while increasing detail around the filter pleat. Testing is done to optimize code settings to:

- minimize the distance covered upstream (*htup*) and downstream (*htdown*) of the filter;

- maximize the grid expansion up (*eta*) and downstream (*zeta*) of the filter;

- minimize the pleat height (*htup*) used to examine a specific pleat angle;

- increase the density of the grid (*nfil_x*);

- maximize the convergence criterion (*epsi*) for faster solution.

3.2 A Sample Run

Before examining the parameters, sample runs are done to demonstrate the format of the output. The output format takes two forms: a printout of the data and a file formatted for creating a vector plot.

The typewritten printout of the input and output data is contained in the file OUTPUT.DAT. The output data include u, v, p, continuity, and angle for every cell in the flowfield. The velocities are in meters per second; the normalized pressure (pressure divided by density) is in meters squared per second squared; the continuity is taken for each cell; the angle is in degrees counterclockwise from a due downstream flow. A sample is shown for an abbreviated flowfield.

The input parameters are contained in the box below. This tells the geometric configuration. This also tells whether convergence was attained and the total number of iterations to obtain convergence, or, if convergence was not attained, then it gives the final value of the convergence criterion. It also gives a value for upstream pressure.

```
 ---------------------------------------------------------------------------
     Pleat Shape:  Triangular       Parameters in meters, degrees, seconds
 ---------------------------------------------------------------------------
    Base Geometry Data                  Derived Geometry Data
  1) pleat height        ht  .242E-01 | x) # cells in x dir  ibar        16
  2) pleat media width   tp  .635E-03 | x) # cells in y dir  jbar         4
  3) pleat angle      thetad   3.000  | x) # x-cells to filt icel         5
  4) rel # cell upstrm  cup    .600   | x) # y-cells to filt jcell        0
  5) rel # cell dnstrm cdown   .700   | x) x cell wdth        delx  .303E-02
  6) # of x filt cells nfil_x    4    | x) y cell wdth        dely  .159E-03
  7) # of y filt cells nfil_y    0    | x) c cell wdth        delc  .000E+00
  8) # of c filt cells nfil_c    0    | x) pleat width        wd    .636E-03
  9) up expans coeff    eta    1.500  | x) total flow lgth    flgth .485E-01
 10) down expans coef   zeta   1.500  | x) filt hts upstrm    htup     .986
 11) max # of iter    jcntmx    20    | x) filt hts dnstrm   htdown   1.600
 12) convergence crit  epsi  .100E-02 | x) est iter runtime  estime .323E+01
 13) x inlet veloc     uin    3.000   | x) est max runtime   estot  .645E+02
 ---------------------------------------------------------------------------
 14) kin. visc'ty      nu   .151E-04  | 17) x permeability    K_x   .780E-10
 15) upstrm flux coef  alpha  1.000   | 18) y permeability    K_y   .780E-10
 16) turb coeff        gamma   .098   | 19) x inertia factor  b_x   .680E+05
                                      | 20) y inertia factor  b_y   .680E+05
 ---------------------------------------------------------------------------
 | Reached Convergence Criterion?       Yes.        No. of iter = 5
 | Upstream Pressure =     .34877E+04 Pa
 ---------------------------------------------------------------------------
```

Table 3.1(a)   Input to a sample run.

The values on the right numbered "x)" are derived values, all others can be input directly.
Once cell dimensions are established (*delx* and *dely*), the height and width are recalculated
based on a set thickness (*tp*) and angle (θ). The exactness with which the height can be
specified is limited by the fineness of the grid (*nfil_x*) (also see Section 2.4.2)

Some of these parameters are further examined in this chapter. It is only noted that the
thickness of the media specified here (6.35e-03 m) is the approximate thickness of the
media used in the Purolator AF3192 filter, a passenger car engine air filter.

Next OUTPUT.DAT gives the variable values per cell. The filter region lies between the slash
"\" marks.

```
U velocity
     1      2      3      4      5      6      7      8      9
6  3.000  3.000  2.999  2.994   .027   .082   .555  3.004 10.229
5  3.000  3.000  2.999  2.994\  .027   .082   .555  3.004\10.229
4  3.000  3.000  3.000  2.997  2.582\  .081   .547  2.996   .579
3  3.000  3.000  3.000  3.002  4.214  4.577\  .533  2.996   .592
2  3.000  3.000  3.001  3.006  5.177  7.260 10.365\ 3.004   .599
1  3.000  3.000  3.001  3.006  5.177  7.260 10.365  3.004   .599

    10     11     12     13     14     15     16     17     18
6  7.694  5.831  4.494  3.775  3.375  3.161  3.057  3.009  3.009
5  7.694  5.831  4.494  3.775  3.375  3.161  3.057  3.009  3.009
4\ 4.233  4.079  3.489  3.261  3.134  3.061  3.023  3.004  3.004
```

```
3   .035\ 2.090  2.407  2.690  2.849  2.935  2.976  2.996  2.996
2   .037  -.001\ 1.610  2.273  2.642  2.844  2.943  2.991  2.991
1   .037  -.001  1.610  2.273  2.642  2.844  2.943  2.991  2.991
--------------
V velocity
      1      2      3      4      5      6      7      8      9
6   .000   .000   .000   .000   .156  -.003  -.025  -.128  -.379
5   .000   .000   .000   .000\  .000   .000   .000   .000\  .000
4   .000   .000   .000   .000  -.156\  .003   .025   .128   .379
3   .000   .000   .000   .000  -.177  -.128\  .049   .257   .252
2   .000   .000   .000   .000  -.114  -.109  -.163\  .386   .126
1   .000   .000   .000   .000   .000   .000   .000   .000   .000

     10     11     12     13     14     15     16     17     18
6   .133   .098   .070   .025   .009   .003   .001   .000   .000
5   .000   .000   .000   .000   .000   .000   .000   .000   .000
4\ -.133  -.098  -.070  -.025  -.009  -.003  -.001   .000   .000
3   .059\ -.106  -.101  -.033  -.012  -.004  -.001   .000   .000
2   .029   .002\ -.084  -.023  -.009  -.003  -.001   .000   .000
1   .000   .000   .000   .000   .000   .000   .000   .000   .000


--------------
angle (positive horizontal equals 0)
      1      2      3      4      5      6      7      8      9
6    .0     .0     .0     .0   80.3   -2.0   -2.6   -2.4   -2.1
5    .0     .0     .0     .0\    .0     .0     .0     .0\    .0
4    .0     .0     .0     .0   -3.4\   2.1    2.6    2.5   33.2
3    .0     .0     .0     .0   -2.4   -1.6\   5.3    4.9   23.0
2    .0     .0     .0     .0   -1.3    -.9    -.9\   7.3   11.9
1    .0     .0     .0     .0     .0     .0     .0     .0     .0

     10     11     12     13     14     15     16     17     18
6   1.0    1.0     .9     .4     .2     .1     .0     .0     .0
5    .0     .0     .0     .0     .0     .0     .0     .0     .0
4\  -1.8   -1.4   -1.1    -.4    -.2    -.1     .0     .0     .0
3   58.9\  -2.9   -2.4    -.7    -.2    -.1     .0     .0     .0
2   38.6  -75.6\  -3.0    -.6    -.2    -.1     .0     .0     .0
1    .0     .0     .0     .0     .0     .0     .0     .0     .0


continuity
      1          11         2          3          4          5          6          7          8          9
10               11         12
6  .0000E+00  .1962E-13 -.7422E-13  .1066E-12 -.1137E-12  .3553E-14 -.2842E-13  .0000E+00 -.4547E-12
5  .0000E+00  .1962E-13 -.7422E-13  .1066E-12\-.1137E-12  .3553E-14 -.2842E-13  .0000E+00\-.4547E-12
4  .0000E+00  .7910E-14 -.3839E-13  .1094E-12 -.8527E-13\ .0000E+00  .0000E+00  .0000E+00  .1137E-12-
3  .0000E+00  .1648E-13 -.3567E-14  .1030E-12 -.5684E-13 -.1421E-13\ .2274E-12 -.2274E-12  .1137E-12
2  .0000E+00  .2106E-13  .1857E-13  .1201E-12 -.2274E-12  .0000E+00 -.1137E-12\-.4547E-12  .0000E+00
1  .0000E+00  .0000E+00  .0000E+00  .0000E+00  .0000E+00  .0000E+00  .0000E+00  .0000E+00  .0000E+00

     10         11         12         13         14         15         16         17         18
6  .1137E-12 -.4547E-12  .2274E-12 -.8527E-13  .7105E-14 -.7105E-14  .1688E-13  .3553E-14  .2109E+01
5  .1137E-12 -.4547E-12  .2274E-12 -.8527E-13  .7105E-14 -.7105E-14  .1688E-13  .3553E-14  .2109E+01
4\-.2274E-12  .1847E-12 -.5684E-13  .5684E-13 -.3553E-14 -.1865E-13  .1421E-13  .2265E-13  .8272E+00
3  .0000E+00\ .0000E+00  .7105E-13 -.7105E-14 -.3553E-14  .1421E-13 -.2354E-13  .8660E-14 -.8641E+00
2  .2842E-13  .3553E-14\-.1137E-12  .5684E-13  .7105E-14 -.3197E-13 -.7105E-14  .3553E-14 -.2072E+01
1  .0000E+00  .0000E+00  .0000E+00  .0000E+00  .0000E+00  .0000E+00  .0000E+00  .0000E+00  .0000E+00


--------------
P pressure  (normalized)
      1          2          3          4          5          6          7          8          9
6  .0000E+00  .3488E+04  .3488E+04  .3488E+04  .3488E+04  .3472E+04  .3423E+04  .3067E+04  .3747E+03
5  .0000E+00  .3488E+04  .3488E+04  .3488E+04\ .3488E+04  .3472E+04  .3423E+04  .3067E+04\ .3747E+03
4  .0000E+00  .3488E+04  .3488E+04  .3488E+04  .3488E+04\ .3472E+04  .3424E+04  .3072E+04  .3900E+03
3  .0000E+00  .3488E+04  .3488E+04  .3488E+04  .3488E+04  .3472E+04\ .3426E+04  .3082E+04  .4002E+03
2  .0000E+00  .3488E+04  .3488E+04  .3488E+04  .3488E+04  .3472E+04  .3426E+04\ .3098E+04  .4053E+03
1  .0000E+00  .3488E+04  .3488E+04  .3488E+04  .3488E+04  .3472E+04  .3426E+04  .3098E+04  .4053E+03

     10         11         12         13         14         15         16         17         18
6  .1366E+02 -.5003E+01 -.4553E+01 -.1221E+01 -.3800E+00 -.1467E+00 -.8942E-01 -.7840E-01  .0000E+00
5  .1366E+02 -.5003E+01 -.4553E+01 -.1221E+01 -.3800E+00 -.1467E+00 -.8942E-01 -.7840E-01  .0000E+00
4\ .1413E+02 -.4934E+01 -.4535E+01 -.1212E+01 -.3787E+00 -.1465E+00 -.8939E-01 -.7840E-01  .0000E+00
3  .1603E+02\-.4854E+01 -.4519E+01 -.1203E+01 -.3770E+00 -.1462E+00 -.8936E-01 -.7840E-01  .0000E+00
2  .1698E+02 -.4794E+01\-.4499E+01 -.1197E+01 -.3761E+00 -.1460E+00 -.8934E-01 -.7841E-01  .0000E+00
1  .1698E+02 -.4794E+01 -.4499E+01 -.1197E+01 -.3761E+00 -.1460E+00 -.8934E-01 -.7841E-01  .0000E+00
```

Table 3.1 (b) Raw data from file OUTPUT.DAT.

47

Results are also output as a set of x,y position and u,v velocity data to be used for vector plotting. A more intuitive understanding of the flow can be gained through a vector plot of the flowfield. For the triangular pleat configuration, the points are taken at the u-position in the cell (see Fig. 2.10). The v-velocity at the u-position is averaged from the two v-velocities northwest and southeast of the u-position, because these are aligned in the filter direction and assure that extra- and intra-filter data are not mixed (for the triangular pleat).

Ideally, vector flowfields would be displayed exactly proportional to the modeled flowfield. However, it is difficult to produce a clear picture when the pleats are nearly vertical and the flowfield is 100 times longer than it is wide. So the flowfield is modified in various ways: either disregarding much of the flow up and downstream of the filter (*x-pruning*), or exaggerating the y-dimension (*y-weighting*).

The latter method also weights the v-velocity component. An example is shown (Fig. 3.1) to exhibit its effect. The expansion only weights the directional component of v not the magnitude.

The vectors' magnitude can be equal-weighted (linear-scale), log-weighted (log-scale), or ignored (equal-length). Examples are shown in Fig. 3.1 (c), (d), and (a), respectively.

Following Fig. 3.1 are sample outputs from the PLEATFLO program representing the range of angles to be tested. Examples using the different vector graphing methods are shown.
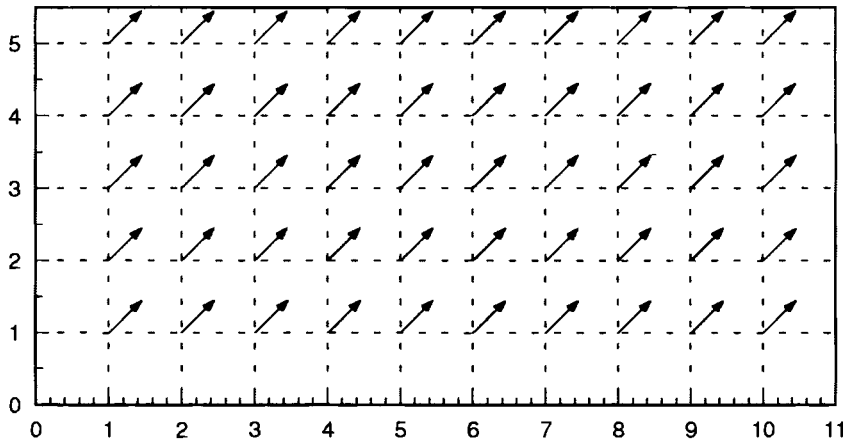
Fig. 3.1(a) Sample of a vector plot, in proportion to the actual size of the flowfield.
The actual flow data is 45° above horizontal. Although the magnitude of the flowfield
varies, the vectors are set equal-length; thus they represent direction only.
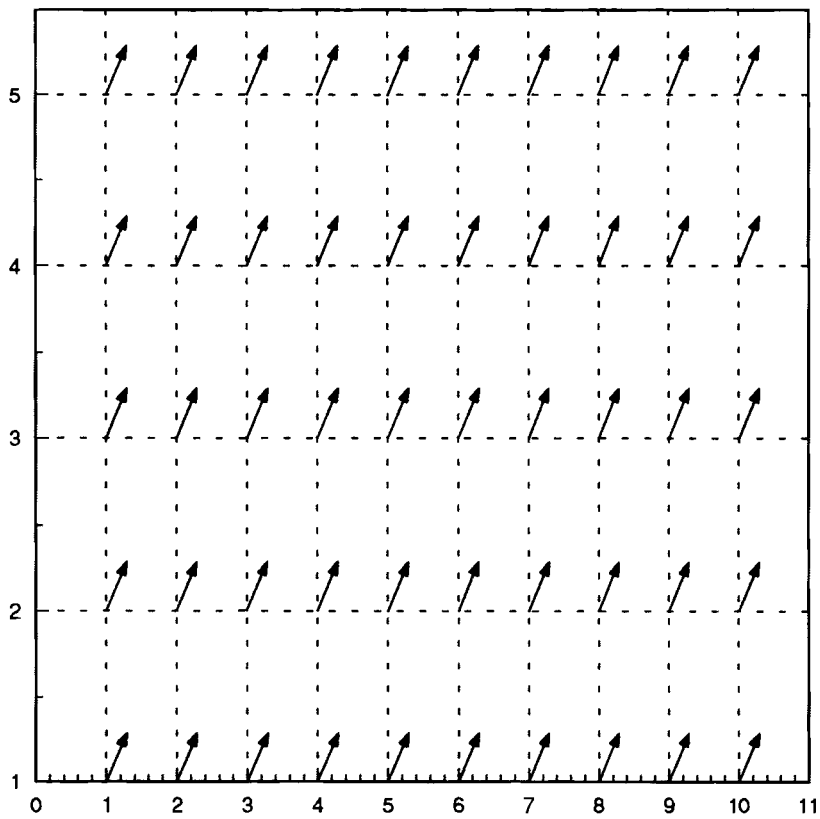
Fig. 3.1(b) Sample of a vector plot for same data, with the y-dimension expanded
200%. Note the magnitude of the vectors is the same as above, but the direction is
weighted equal in amount to the expansion.

49
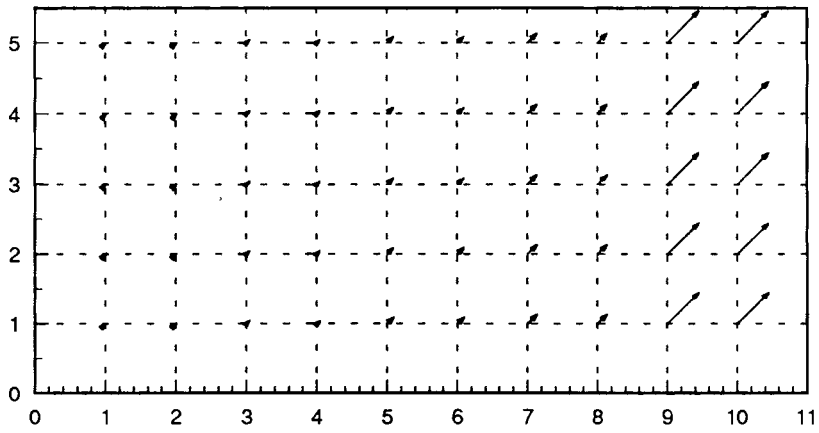
Fig. 3.1(c) Same as (a), but the vectors are scaled linearly to represent magnitude.
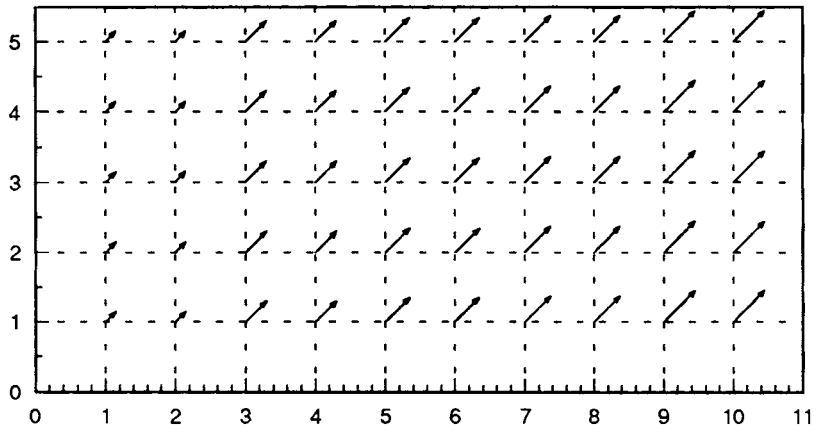
Fig. 3.1(d) Same as (a), but the vectors are log-scale. This is better to represent magnitude if the magnitude within the flowfield varies greatly.

50

```
-----------------------------------------------------------------------
    Pleat Shape:  Triangular      Parameters in meters, degrees, seconds
-----------------------------------------------------------------------
|  Base Geometry Data_____  |___Derived Geometry Data_____
1) pleat height      |  ht  |.202E-02 | x) # cells in x dir | ibar        24
2) pleat media width |  tp  |.635E-03 | x) # cells in y dir | jbar         5
3) pleat angle       |thetad| 45.000  | x) # x-cells to filt| icel         8
4) rel # cell upstrm |  cup |   .800  | x) # y-cells to filt| jcel         0
5) rel # cell dnstrm | cdown| 1.000   | x) x cell wdth      | delx |.225E-03
6) # of x filt cells |nfil_x|   4     | x) y cell wdth      | dely |.225E-03
7) # of y filt cells |nfil_y|   0     | x) c cell wdth      | delc |.000E+00
8) # of c filt cells |nfil_c|   0     | x) pleat width      | wd   |.112E-02
9) up expans coeff   | eta  | 1.000   | x) total flow lgth  | flgth|.540E-02
10) down expans coef | zeta | 1.000   | x) filt hts upstrm  | htup |   .786
11) max # of iter    |jcntmx|  25     | x) filt hts dnstrm  |htdown|  1.010
12) convergence crit | epsi |.100E-02 | x) est iter runtime |estime|.118E+02
13) x inlet veloc    | uin  | 3.000   | x) est max runtime  | estot|.294E+03
|----------------------------------------------------------------------
|                         Flow Parameters
|----------------------------------------------------------------------
14) kin. visc'ty  | nu   |.151E-04 | 17) x permeability   | K_x |.780E-10
15) upstrm flux coef| alpha| 1.000 | 18) y permeability   | K_y |.780E-10
16) turb coeff    | gamma|  .098   | 19) x inertia factor | b_x |.680E+05
|                                  | 20) y inertia factor | b_y |.680E+05
|----------------------------------------------------------------------
| Reached Convergence Criterion?      Yes.           No. of iter = 18
| Upstream Pressure =     .49748E+03 Pa
-----------------------------------------------------------------------
```

Table 3.2 Input summary for a 45° pleat, 2 mm high.
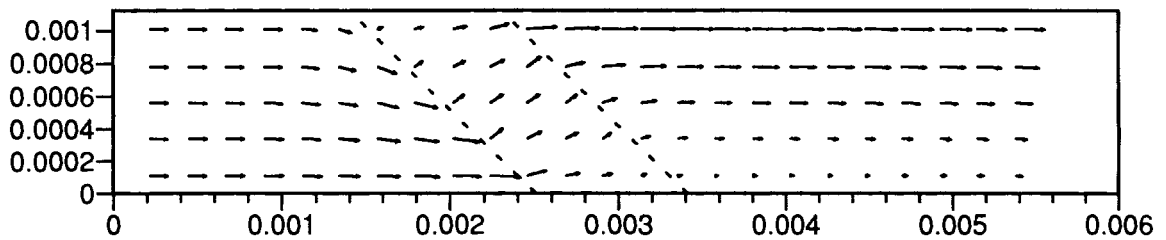
Fig. 3.2(a) Full and proportional flowfield, linear-scaled vectors.
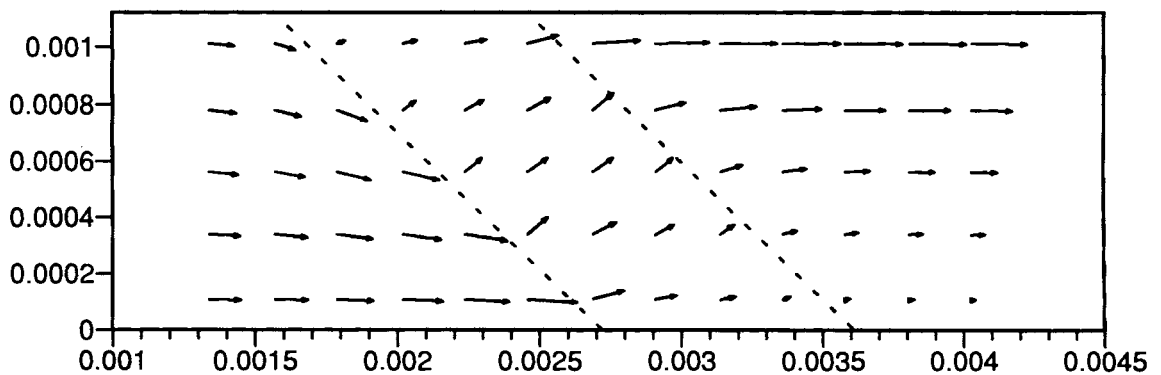
Fig. 3.2(b) Pruned and proportional flowfield, linear-scaled vectors.

Figs. 3.2 Vector flowfields for 45° pleat, 2 mm high.

```
| ------------------------------------------------------------------------------
|   Pleat Shape:  Triangular       Parameters in meters, degrees, seconds
| ------------------------------------------------------------------------------
|   Base Geometry Data_____|___Derived Geometry Data_____
1)  pleat height      :    ht  |.822E-02 | x) # cells in x dir    ibar       27
2)  pleat media width.     tp  |.635E-03 | x) # cells in y dir .  jbar        5
3)  pleat angle        |thetad;  10.000  | x) # x-cells to filt  icell        9
4)  rel # cell upstrm| cup |      .900 , | x) # y-cells to filt| jcell        0
5)  rel # cell dnstrm| cdown|    1.200 | | x) x cell wdth      |  delx |.914E-03
6)  # of x filt cells|nfil_x|       4 | | x) y cell wdth      |  dely |.161E-03
7)  # of y filt cells|nfil_y|       0 | | x) c cell wdth      |  delc |.000E+00
8)  # of c filt cells|nfil_c|       0 | | x) pleat width      |  wd   |.805E-03
9)  up expans coeff  |  eta |    1.000 | | x) total flow lgth  | flgth|.247E-01
10) down expans coef| zeta |     1.000 | | x) filt hts upstrm  | htup |    .892 |
11) max # of iter    |jcntmx|       25 | | x) filt hts dnstrm  |htdown|   1.226 |
12) convergence crit| epsi |.100E-02 | | x) est iter runtime |estime|.149E+02 |
13) x inlet veloc    | uin !    3.000 | | x) est max runtime  | estot|.372E+03 !
| ------------------------------------------------------------------------------
|                              Flow Parameters
| ------------------------------------------------------------------------------
14) kin. visc'ty     |  nu  |.151E-04 | 17) x permeability  :  K_x |.780E-10 ;
15) upstrm flux coef| alpha|    1.000 | 18) y permeability  |  K_y |.780E-10 '
16) turb coeff       | gamma|     .098 | 19) x inertia factor|  b_x |.680E+05 :
|                                      | 20) y inertia factor|  b_y |.680E+05 '
| ------------------------------------------------------------------------------
| Reached Convergence Criterion?         Yes.            No. of iter =  11    |
| Upstream Pressure =       .62404E+03 Pa                                      |
| ------------------------------------------------------------------------------
```

Table 3.3 Input summary for a 10° pleat, 8 mm high.
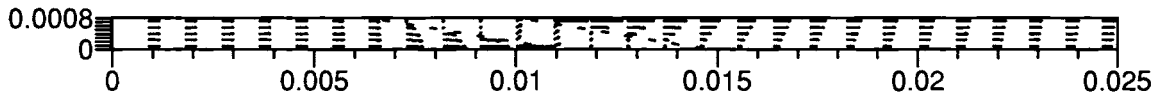
Fig. 3.3(a) Full and proportional flowfield, linear-scaled vectors.
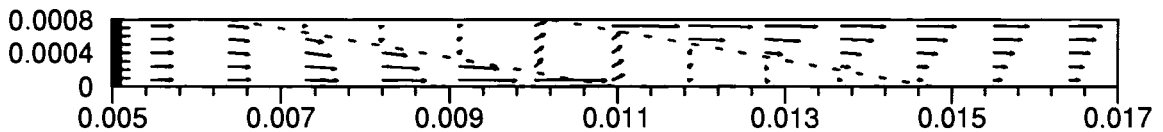
Fig. 3.3(b) Pruned and proportional flowfield, linear-scaled vectors.
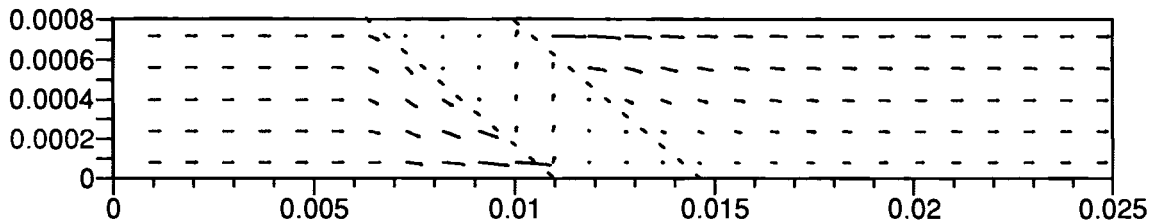
Fig. 3.3(c) Full and expanded flowfield [y-weighted 500%], linear-scaled vectors.

Figs. 3.3 Vector flowfields for 10° pleat, 8 mm high.

```
 ------------------------------------------------------------------------
| ---------------------------------------------------------------------- |
|    Pleat Shape:  Triangular      Parameters in meters, degrees, seconds |
| ---------------------------------------------------------------------- |
|   Base Geometry Data            |   Derived Geometry Data              |
| 1) pleat height    |   ht  |.273E-01 | x) # cells in x dir : ibar :    27 .
| 2) pleat media width|  tp  |.635E-03 | x) # cells in y dir : jbar :     5
| 3) pleat angle     |thetad|  3.000   | x) # x-cells to filt: icell,     9
| 4) rel # cell upstrm|  cup |   .900  | x) # y-cells to filt: jcell:     0
| 5) rel # cell dnstrm| cdown|  1.200  | x) x cell wdth      | delx |.303E-02
| 6) # of x filt cells|nfil_x|    4    | x) y cell wdth      | dely |.159E-03
| 7) # of y filt cells|nfil_y|    0    | x) c cell wdth      | delc |.000E+00
| 8) # of c filt cells|nfil_c|    0    | x) pleat width      | wd   |.795E-03
| 9) up expans coeff  | eta  |  1.000  | x) total flow lgth  | flgth|.818E-01
| 10) down expans coef| zeta |  1.000  | x) filt hts upstrm  | htup |   .809
| 11) max # of iter   |jcntmx|   25    | x) filt hts dnstrm  |htdown|  1.112
| 12) convergence crit| epsi |.100E-02 | x) est iter runtime |estime|.149E+02
| 13) x inlet veloc   | uin  |  3.000  | x) est max runtime  . estot|.372E+03 |
| ---------------------------------------------------------------------- |
|                         Flow Parameters                                |
| ---------------------------------------------------------------------- |
| 14) kin. visc'ty    |  nu  |.151E-04 | 17) x permeability : K_x |.780E-10 |
| 15) upstrm flux coef| alpha|  1.000  | 18) y permeability : K_y |.780E-10 |
| 16) turb coeff      | gamma|   .098  | 19) x inertia factor| b_x |.680E+05 |
|                                      | 20) y inertia factor| b_y |.680E+05 |
| ---------------------------------------------------------------------- |
| Reached Convergence Criterion?       Yes.          No. of iter =   6   |
| Upstream Pressure =    .14310E+04 Pa                                   |
| ---------------------------------------------------------------------- |
```

Table 3.4 Input summary for a 3° pleat, 3 cm high.
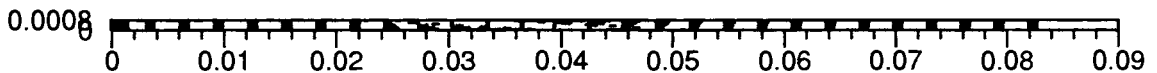
Fig. 3.4(a) Full and proportional flowfield, linear-scaled vectors.
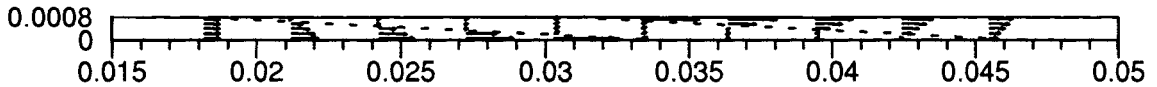
Fig. 3.4(b) Pruned and proportional flowfield, linear-scaled vectors.
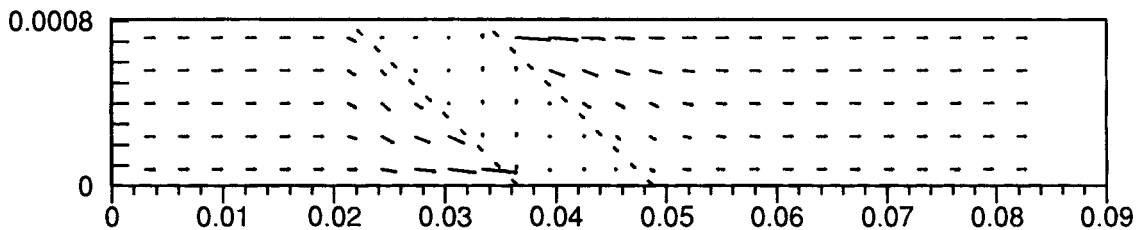
Fig. 3.4(c) Full and expanded flowfield [y-weighted 1600%], linear-scaled vectors.
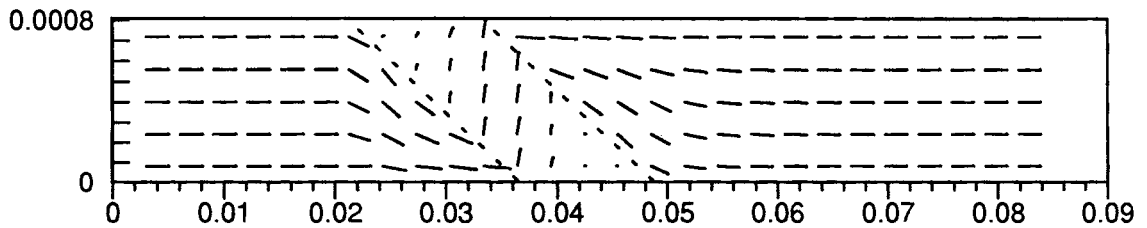
Fig. 3.4(d) Full and expanded flowfield [y-weighted 1600%], log-scaled vectors.

Figs. 3.4 Vector flowfields for 3° pleat, 3 cm high.

The significance of the results is discussed in chapter 4. The examples of a 45° and 3° pleat represent the extremes to be observed. Note that the height of the 45° example is significantly less than that of the 3° pleat. This is because the x cell dimension (*delx*) is set by the pleat thickness (*tp*) and the prescribed fineness (*nfil_x*), and then since the cells must align diagonally to fit the prescribed pleat angle, the y cell dimension *dely* is set by the angle (θ_Δ). If, from this, *dely* turns out to be 0.1mm, and a 45°, 3 cm high pleat is sought, 300 cells would be needed lengthwise and widthwise to cover just the pleat region of the flowfield. If *dely* is 0.1 mm, and a 3°, 3 cm high pleat is sought, less than two cells would be needed lengthwise and widthwise to cover the pleat region; by virtue that for the 3° angle, *delx* is 19 times *dely*, and the width of the flowfield would be only 0.2 mm.

One other remark is made about the presentation of the flowfield. With the smaller pleat angles, the flow through the pleats appears rather minimal, and one might wonder how continuity is maintained. With the smaller pleats the cells are much longer (flow-wise) than they are wide. Thus only a small degree of cross velocity is necessary to counter a large influx of flow-wise velocity. The magnitude of the continuity error calculated cell-by-cell shown in Table 3.1(b) is typical of all program runs.

3.3 The Upstream Differencing Parameter (α)

The convective terms of the Navier-Stokes equations are translated into FDEs using some proportion of upstream differencing represented by α. The form of upstream differencing has been adapted from the SOLA program [Hirt et al., 1975]. In that CFD code for viscous flow, transient effects were also included, thus making the stability criteria different than those for the present steady-state analysis. However, instability still exists in central-difference representations of convection [Patankar, 1980, p. 83f], and upstream differencing is necessary to maintain stability. Although a thorough stability analysis is not

done here, empirical testing is done over the range of Δx and Δy used in practice. Any

departure away from full upstream differencing brings on the likelihood of instability.

However, although full upstream differencing is always stable, it is not always accurate.
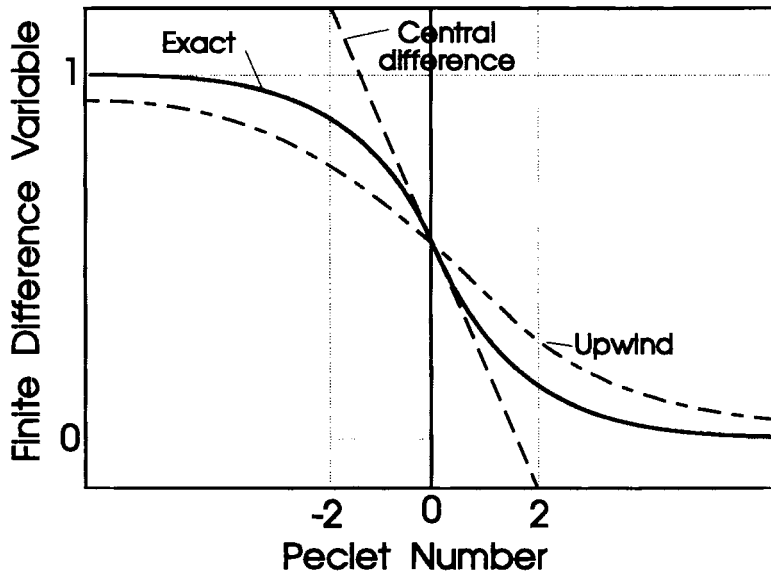
Fig. 3.5   Solution of 1-d convection-diffusion problem with uniform grid and solutions east and west of the variable equal to 1 and 0 respectively, adapted from Patankar [1980, p. 96].

Patankar shows results using different differencing schemes [Patankar, 1980, p. 96] (Fig. 3.5). From this it can be seen what the upstream flux coefficient is doing -- essentially providing an approximation of the exact solution using the central and upstream differenced results.

To get a clearer view of the effect of the upstream differencing parameter for this CFD code, some runs are made with varying values of α. If α is set at zero, correspondent to full central differencing for the convective terms, the flowfield is as follows.
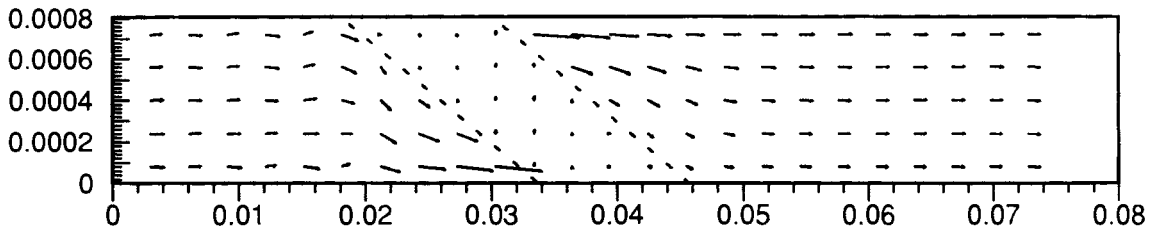
Fig. 3.6(a) Flow through 3° pleat as in Fig. 4.4, α *= 0*
(full and expanded [y-weighted 1600%], linear-scale vectors).

The instability can be seen in the periodic waving of the vectors upstream of the pleat. The instability is even clearer with the solution of the 45° pleat found with full central differencing.
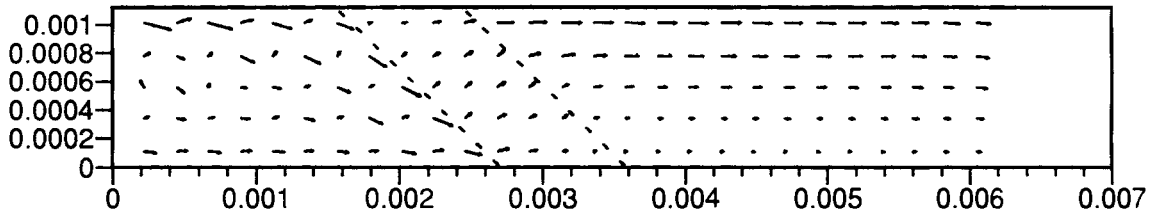
Fig. 3.6(b) Flow through 45° pleat as in Fig. 4.2, α *= 0*
(full and proportional, linear-scale vectors).

As α is increased, the magnitude of the instability is less discernible. It can best be observed by viewing the numbers themselves. Below are the *u*-velocity values for the cells upstream of the pleat for varying values of α for the 3° pleat.

56

α = 0

```
---------------------------------------------------------------------
Reached Convergence Criterion?      Yes.          No. of iter = ..
Upstream Pressure =      .13506E+04 Pa
---------------------------------------------------------------------

--------------
  U velocity
     1      2      3      4      5      6      7      8      9     10     11     12     13     14     15     16
 7 3.000  2.709  3.182  2.596  3.458  2.221  4.131   .020   .042   .155   .870 .1.400  9.340  7.095  5.697  4.428
 6 3.000  2.709  3.182  2.596  3.458  2.221  4.131\  .020   .042   .155   .870\11.400  9.340  7.095  5.697  4.427
 5 3.000  2.830  3.110  2.770  3.276  2.579  3.687  2.075\  .042   .153   .845   .866\ 5.343  5.169  4.587  3.784
 4 3.000  3.003  3.002  3.008  3.009  3.033  3.024  3.549  3.119\  .149   .821   .888   .102\ 2.717  3.141  2.976
 3 3.000  3.172  2.891  3.235  2.731  3.447  2.336  4.465  5.302  5.596\  .798   .911   .106   .010\ 1.576  2.195
 2 3.000  3.286  2.814  3.390  2.525  3.721  1.821  4.891  6.495  8.947 11.667\  .936   .109   .010  -.001\ 1.625
 1 3.000  3.286  2.814  3.390  2.525  3.721  1.821  4.891  6.495  8.947 11.667   .936   .109   .010  -.001  1.625
```

α = 0.5

```
|--------------------------------------------------------------------|
| Reached Convergence Criterion?      Yes.          No. of iter =   7  |
| Upstream Pressure =      .13914E+04 Pa                              |
|--------------------------------------------------------------------|

--------------
  U velocity
     1      2      3      4      5      6      7      8      9     10     11     12     13     14     15     16
 7 3.000  2.999  3.002  2.992  3.030  2.883  3.427   .020   .041   .156   .896 11.302  9.330  7.126  5.718  4.507
 6 3.000  2.999  3.002  2.992  3.030  2.883  3.427\  .020   .041   .156   .896\11.302  9.330  7.126  5.718  4.507
 5 3.000  3.000  3.001  2.995  3.019  2.930  3.282  2.082\  .041   .154   .871   .891\ 5.342  5.149  4.573  3.817
 4 3.000  3.000  3.000  3.000  3.000  3.001  3.030  3.525  3.095\  .150   .847   .912   .106\ 2.706  3.126  2.963
 3 3.000  3.000  2.999  3.005  2.982  3.070  2.744  4.447  5.264  5.577\  .825   .935   .110   .009\ 1.584  2.150
 2 3.000  3.001  2.998  3.008  2.969  3.116  2.517  4.926  6.558  8.963 11.561\  .960   .112   .009  -.001\ 1.563
 1 3.000  3.001  2.998  3.008  2.969  3.116  2.517  4.926  6.558  8.963 11.561   .960   .112   .009  -.001  1.563
```

α = 0.8

```
|--------------------------------------------------------------------|
| Reached Convergence Criterion?      Yes.          No. of iter =   6  |
| Upstream Pressure =      .14153E+04 Pa                              |
|--------------------------------------------------------------------|

--------------
  U velocity
     1      2      3      4      5      6      7      8      9     10     11     12     13     14     15     16
 7 3.000  3.000  3.000  3.000  3.001  2.986  3.146   .020   .041   .156   .911 11.245  9.325  7.143  5.733  4.551
 6 3.000  3.000  3.000  3.000  3.001  2.986  3.146\  .020   .041   .156   .911\11.245  9.325  7.143  5.733  4.551
 5 3.000  3.000  3.000  3.000  3.001  2.991  3.099  2.072\  .041   .154   .886   .906\ 5.341  5.139  4.566  3.833
 4 3.000  3.000  3.000  3.000  3.000  3.000  3.013  3.499  3.081\  .151   .863   .927   .108\ 2.700  3.116  2.956
 3 3.000  3.000  3.000  3.000  2.999  3.008  2.912  4.439  5.245  5.568\  .841   .949   .112   .009\ 1.586  2.128
 2 3.000  3.000  3.000  3.000  2.999  3.015  2.830  4.970  6.592  8.971 11.499\  .974   .115   .009  -.001\ 1.532
 1 3.000  3.000  3.000  3.000  2.999  3.015  2.830  4.970  6.592  8.971 11.499   .974   .115   .009  -.001  1.532
```

α = 0.9

```
|--------------------------------------------------------------------|
| Reached Convergence Criterion?      Yes.          No. of iter =   6  |
| Upstream Pressure =      .14232E+04 Pa                              |
|--------------------------------------------------------------------|

--------------
  U velocity
     1      2      3      4      5      6      7      8      9     10     11     12     13     14     15     16
 7 3.000  3.000  3.000  3.000  3.000  2.997  3.067   .020   .041   .157   .916 11.226  9.323  7.148  5.738  4.564
 6 3.000  3.000  3.000  3.000  3.000  2.997  3.067\  .020   .041   .157   .916\11.226  9.323  7.148  5.738  4.564
 5 3.000  3.000  3.000  3.000  3.000  2.998  3.045  2.068\  .041   .155   .891   .911\ 5.340  5.136  4.564  3.838
 4 3.000  3.000  3.000  3.000  3.000  3.000  3.000  3.490  3.077\  .151   .868   .931   .108\ 2.699  3.113  2.954
 3 3.000  3.000  3.000  3.000  3.000  3.002  2.960  4.437  5.239  5.565\  .846   .954   .113   .009\ 1.586  2.121
 2 3.000  3.000  3.000  3.000  3.000  3.003  2.922  4.986  6.603  8.973 11.479\  .978   .115   .009  -.001\ 1.523
 1 3.000  3.000  3.000  3.000  3.000  3.003  2.922  4.986  6.603  8.973 11.479   .978   .115   .009  -.001  1.523
```

α = 1.0

```
|--------------------------------------------------------------------|
| Reached Convergence Criterion?      Yes.          No. of iter =   6  |
| Upstream Pressure =      .14310E+04 Pa                              |
|--------------------------------------------------------------------|

--------------
  U velocity
     1      2      3      4      5      6      7      8      9     10     11     12     13     14     15     16
 7 3.000  3.000  3.000  3.000  3.000  3.000  2.993   .020   .041   .157   .920 11.208  9.321  7.152  5.743  4.577
 6 3.000  3.000  3.000  3.000  3.000  3.000  2.993\  .020   .041   .157   .920\11.208  9.321  7.152  5.743  4.577
 5 3.000  3.000  3.000  3.000  3.000  3.000  2.994  2.063\  .041   .155   .896   .916\ 5.340  5.133  4.562  3.842
 4 3.000  3.000  3.000  3.000  3.000  3.000  2.999  3.480  3.072\  .151   .873   .936   .109\ 2.697  3.110  2.952
 3 3.000  3.000  3.000  3.000  3.000  3.000  3.005  4.436  5.233  5.562\  .851   .958   .114   .009\ 1.586  2.115
 2 3.000  3.000  3.000  3.000  3.000  3.000  3.009  5.002  6.614  8.976 11.459\  .983   .116   .009  -.001\ 1.514
 1 3.000  3.000  3.000  3.000  3.000  3.000  3.009  5.002  6.614  8.976 11.459   .983   .116   .009  -.001  1.514
```

Table 3.5(a)   Effect of α   on program stability, 3° pleat.

Note that there is instability even when α is set as high as 0.90 (see columns 6 & 7).

For a 45° pleat, the instability is greater at low α's, but seemingly entirely damped out at an α of only 0.50.

α = 0

```
|----------------------------------------------------------------------|
! Reached Convergence Criterion?        No.          Final epsi =-.61E-01!
! Upstream Pressure =      .48964E+03 Pa                                ;
|----------------------------------------------------------------------!

   --------------
   U velocity
       1      2      3      4      5      6      7      8      9     10     11     12     13     14     15     16
  7  3.000  8.722  4.438  7.624  3.615  6.020  2.429  4.903   .830  1.505  2.228  3.184  5.042  5.457  6.070  6.012
  6  3.000  8.722  4.438  7.624  3.615  6.020  2.429  4.903\  .830  1.505  2.228  3.184\ 5.042  5.457  6.070  6.012
  5  3.000  2.020  2.351  1.339  4.033  1.213  5.000   .921  5.416\ 1.375  1.947  2.372  2.131\ 3.403  3.990  4.189
  4  3.000 -1.181  2.353   .338  1.587  2.603  1.622  4.032  1.593  5.839\ 1.765  2.105  2.136  1.847\ 1.978  2.489
  3  3.000  1.506  2.651  1.962  2.767  1.712  3.204  1.695  4.368  2.038  5.919\ 2.084  2.407  2.003  1.425\ 1.510
  2  3.000  3.934  3.206  3.737  2.998  3.453  2.744  3.449  2.793  4.243  3.141  5.256\ 3.283  2.290  1.537   .800\
  1  3.000  3.934  3.206  3.737  2.998  3.453  2.744  3.449  2.793  4.243  3.141  5.256  3.283  2.290  1.537   .800
```

α = 0.5

```
|----------------------------------------------------------------------|
! Reached Convergence Criterion?        No.          Final epsi =-.14E-02!
! Upstream Pressure =      .49242E+03 Pa                                !
|----------------------------------------------------------------------!

   --------------
   U velocity
       1      2      3      4      5      6      7      8      9     10     11     12     13     14     15     16
  7  3.000  2.996  2.987  2.970  2.928  2.878  2.665  2.614   .833  1.512  2.231  3.177  5.005  5.683  5.972  6.078
  6  3.000  2.996  2.987  2.970  2.928  2.878  2.665  2.614\  .833  1.512  2.231  3.177\ 5.005  5.683  5.972  6.078
  5  3.000  2.998  2.992  2.981  2.965  2.921  2.919  2.686  3.582\ 1.387  1.958  2.384  2.164\ 3.186  3.799  4.134
  4  3.000  3.000  3.000  3.001  3.005  3.009  3.050  3.068  3.410  4.362\ 1.783  2.119  2.148  1.841\ 2.263  2.518
  3  3.000  3.002  3.008  3.019  3.041  3.077  3.157  3.269  3.570  3.806  4.864\ 2.100  2.411  2.003  1.429\ 1.468
  2  3.000  3.004  3.012  3.029  3.060  3.115  3.210  3.363  3.604  3.934  4.163  5.220\ 3.271  2.286  1.537   .801\
  1  3.000  3.004  3.012  3.029  3.060  3.115  3.210  3.363  3.604  3.934  4.163  5.220  3.271  2.286  1.537   .801
```

α = 0.8

```
|----------------------------------------------------------------------|
| Reached Convergence Criterion?        Yes.          No. of iter =  22  |
| Upstream Pressure =      .49494E+03 Pa                                 |
|----------------------------------------------------------------------|

   --------------
   U velocity
       1      2      3      4      5      6      7      8      9     10     11     12     13     14     15     16
  7  3.000  2.995  2.984  2.961  2.918  2.833  2.657  2.305   .832  1.513  2.232  3.174  4.992  5.673  5.963  6.069
  6  3.000  2.995  2.984  2.961  2.918  2.833  2.657  2.305\  .832  1.513  2.232  3.174\ 4.992  5.673  5.963  6.069
  5  3.000  2.997  2.991  2.978  2.955  2.915  2.854  2.772  3.267\ 1.389  1.961  2.388  2.174\ 3.191  3.791  4.118
  4  3.000  3.000  3.001  3.002  3.005  3.016  3.050  3.140  3.529  4.020\ 1.789  2.125  2.153  1.845\ 2.278  2.529
  3  3.000  3.003  3.010  3.023  3.049  3.097  3.186  3.347  3.655  4.017  4.558\ 2.109  2.414  2.005  1.430\ 1.481
  2  3.000  3.005  3.015  3.036  3.073  3.139  3.253  3.437  3.717  4.062  4.460  5.204\ 3.267  2.286  1.538   .803\
  1  3.000  3.005  3.015  3.036  3.073  3.139  3.253  3.437  3.717  4.062  4.460  5.204  3.267  2.286  1.538   .803
```

α = 1.0

```
|----------------------------------------------------------------------|
| Reached Convergence Criterion?        Yes.          No. of iter =  20  |
| Upstream Pressure =      .49656E+03 Pa                                 |
|----------------------------------------------------------------------|

   --------------
   U velocity
       1      2      3      4      5      6      7      8      9     10     11     12     13     14     15     16
  7  3.000  2.995  2.982  2.957  2.908  2.813  2.617  2.169   .833  1.514  2.232  3.172  4.982  5.665  5.957  6.063
  6  3.000  2.995  2.982  2.957  2.908  2.813  2.617  2.169\  .833  1.514  2.232  3.172\ 4.982  5.665  5.957  6.063
  5  3.000  2.997  2.989  2.975  2.949  2.904  2.833  2.770  3.121\ 1.392  1.963  2.390  2.180\ 3.194  3.787  4.110
  4  3.000  3.000  3.001  3.002  3.006  3.018  3.056  3.174  3.531  3.843\ 1.792  2.128  2.157  1.848\ 2.286  2.535
  3  3.000  3.003  3.011  3.026  3.055  3.109  3.209  3.395  3.716  4.074  4.398\ 2.115  2.416  2.007  1.431\ 1.489
  2  3.000  3.005  3.017  3.040  3.082  3.157  3.284  3.492  3.799  4.177  4.614  5.194\ 3.265  2.286  1.539   .803\
  1  3.000  3.005  3.017  3.040  3.082  3.157  3.284  3.492  3.799  4.177  4.614  5.194  3.265  2.286  1.539   .803
```

Table 3.5(b)   Effect of α   on program stability, 45° pleat.

58

In order to ensure stability under all configurations, α is set at unity consistently. It is borne in mind that this could produce excessive damping under certain conditions.

3.4 The Mixing Length Constant (γ)

The model used to determine the turbulent stresses calculates a mixing length that is a direct function of the flow half-width (d) (see Section 2.2.2).

$$-\overline{uv} = l_{mix}^2 \left| \frac{dU}{dy} \right| \frac{dU}{dy} \quad \text{where } l_{mix} = \gamma \cdot d \quad \text{and } d \equiv \text{flow half-width}$$
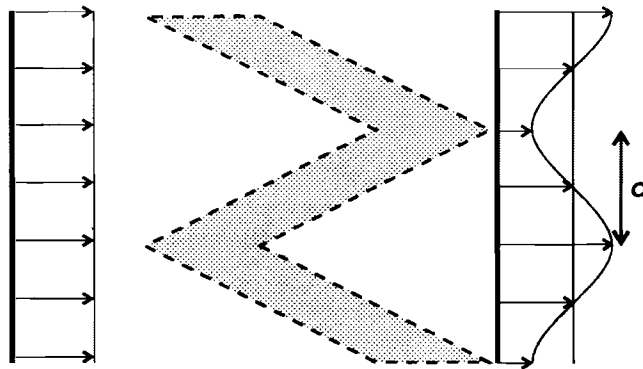
Fig. 3.7   Flow downstream of filter.

This turbulence model is based on an idealized jet flow (Fig. 2.4). There are several conditions in the ideal model that are not met in the flow conditions downstream of the filter.

- The jet is not surrounded by non-turbulent flow.

- Its width does not spread moving downstream.

- Velocities within the jet stream range above and below the inlet flow velocity, rather than being solely greater or less than an ambient velocity.

- The flow is not a fully-developed self-preserving flow.

The main divergence with the idealized model is that instead of a single jet in an ambient fluid, there are a series of jet flows lined up beside one another; hence the jets are unable to expand widthwise. In the self-preserving flow of an expanding jet, the effect of width expansion (see Eq. 2.14) is to increase the magnitude of the turbulent stress moving downstream. The effect of containing the width of the jet downstream is therefore to decrease the turbulent stresses downstream. This makes sense as the stresses would be expected to lessen as the velocity gradient weakens.

So, although the model does not simulate the exact conditions, it is still reasonable to apply this algebraic model because:
- It is still a jet-like flow.
- The mixing length is still assumed to be based on a direct relation to the jet half-width.
- The magnitude of the turbulence constant (γ) will still be essentially the same. Even for widely varying types of free-shear flows, the values of γ are all of the same magnitude, from 0.071 for mixing layers (which can produce the largest velocity gradients) to 0.180 for wakes (which produce small velocity gradients). The value Wilcox [1993] suggests for a plane jet is

$$\gamma = 0.098 \tag{3-1}$$

The main consequence of turbulent stress on the mean flow is an increased viscous effect that acts to flatten out the velocity profile. The effect can be seen in the comparison of the flowfield for the 45° pleat derived assuming the following turbulent stress conditions: laminar flow, our modeled turbulence coefficient, and double that value.
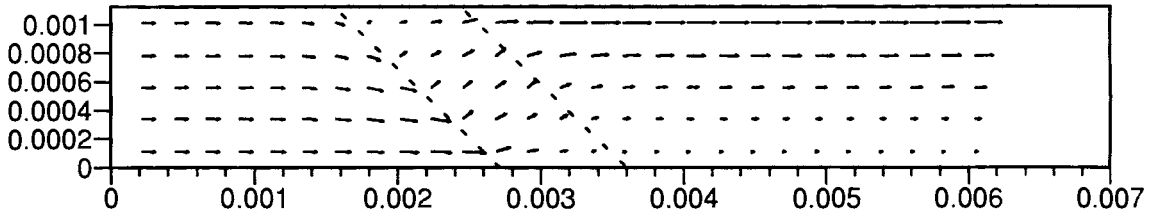
Fig. 3.8(a)   Flowfield for γ   *= 0 (full and proportional, linear-scale vectors).*
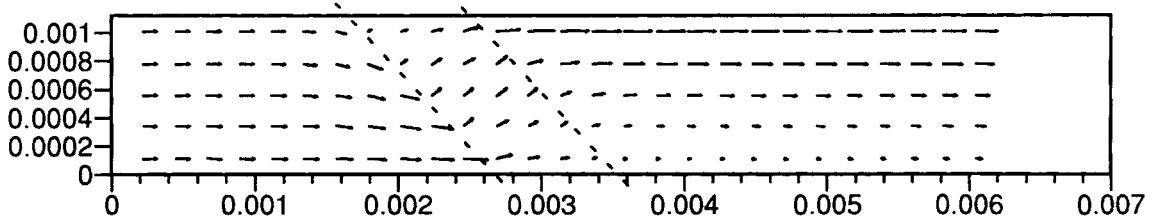
Fig. 3.8(b)   Flowfield for γ   *= 0.098 (full and proportional, linear-scale vectors).*
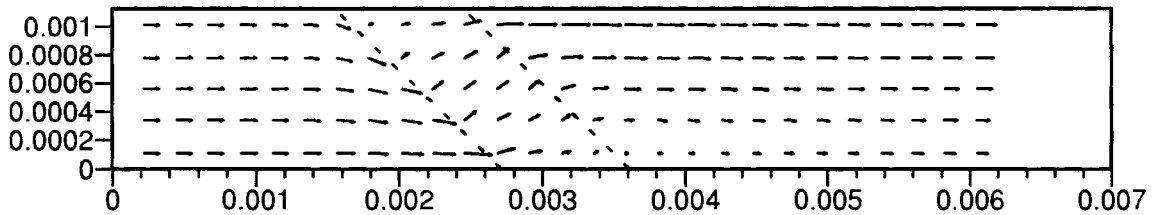
Fig. 3.8(c)   Flowfield for γ   *= 0.196 (full and proportional, linear-scale vectors).*

Figs. 3.8   The effect of γ   *on the downstream flow.*

One side effect of applying this turbulence model in all non-media regions of the flowfield

is that it is operative in the crevasse of the pleat as well. This increases the viscous and

turbulent drag within the crevasse even though the region may be prohibitively small for

the development of turbulence. One solution would be to turn the turbulence model off

within the pleat crevasse. However, this was not done here. The effects of this

phenomenon are noted in Section 4.4.

61

3.5 Upstream and Downstream Coverage (*htup* and *htdown*)

The remaining parameters examined affect the run time of the program. As the portion of the flowfield that is of particular interest is the flow immediately entering, within, and exiting the filter media, the flow far upstream and downstream of the filter is only of interest insofar as it affects the filter region.

The flow upstream of the filter is affected by the left-hand boundary condition, a uniform inlet flow. If this boundary condition is set too close to the filter, an artificially large velocity gradient is created. Ideally, there should be enough distance between the left-hand boundary and the filter so that the left-hand boundary condition has no effect on the gradient.

As this effect is difficult to distinguish in a vector plot, the values of the *u*-velocity before the pleat are shown for two values of *htup* (0.5 and 1.63) for a 45° pleat (Table 3.6). The numbers are aligned so that the filter regions coincide.

As can be observed, a very short run-up (*htup* = 0.50) to the filter forces the velocity gradient; this has some effect on the intra-filter flow as well. With a long run-up (*htup* = 1.63) to the filter, the velocity gradient develops naturally.

On the downstream side, upstream differencing used in the finite difference approximation for the convective terms limits the influence of downstream phenomena on upstream locations. The right-hand boundary condition assumes the velocity gradient has disappeared before reaching the exit. However, this is not true unless a very lengthy exit length is used. If a gradient does actually exist at the exit, the continuitive outflow condition will artificially force the gradient at the exit.

The effect of this artificial condition can be observed by comparing a flowfield solved for different values of *htdown* (Table 3.7). It can be seen that the exit boundary condition does affect the flowfield near the exit, but barely affects the flow near and within the filter.

htup = 0.50:   *htup = 1.63:*

```
|------------------------------------------------|
| Reached Convergence Criterion?        Yes.     |
| No. of iter =  20                              |
| Upstream Pressure =      .49653E+03 Pa         |
|------------------------------------------------|
```

    U velocity

	1	2	3	4
7	3.000	3.000	2.999	2.998
6	3.000	3.000	2.999	2.998
5	3.000	3.000	2.999	2.999
4	3.000	3.000	3.000	3.000
3	3.000	3.000	3.001	3.001
2	3.000	3.000	3.001	3.002
1	3.000	3.000	3.001	3.002

	5	6	7	8	9	10
7	2.996	2.992	2.985	2.971	2.946	2.897
6	2.996	2.992	2.985	2.971	2.946	2.897
5	2.997	2.995	2.991	2.983	2.968	2.942
4	3.000	3.000	3.000	3.001	3.002	3.006
3	3.003	3.005	3.009	3.018	3.033	3.062
2	3.004	3.008	3.015	3.028	3.051	3.093
1	3.004	3.008	3.015	3.028	3.051	3.093

```
|------------------------------------------------|
| Reached Convergence Criterion?        Yes.     |
| | No. of iter =  20                            |
| Upstream Pressure =      .49755E+03 Pa         |
|------------------------------------------------|
```

    U velocity

	1	2	3	4	5	6
7	3.000	2.821	2.325	.843	1.518	2.234
6	3.000	2.821	2.325\	.843	1.518	2.234
5	3.000	2.948	2.887	3.244\	1.393	1.965
4	3.000	3.047	3.191	3.599	3.934\	1.793
3	3.000	3.088	3.292	3.666	4.075	4.435
2	3.000	3.096	3.305	3.648	4.079	4.573
1	3.000	3.096	3.305	3.648	4.079	4.573

	7	8	9	10	11	12
7	3.174	4.984	5.667	5.958	6.064	6.062
6	3.174\	4.984	5.667	5.958	6.064	6.062
5	2.391	2.180\	3.194	3.787	4.110	4.282
4	2.129	2.157	1.847\	2.286	2.535	2.667
3\	2.115	2.416	2.006	1.431\	1.488	1.452
2	5.192\	3.263	2.285	1.538	.803\	.537
1	5.192	3.263	2.285	1.538	.803	.537

	11	12	13	14	15	16
7	2.802	2.609	2.163	.832	1.514	2.232
6	2.802	2.609	2.163\	.832	1.514	2.232
5	2.898	2.827	2.764	3.116\	1.391	1.963
4	3.018	3.055	3.173	3.528	3.840\	1.792
3	3.115	3.215	3.399	3.718	4.074	4.397
2	3.167	3.294	3.500	3.806	4.182	4.616
1	3.167	3.294	3.500	3.806	4.182	4.616

	17	18	19	20	21	22
7	3.172	4.982	5.665	5.957	6.063	6.061
6	3.172\	4.982	5.665	5.957	6.063	6.061
5	2.390	2.180\	3.194	3.787	4.110	4.282
4	2.128	2.157	1.848\	2.286	2.535	2.667
3\	2.115	2.416	2.007	1.431\	1.489	1.452
2	5.195\	3.265	2.286	1.539	.803\	.538
1	5.195	3.265	2.286	1.539	.803	.538

Table 3.6 The effect of htup *on the upstream flow.*

htdown = 0.88

U velocity

```
       1      2      3      4      5      6
7   3.000  2.995  2.982  2.957  2.908  2.813
6   3.000  2.995  2.982  2.957  2.908  2.813
5   3.000  2.997  2.989  2.975  2.949  2.904
4   3.000  3.000  3.001  3.002  3.006  3.018
3   3.000  3.003  3.011  3.026  3.055  3.109
2   3.000  3.005  3.017  3.040  3.082  3.157
1   3.000  3.005  3.017  3.040  3.082  3.157

       7      8      9     10     11     12
7   2.617  2.169   .833  1.514  2.232  3.172
6   2.617  2.169\  .833  1.514  2.232  3.172
5   2.833  2.770  3.121\ 1.392  1.963  2.390
4   3.056  3.174  3.531  3.843\ 1.792  2.128
3   3.209  3.395  3.716  4.074  4.398\ 2.115
2   3.284  3.492  3.799  4.177  4.614  5.194
1   3.284  3.492  3.799  4.177  4.614  5.194

       13     14     15     16     17     18
7   4.982  5.665  5.957  6.062  6.056  5.983
6\  4.982  5.665  5.957  6.062  6.056  5.983
5   2.180\ 3.194  3.787  4.110  4.282  4.363
4   2.157  1.848\ 2.286  2.536  2.668  2.755
3   2.416  2.007  1.431\ 1.490  1.454  1.436
2\  3.265  2.286  1.539   .803\  .539   .463
1   3.265  2.286  1.539   .803   .539   .463

       19     20     21     22     23
7   5.868  5.721  5.534  5.279  5.279
6   5.868  5.721  5.534  5.279  5.279
5   4.378  4.349  4.288  4.199  4.199
4   2.819  2.866  2.908  2.960  2.960
3   1.464  1.530  1.626  1.760  1.760
2    .470   .534   .645   .802   .802
1    .470   .534   .645   .802   .802
```

htdown = 3.38

```
       1      2      3      4      5      6
7   3.000  2.995  2.982  2.957  2.908  2.813
6   3.000  2.995  2.982  2.957  2.908  2.813
5   3.000  2.997  2.989  2.975  2.949  2.904
4   3.000  3.000  3.001  3.002  3.006  3.018
3   3.000  3.003  3.011  3.026  3.055  3.109
2   3.000  3.005  3.017  3.040  3.082  3.157
1   3.000  3.005  3.017  3.040  3.082  3.157

       7      8      9     10     11     12
7   2.617  2.169   .833  1.514  2.232  3.172
6   2.617  2.169\  .833  1.514  2.232  3.172
5   2.833  2.770  3.121\ 1.392  1.963  2.390
4   3.056  3.174  3.531  3.843\ 1.792  2.128
3   3.209  3.395  3.716  4.074  4.398\ 2.115
2   3.284  3.492  3.799  4.177  4.614  5.194
1   3.284  3.492  3.799  4.177  4.614  5.194

       13     14     15     16     17     18
7   4.982  5.665  5.957  6.063  6.061  5.995
6\  4.982  5.665  5.957  6.063  6.061  5.995
5   2.180\ 3.194  3.787  4.110  4.282  4.366
4   2.157  1.848\ 2.286  2.535  2.667  2.749
3   2.416  2.007  1.431\ 1.489  1.452  1.431
2\  3.265  2.286  1.539   .803\  .538   .459
1   3.265  2.286  1.539   .803   .538   .459

       19     20     21     22     23     24
7   5.896  5.781  5.660  5.538  5.420  5.308
6   5.896  5.781  5.660  5.538  5.420  5.308
5   4.388  4.373  4.338  4.293  4.243  4.192
4   2.809  2.849  2.875  2.892  2.905  2.914
3   1.448  1.493  1.550  1.612  1.673  1.732
2    .459   .504   .577   .665   .759   .853
1    .459   .504   .577   .665   .759   .853

       25     26     27     28     29     30
7   5.202  5.103  5.010  4.925  4.845  4.771
6   5.202  5.103  5.010  4.925  4.845  4.771
5   4.143  4.096  4.051  4.009  3.970  3.934
4   2.922  2.928  2.934  2.939  2.943  2.948
3   1.789  1.842  1.891  1.938  1.981  2.021
2    .945  1.031  1.113  1.189  1.261  1.327
1    .945  1.031  1.113  1.189  1.261  1.327

       31     32     33     34     35     36
7   4.702  4.637  4.577  4.521  4.467  4.417
6   4.702  4.637  4.577  4.521  4.467  4.417
5   3.900  3.868  3.838  3.810  3.783  3.758
4   2.951  2.954  2.958  2.960  2.963  2.965
3   2.058  2.093  2.125  2.156  2.185  2.212
2   1.389  1.448  1.502  1.553  1.602  1.648
1   1.389  1.448  1.502  1.553  1.602  1.648

       37     38     39     40     41     42
7   4.369  4.323  4.277  4.229  4.175  4.107
6   4.369  4.323  4.277  4.229  4.175  4.107
5   3.734  3.710  3.687  3.663  3.636  3.606
4   2.968  2.970  2.972  2.975  2.979  2.987
3   2.238  2.263  2.289  2.315  2.345  2.382
2   1.691  1.734  1.775  1.818  1.864  1.917
1   1.691  1.734  1.775  1.818  1.864  1.917

(column 43 = 42)
```

Table 3.7 The effect of htdown *on the downstream flow.*

3.6 The Grid Expansion Coefficients (*eta* and *zeta*)

One theoretically simple method to deal with the entrance and exit boundary conditions is to introduce an expandable grid. As detail becomes less important moving up and downstream of the filter, the cells can be expanded in those directions. In this way, the effect of the boundary conditions at the up- and downstream positions is diminished, while keeping the cell count low. The cell expansions begin at the x-cells two positions upstream and downstream of the pleat.

The initial sample of the 10° pleat (Fig. 3.3) had a long enough run-up to the filter so that the flow could develop naturally from the upstream boundary condition. For comparison, *eta* is increased to 1.2 and *icell* is adjusted (via *cup*) so that the upstream distance (*htup*) is kept nearly the same; so only five upstream cells are used on the right but eight on the left.

eta = 1.00, cup = 0.90, htup = 0.892

```
 U velocity

        1       2       3       4       5       6
 6   3.000   3.000   3.000   3.000   3.000   2.999
 5   3.000   3.000   3.000   3.000   3.000   3.000
 4   3.000   3.000   3.000   3.000   3.000   3.000
 3   3.000   3.000   3.000   3.000   3.000   3.000
 2   3.000   3.000   3.000   3.000   3.000   3.001

        7       8       9      10      11      12
 6   2.992   2.880\   .047    .095    .360   1.490
 5   2.995   2.927   2.392\   .088    .329   1.283
 4   3.000   3.005   3.621   3.390\   .275   1.096
 3   3.005   3.074   4.299   5.207   5.697\   .916
 2   3.008   3.114   4.641   6.220   8.339  10.216

       13      14      15      16      17      18
6\   9.638   9.135   7.566   6.401   5.582   5.029
 5   1.084\  5.025   5.019   4.647   4.289   4.036
 4   1.238    .225\  2.400   2.785   2.859   2.905
 3   1.415    .290    .003\  1.182   1.589   1.882
2\   1.624    .326    .012   -.015\   .681   1.147

       19      20      21      22      23      24
 6   4.642   4.359   4.145   3.979   3.847   3.740
 5   3.854   3.719   3.614   3.531   3.464   3.408
 4   2.935   2.954   2.967   2.975   2.981   2.985
 3   2.090   2.242   2.358   2.448   2.521   2.579
 2   1.479   1.726   1.917   2.067   2.187   2.287
```

eta = 1.24, cup = 0.50, htup = 0.897

```
 U velocity

        1       2       3
 6   3.000   3.000   2.999
 5   3.000   3.000   2.999
 4   3.000   3.000   3.000
 3   3.000   3.000   3.001
 2   3.000   3.000   3.001

        4       5       6       7       8       9
 6   2.986   2.876\   .047    .095    .360   1.490
 5   2.992   2.925   2.391\   .088    .329   1.283
 4   3.000   3.004   3.620   3.390\   .275   1.096
 3   3.008   3.076   4.299   5.207   5.697\   .916
 2   3.014   3.119   4.642   6.221   8.339  10.216

       10      11      12      13      14      15
6\   9.638   9.135   7.566   6.401   5.582   5.029
 5   1.084\  5.025   5.019   4.647   4.289   4.036
 4   1.238    .225\  2.400   2.785   2.859   2.905
 3   1.415    .290    .003\  1.182   1.589   1.882
2\   1.624    .326    .012   -.015\   .681   1.147

       16      17      18      19      20      21
 6   4.642   4.359   4.145   3.979   3.847   3.740
 5   3.854   3.719   3.614   3.531   3.464   3.408
 4   2.935   2.954   2.967   2.975   2.981   2.985
 3   2.090   2.242   2.358   2.448   2.521   2.579
 2   1.479   1.726   1.917   2.067   2.187   2.287
```

Table 3.8 Effect of eta *on the flow upstream of pleat.*

It can be seen that the velocity values entering the pleat and within the pleat are the same.

Likewise, an increased *zeta* grid expansion coefficient downstream can allow the flow profile distance enough to re-establish a flat profile under viscous forces. Note that the expanded grid on the right reaches the standard uniform flow condition.

zeta = 1.0, cdown = 1.2, htdown = 1.226   **zeta = 1.8, cdown = 1.2, htdown = 89.42**

```
    --------------                               --------------
    U velocity                                   U velocity


        1       2       3       4       5       6           1       2       3       4       5       6
    6  3.000   3.000   3.000   3.000   3.000   2.999    6  3.000   3.000   3.000   3.000   3.000   2.999
    5  3.000   3.000   3.000   3.000   3.000   3.000    5  3.000   3.000   3.000   3.000   3.000   3.000
    4  3.000   3.000   3.000   3.000   3.000   3.000    4  3.000   3.000   3.000   3.000   3.000   3.000
    3  3.000   3.000   3.000   3.000   3.000   3.000    3  3.000   3.000   3.000   3.000   3.000   3.000
    2  3.000   3.000   3.000   3.000   3.000   3.001    2  3.000   3.000   3.000   3.000   3.000   3.001

        7       8       9      10      11      12           7       8       9      10      11      12
    6  2.992  2.880\   .047    .095    .360   1.490    6  2.992  2.880\   .047    .095    .360   1.490
    5  2.995   2.927  2.392\   .088    .329   1.283    5  2.995   2.927  2.392\   .088    .329   1.283
    4  3.000   3.005   3.621  3.390\   .275   1.096    4  3.000   3.005   3.621  3.390\   .275   1.096
    3  3.005   3.074   4.299   5.207  5.697\   .916    3  3.005   3.074   4.299   5.207  5.697\   .916
    2  3.008   3.114   4.641   6.220   8.339  10.216   2  3.008   3.114   4.641   6.220   8.339  10.216

       13      14      15      16      17      18          13      14      15      16      17      18
    6\ 9.638   9.135   7.566   6.401   5.582   5.029   6\ 9.638   9.135   7.566   6.400   5.561   4.823
    5  1.084\  5.025   5.019   4.647   4.289   4.036    5  1.084\  5.025   5.019   4.647   4.283   3.945
    4  1.238    .225\  2.400   2.785   2.859   2.905    4  1.238    .225\  2.400   2.786   2.868   2.930
    3  1.415    .290    .003\  1.182   1.589   1.882    3  1.415    .290    .003\  1.183   1.602   1.995
    2\ 1.624    .326    .012  -.015\   .681   1.147    2\ 1.624    .326    .012  -.016\   .685   1.307

       19      20      21      22      23      24          19      20      21      22      23      24
    6  4.642   4.359   4.145   3.979   3.847   3.740    6  4.177   3.684   3.346   3.142   3.043   3.009
    5  3.854   3.719   3.614   3.531   3.464   3.408    5  3.627   3.375   3.196   3.083   3.026   3.005
    4  2.935   2.954   2.967   2.975   2.981   2.985    4  2.964   2.984   2.994   2.998   3.000   3.000
    3  2.090   2.242   2.358   2.448   2.521   2.579    3  2.342   2.611   2.799   2.915   2.974   2.995
    2  1.479   1.726   1.917   2.067   2.187   2.287    2  1.890   2.346   2.665   2.861   2.957   2.991

       25      26      27      28      29                  25      26      27      28      29
    6  3.652   3.578   3.511   3.415   3.415            6  3.001   3.000   3.000   3.000   3.000
    5  3.362   3.323   3.288   3.237   3.237            5  3.001   3.000   3.000   3.000   3.000
    4  2.989   2.991   2.994   2.997   2.997            4  3.000   3.000   3.000   3.000   3.000
    3  2.628   2.669   2.706   2.761   2.761            3  2.999   3.000   3.000   3.000   3.000
    2  2.369   2.439   2.500   2.590   2.590            2  2.999   3.000   3.000   3.000   3.000
    --------------                               --------------
```

Table 3.9 Effect of zeta on the flow downstream of pleat.

3.7 The Pleat Height (*ht*)

As the number of cells widthwise in the grid (*jbar*) for a given pleat angle (θ) and given pleat thickness (*tp*) is a function of the pleat height (*ht*) (see Table 2.1), reducing the pleat

height is one way of reducing the number of grid cells. Obviously, reducing the pleat

height will create a different (higher) pressure drop across the pleat, but it may be an

effective way to observe flow trends just the same. With regard to the latter, the main

concern with this grid reduction is its affect on distinguishing the flow trend through the

section of the filter away from the direct effect of the pleat folds, defined as the *freelength*

of the pleat.

$$freelength = ht - 2tx$$
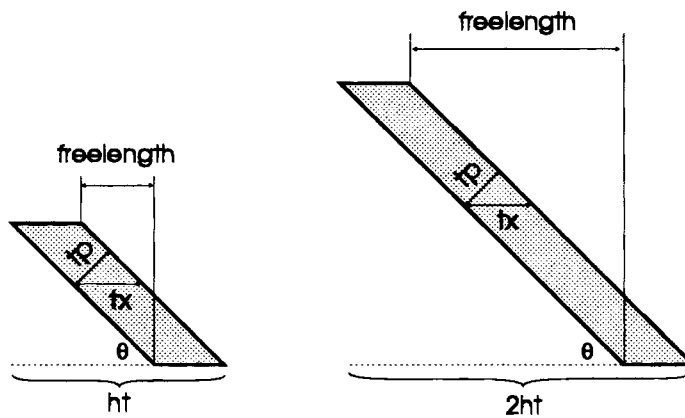
Fig. 3.9   Freelength as related to filter height.

If the height of the pleat is reduced so that *ht* is in the same range as *tx*, then the flowfield

is dominated by the pleat folds. If we are trying to simulate a flow for a pleat of a greater

height, the simulation will not be realistic. In the case of a small pleat angle (i.e. 3°) with

the triangle geometry, the pleat folds do dominate, and this is a realistic portrayal of the

flow. For larger pleat angles, the pleat fold area should not dominate.

So if *ht* ≈ *2tx*, there is little freelength. For comparison, flowfields are obtained for a 45°

pleat with varying pleat heights. Note that the increase in freelength leads to a decrease in

the influence of the pleat folds and an increase in the filter area which in turn decreases the

overall pressure drop.

67
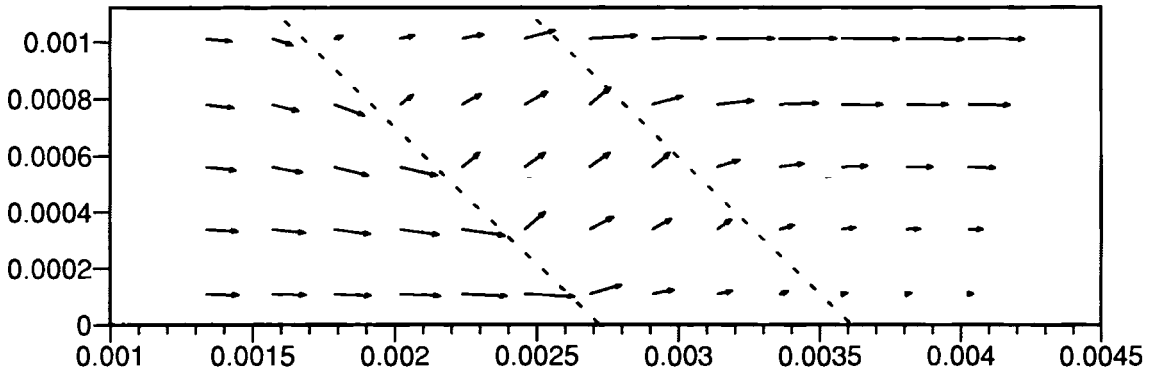
Fig. 3.10(a) ht = 1.79 mm, 0 freelength cells, upstream pressure = 414 Pa.
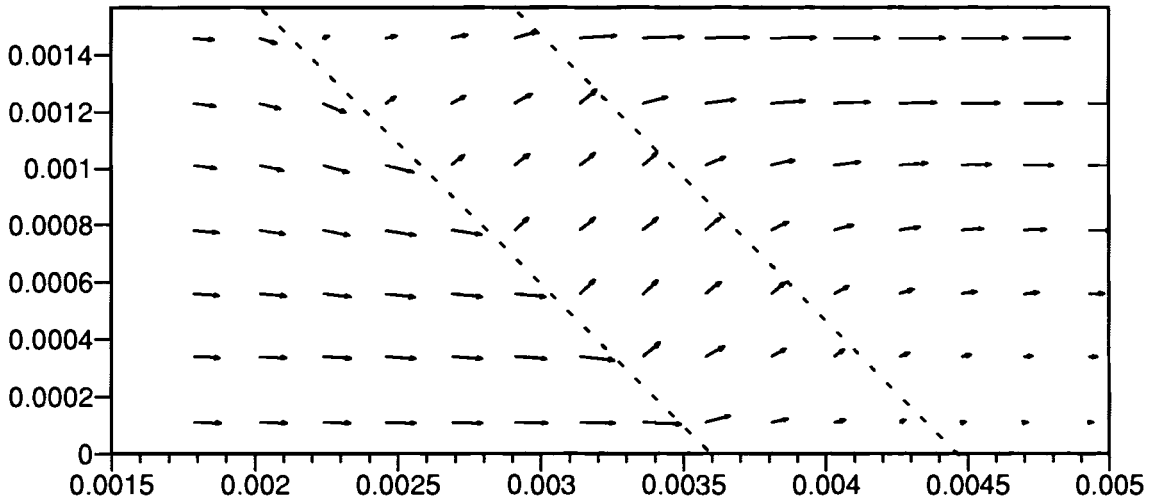
Fig. 3.10(b) ht = 2.50 mm, 2 freelength cells, upstream pressure = 377 Pa.
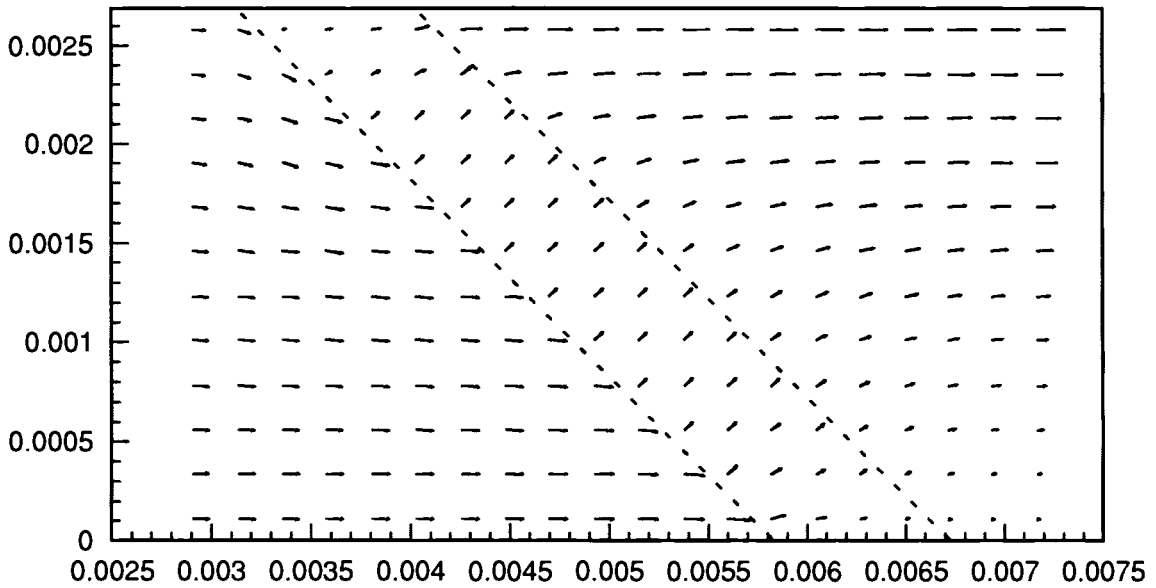
Fig. 3.10(c) ht = 3.60 mm, 7 freelength cells, upstream pressure = 349 Pa.

Figs. 3.10 Effect of pleat height on the flowfield
45° pleat (pruned and proportional, linear-scale vectors).

It can be seen that with no area of the filter outside of the influence of the folds ($ht = 1.79$ mm), there is no region of the flow that orients normal to the pleat. Whereas with a larger freelength ($ht = 2.50$ or 3.60 mm), there is a region of flow oriented normal to the pleat. Judging from the similarities seen in the freelength region of the last two plots, it is suspected that this flow trend continues for greater pleat heights as well.

So the pleat height can be set for a minimal number of freelength cells (2 ~ 4), where the number of freelength cells is given by:

$$\text{\# of freelength cells} = jbar - (nnode + 1)$$

3.8 The Grid Density (*nfil_x*)

Obviously, the denser the grid, the clearer the trends in the flow and the better the approximations to the PDE are, and vice versa. On the other hand, the denser the grid is, the longer a solution will take. Thus the effects of varying the fineness of the grid (determined by *nfil_x* only, for the triangular pleat) are examined to see the consequences.

It is kept in mind that there comes a point where the grid is too fine. Recall that the velocity within the filter represents an area-average macroscopic velocity. The real velocity is related to the macroscopic velocity by media porosity:

$$\vec{V}_{actual} = \frac{\vec{V}_{darcy}}{\delta} \tag{3-2}$$

So if the grid were to shrink below the actual size of the filter pore, the velocities would no longer be describing a true macroscopic velocity for the cell. Thus a minimum cell dimension is specified by the pore size. The average distance between fibers given an

69

average fiber diameter of 39 μm and a porosity of 0.77 [Sabnis, 1993] is about 32 μm,

assuming a face-centered cubic geometry. The average pore size based on the square root

of the permeability of the media, following Bejan [1984], is 9 μm. As the media thickness

considered in this report is only about 600 μm, this would set a limit to the grid detail

specified.

For the 3° pleat, runs are made with the grid fineness varied (Fig. 3.11).
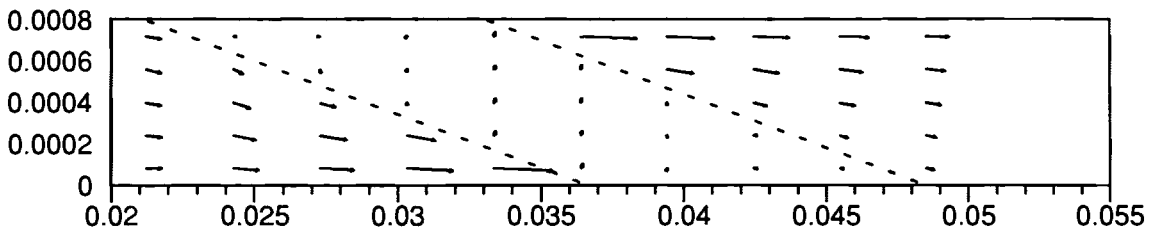
Fig. 3.11(a) nfil_x = 4.
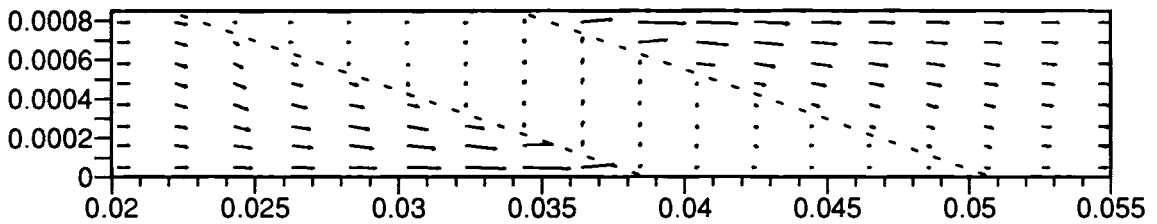
Fig. 3.11(b) nfil_x = 6.
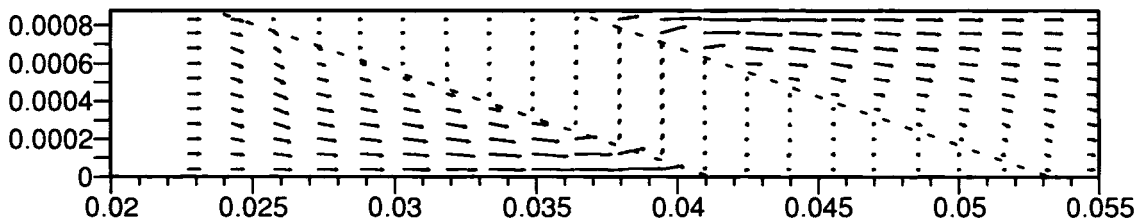
Fig. 3.11(c) nfil_x = 8.

Figs. 3.11 Single geometry with grid fineness varied, 3° pleat
(pruned and expanded [y-weighted ~700%]).

Although the increased resolution reveals greater detail, it does not reveal phenomena

otherwise hidden. The main quality discovered is that the flow is oriented more normal to

70

the filter at the pleat entrance and exit, however this can be ascertained without the finer grid. As the greater detail comes at a high cost (computing time), it is not always sought on its own merit.

3.9 Selecting a Convergence Criterion (*epsi*)

As the solution of the set of non-linear equations is approached *iteratively*, some arbitrary condition of solution convergence must be specified to halt the iteration. Any or all of the three variables being solved (p,u,v) can be used in the convergence criteria. The key standard for the criterion is that it ensures iteration has been carried far enough so that a certain level of precision has been reached and will not be further influenced by continued iteration.

Pressure could be used as a standard for convergence, but determining a standard value is not possible as the magnitude of the pressure would vary greatly with different configurations. However, it is useful when only a pressure drop measurement is sought from running the program. A common value used in this study was 1.0 Pa.

Velocity is simpler to set. The velocity scale is 01 m/s. The precision sought is two orders of magnitude below this, or 0.01 m/s. This is assumed to be sufficiently satisfied when a further iteration produces no greater than a 0.001 m/s change throughout the field (as long as the iteration is still converging).

3.10 The Square Pleat Geometry

As the actual shape of a pleat lies between the simple geometries of a triangle and a square, the latter is modeled as well (see Figs. 1.5, 2.13(b) for geometry). There are

several significant differences with the square pleat. The x and y fineness are specified separately by *nfil_x* and *nfil_y* respectively. There is an additional cell expansion along the median of the pleat (determined by *nfil_c*). The flow contraction is much more sudden, thus the gradient is stronger and requires more distance up- and downstream to reach standard flow conditions (uniform flow).

The main problem that arises with this geometry is instability. There is no boundary condition at the pleat interface (see Section 2.6), so the fluid FDEs and filter FDEs overlap. In the triangular configuration, these contrasting models consistently meet at the same geometric position throughout $(i \pm 1, j \pm 1)$, so any disturbance is damped out. With the square geometry the boundary is approached from different directions. So, especially at the pleat corners, the instability develops uncontrolled. The problem could be resolved with an additional boundary condition at the interface to segregate the regions. However, this has not yet been done in this model.

The instability in the square pleat is inconsistent. An apparent solution is attained in some configurations but not in others, with solution being more common with a small number of cross-flow cells (*jbar*). If the solution process is halted before the disturbance is allowed to develop, a reasonable solution is obtained in almost all cases. Some comparisons of the results from each geometry are shown in Chapter 4.

Chapter 4

Flow Simulations and Discussion

4.1 Introduction

Using the PLEATFLO program, a simulation for a geometry closest to our modeled filter (Purolator AF3192) is done to examine the characteristics of the flow entering, within, and exiting the filter. The calculated pressure drop over the simulated pleat is compared to that of experiment.

Following, simulations are done to determine the effect of different flow conditions and different geometries on velocity and pressure drop. Results are compared to examine the effects of:

- inlet velocity,
- pleat angle,
- pleat height,
- dust loading (simulated via altered Darcy parameters),
- and geometry (square pleat).

4.2 Flow through the AF3192 Filter

Flow through the AF3192 filter is simulated using the following criteria. The angle was calculated based on the filter pleats being 3 cm high and running 19 cm in length with 60 pleats. This yields an angle of 4.2°; equivalent to exactly 8 pleats per inch. Recall that for the triangular geometry, the angle represents the angle of the media *face* versus the inlet flow.

```
|--------------------------------------------------------------------------|
|    Pleat Shape:   Triangular       Parameters in meters, degrees, seconds |
|--------------------------------------------------------------------------|
|   Base Geometry Data              |   Derived Geometry Data               |
1)  pleat height       |  ht  |.294E-01 | x) # cells in x dir | ibar |      39 |
2)  pleat media width|  tp  |.635E-03 | x) # cells in y dir | jbar |      12 |
3)  pleat angle        |thetad|   4.210 | x) # x-cells to filt| icell|      10 |
4)  rel # cell upstrm|  cup |    .500 | x) # y-cells to filt| jcell|       0 |
5)  rel # cell dnstrm| cdown|    .800 | x) x cell wdth      | delx |.173E-02 |
6)  # of x filt cells|nfil_x|       5 | x) y cell wdth      | dely |.127E-03 |
7)  # of y filt cells|nfil_y|       0 | x) c cell wdth      | delc |.000E+00 |
8)  # of c filt cells|nfil_c|       0 | x) pleat width      | wd   |.153E-02 |
9)  up expans coeff  | eta  |   1.200 | x) total flow lgth  | flgth|.542E+00 |
10) down expans coef| zeta |   1.400 | x) filt hts upstrm  | htup |   1.223 |
11) max # of iter   |jcntmx|       8 | x) filt hts dnstrm  |htdown|  16.194 |
12) convergence crit| epsi |.300E+01 | x) est iter runtime |estime|.194E+03 |
13) x inlet veloc   | uin  |   3.000 | x) est max runtime  | estot|.155E+04 |
|--------------------------------------------------------------------------|
|                           Flow Parameters                                 |
|--------------------------------------------------------------------------|
14) kin. visc'ty    | nu   |.151E-04 | 17) x permeability   | K_x |.780E-10 |
15) upstrm flux coef| alpha|   1.000 | 18) y permeability   | K_y |.780E-10 |
16) turb coeff      | gamma|    .098 | 19) x inertia factor| b_x |.680E+05 |
|                                    | 20) y inertia factor| b_y |.680E+05 |
|--------------------------------------------------------------------------|
| Reached Convergence Criterion?        Yes.             No. of iter =   5   |
| Upstream Pressure =      .26088E+03 Pa                                     |
|--------------------------------------------------------------------------|
```

Table 4.1   Input parameters for AF3192 filter flow simulation.

Observing the flowfield (Fig. 4.1) shows the trends in the flow. As the flow enters from upstream (left), it enters a contraction formed by the pleat. Much of the flow squeezes down the "V" to where pressure is lower. The flow at the surface of the media (as represented by the first vector within the surface) loses much of its momentum, and orients more toward the media surface. Within the filter, the flow takes the path of least resistance across the filter; it can be seen in Fig. 4.1(b) that the majority of flow crosses the media along the narrowest path. However, it is clear that inertia plays a part as well.
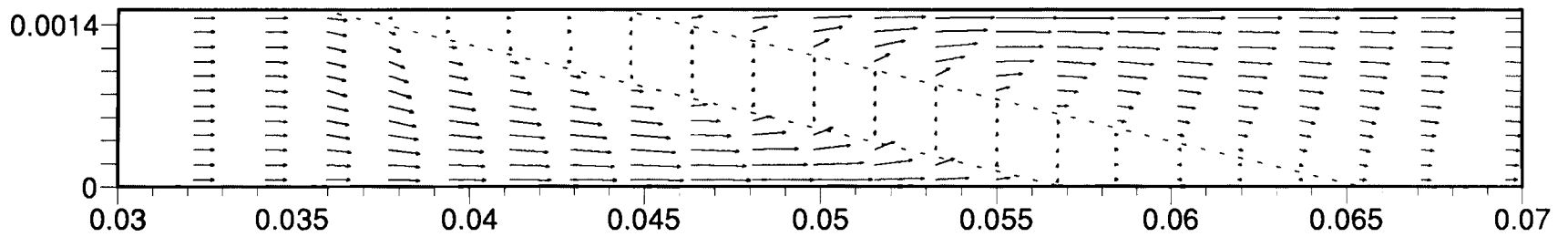
74

Fig. 4.1(a)   [Y-Weighted 327%, Linear-scale Vectors]
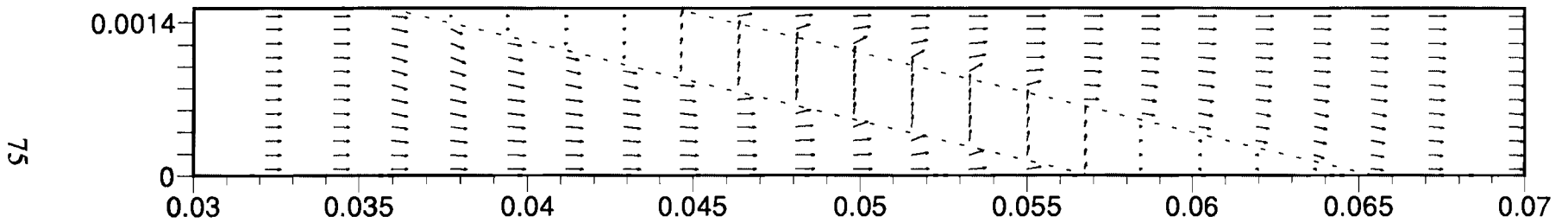

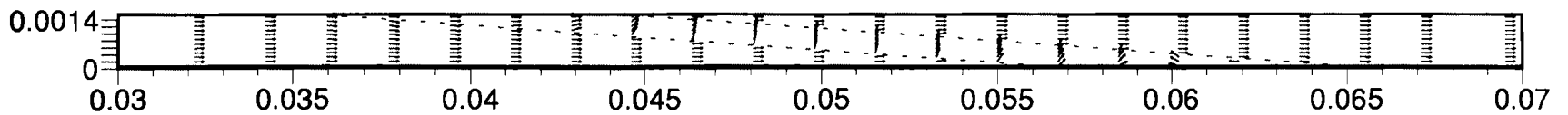*Fig. 4.1(b)   [Y-Weighted 327%, Log-scale Vectors]*

Fig. 4.1(c)   [Proportional, Equal-length Vectors]

Figs. 4.1   Simulated flow through an AF3192 filter pleat. (4 ° pleat, 3 cm high)

```
angle (positive horizontal equals 0, disregard angles above 90°)


         1       2       3       4       5       6       7       8       9      10      11      12
   13   .0      .0      .0      .0      .0      .0      .0      .0      .0\     .0      .0      .0
   12   .0      .0      .0      .0      .0      .0      .0      .0     -.2    -11.6\   -2.0     1.1
   11   .0      .0      .0      .0      .0      .0      .0     -.1     -.6    -10.7    -4.3\    2.3
   10   .0      .0      .0      .0      .0      .0      .0     -.1    -1.0     -9.6    -4.1    -3.5
    9   .0      .0      .0      .0      .0      .0      .0     -.1    -1.5     -8.4    -3.9    -3.3
    8   .0      .0      .0      .0      .0      .0      .0     -.1    -1.8     -7.3    -3.5    -2.9
    7   .0      .0      .0      .0      .0      .0      .0     -.2    -1.9     -6.2    -3.1    -2.6
    6   .0      .0      .0      .0      .0      .0      .0     -.2    -1.7     -5.1    -2.6    -2.2
    5   .0      .0      .0      .0      .0      .0      .0     -.1    -1.5     -4.1    -2.1    -1.8
    4   .0      .0      .0      .0      .0      .0      .0     -.1    -1.1     -3.1    -1.6    -1.4
    3   .0      .0      .0      .0      .0      .0      .0     -.1     -.7     -2.1    -1.1     -.9
    2   .0      .0      .0      .0      .0      .0      .0      .0     -.3     -1.0     -.6     -.5


        13      14      15      16      17      18      19      20      21      22      23      24
   13   .0      .0\     .0      .0      .0      .0      .0      .0      .0      .0      .0      .0
   12  1.6     3.1     40.3\    4.0     2.0     1.2      .7      .2     -.3     -.5     -.4     -.4
   11  3.3     6.6     44.8    63.1\    7.3     3.4     1.7      .5     -.5     -.9     -.9     -.8
   10\ 4.9    10.4     49.6    65.5    71.5\    9.8     4.0     1.2     -.7    -1.4    -1.4    -1.2
    9 -3.3\   14.8     54.7    67.9    72.5    75.4\   10.6     2.9     -.7    -2.0    -1.9    -1.7
    8 -3.0    -2.9\    60.1    70.3    73.6    75.4    77.8\    8.4     -.3    -2.5    -2.4    -2.1
    7 -2.6    -2.7     -.1\    72.8    74.6    75.4    76.6    79.4\    2.2    -3.0    -3.0    -2.6
    6 -2.2    -2.3    -1.2     3.3\    75.7    75.4    75.3    76.8    80.5\   -3.4    -3.5    -3.1
    5 -1.8    -1.9    -1.3      .6     5.8\    75.4    74.1    74.1    76.4    79.4\   -4.1    -3.6
    4 -1.4    -1.4    -1.1     -.1     1.8     7.0\    72.9    71.4    72.3    73.5   -54.4\   -4.2
    3 -1.0    -1.0     -.8     -.3      .6     2.3     7.2\    68.8    68.0    64.6   -46.2    -4.3
    2  -.5     -.5     -.4     -.2      .2      .8     2.1     6.1\    63.5    46.5   -29.0    -2.2


        25      26      27      28      29      30      31      32      33      34      35      36
   13   .0      .0      .0      .0      .0      .0      .0      .0      .0      .0      .0      .0
   12  -.4     -.4     -.4     -.3     -.2     -.1     -.1      .0      .0      .0      .0      .0
   11  -.7     -.8     -.8     -.5     -.4     -.2     -.1     -.1      .0      .0      .0      .0
   10 -1.1    -1.3    -1.1     -.8     -.5     -.3     -.2     -.1     -.1      .0      .0      .0
    9 -1.5    -1.8    -1.5    -1.0     -.7     -.4     -.2     -.1     -.1      .0      .0      .0
    8 -1.9    -2.3    -1.9    -1.3     -.8     -.5     -.3     -.2     -.1      .0      .0      .0
    7 -2.4    -3.0    -2.3    -1.4     -.9     -.5     -.3     -.2     -.1      .0      .0      .0
    6 -2.8    -3.7    -2.6    -1.6     -.9     -.5     -.3     -.2     -.1      .0      .0      .0
    5 -3.3    -4.5    -2.7    -1.6     -.9     -.5     -.3     -.2     -.1      .0      .0      .0
    4 -3.7    -5.2    -2.7    -1.5     -.8     -.4     -.2     -.1     -.1      .0      .0      .0
    3\ -4.2   -5.5    -2.3    -1.2     -.6     -.3     -.2     -.1      .0      .0      .0      .0
    2  -.9\   -4.2    -1.4     -.7     -.3     -.2     -.1     -.1      .0      .0      .0      .0
```

Table 4.2   Angle of flow for AF3192 simulation.

76

The flow does not orient completely normal to the media even though the pressure drop is strong; a perpendicular angle to the pleat would be 85.8°. Compare this to Fig. 4.1(c) and the numerical angle data in Table 4.2. The flow streamlines within the filter hold the trend forecast in Fig. 2.2, curving slightly under the influences of the pleat folds. The flow exiting the filter is essentially inverse reflective of that entering.

The pressure drop across the filter in this simulation is 217 Pa. This is equivalent to 0.87 in. H_2O. In practice, a standard flow rate for flow through an air filter is 3.54 m^3/s (125 cfm). If the edges of the filter are discounted somewhat, this flow rate yields an area-average velocity of 3.0 ± 0.2 m/s. Experiment has shown that at this flow rate the pressure drop across a clean AF3192 filter is 248 ± 10 Pa (1.00 ± 0.05 in. H_2O) (G. Liu, 1995). The numerical and experimental results were not expected to be in perfect agreement. There are certain disparities between the simulated and actual conditions which make such accuracy unlikely, for instance, the difference in geometry (Fig. 1.3) as well as other reasons discussed below.

4.3 Inlet Velocity

The velocity of the flow directly influences the pressure across the pleat via the filter momentum equations (Eq. 2.25). Velocity's influence increases exponentially when greater than 1 m/s, as pressure drop is related to the inertia of the flow. Since the extremes in the range of local inlet velocities in practice run from 0.5 to 10 m/s, simulations are done for velocities at the bottom and top of that range.

These two cases are simulated and the flowfield results are shown in Figs. 4.2. For the slower flow, the flow angles orient virtually normal to the pleat. However, the momentum

of the high velocity flow is clearly carried inside of the filter indicated by the relative downstream orientation of the intra-filter flow vectors (see also Table 4.3).

This phenomenon has an interesting indirect effect. In addition to the increased pressure gradient due to the direct effect of the Darcy law, the extra travel distance through the high resistance media serves to indirectly increase the pressure drop as well. This effect is shown in the graph of Fig. 4.3. The pressure drop for flows at 0.5, 3.0, and 10.0 m/s are plotted for flow through the flat media, and pleats of 13°, 4°, and 3°. The flat pleat pressure drop is calculated analytically using Eq. 2.25. The curves are scaled so that they all meet at the low velocity datum point. Compared to the flat media, the pleated results show an increase in pressure drop beyond the direct effect of inertia. One factor is the increased travel distance through the media. This phenomenon is intensified as the pleat angle gets closer to vertical. However, the large deviation in the near-vertical pleats has other grounds as well (see Sections 4.4 and 4.5).

At the exit of the pleat, the higher momentum of the high velocity flow influences flow direction somewhat, but, otherwise, the different velocities have little influence on the flowfield or gradients outside of the filter. With the high velocity flow, a slight pressure deficit registers at the bottom tip of the filter causing some reverse flow of very small magnitude.
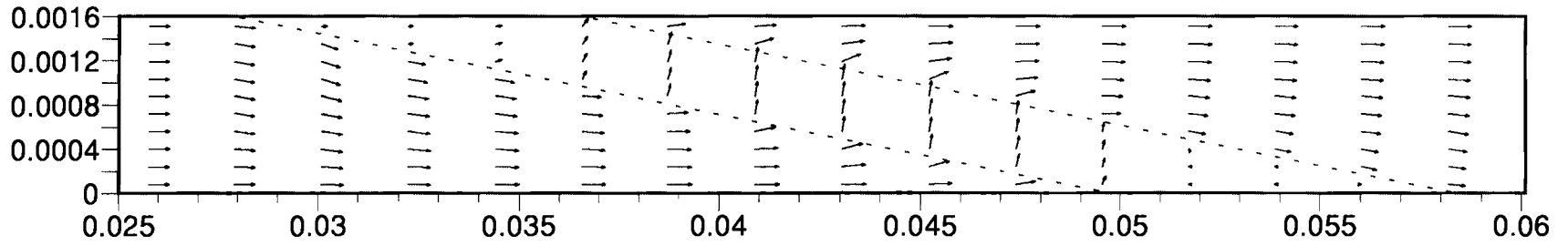
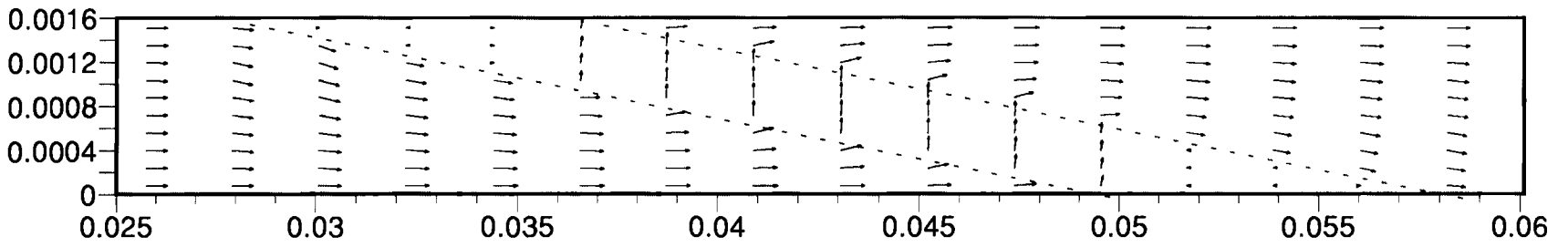*Fig. 4.2(a)   Inlet velocity of 10 m/s [Y-Weighted 273%, Log-scale Vectors]*

Fig. 4.2(b)   Inlet velocity of 0.5 m/s [Y-Weighted 273%, Log-scaled Vectors]
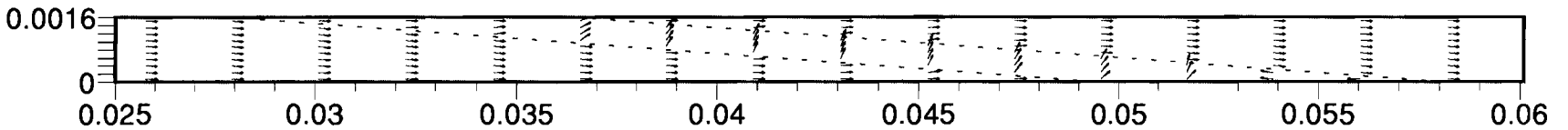

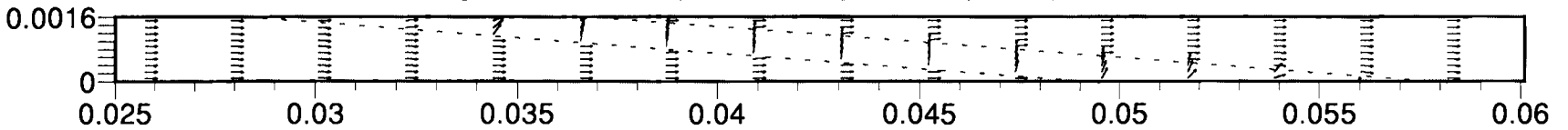*Fig. 4.2(c)   Inlet velocity of 10 m/s [Proportional, Equal-length Vectors]*

Fig. 4.2(d)   Inlet velocity of 0.5 m/s [Proportional, Equal-length Vectors]

Figs. 4.2   Flowfields for two different inlet velocities

	7	8	9	10	11	12	13	14	15	16	17	18	19	20	21
11	.0\	.0	.0	.0	.0\	.0	.0	.0	.0	.0	.0	.0	.0	.0	.0
10	.0	-10.1\	-.7	1.4	2.3	28.9\	4.0	2.1	1.2	.4	-.2	-.5	-.5	-.4	-.5
9	.0	-9.2	-4.0\	2.8	4.6	32.4	52.2\	7.4	3.4	1.2	-.4	-1.0	-1.0	-.9	-1.0
8	-.1	-8.2	-3.8	-3.3\	7.0	36.2	54.6	62.8\	9.4	2.9	-.5	-1.6	-1.5	-1.4	-1.5
7	-.2	-7.1	-3.5	-3.0	-2.8\	40.2	57.1	63.7	68.0\	8.3	.0	-2.2	-2.1	-1.9	-2.1
6	-.2	-5.9	-3.1	-2.6	-2.5	-.4\	59.8	64.6	67.1	70.9\	2.4	-2.8	-2.7	-2.4	-2.8
5	-.3	-4.8	-2.6	-2.2	-2.1	-1.2	2.7\	65.6	66.2	68.1	73.3\	-3.2	-3.4	-3.0	-3.6
4	-.3	-3.6	-2.0	-1.7	-1.6	-1.2	.4	5.1\	65.4	65.4	68.8	83.2\	-4.1	-3.6	-4.4
3	-.2	-2.4	-1.4	-1.2	-1.1	-.9	-.1	1.5	6.4\	62.7	64.1	76.8	-13.0\	-4.2	-5.0
2	-.1	-1.2	-.7	-.6	-.6	-.5	-.2	.5	1.8	6.3\	59.1	63.0	-6.8	-1.0\	-4.2

Table 4.3 (a)   Flow direction angle for inlet flow = 10 m/s (4° pleat, 3 cm high).

	7	8	9	10	11	12	13	14	15	16	17	18	19	20	21
11	.0\	.0	.0	.0	.0\	.0	.0	.0	.0	.0	.0	.0	.0	.0	.0
10	-.3	-10.1\	-.1	2.4	5.0	71.5\	3.0	1.2	.6	.2	-.2	-.5	-.5	-.5	-.6
9	-.5	-8.9	-4.0\	5.1	12.4	74.6	80.9\	5.2	2.1	.8	-.3	-1.1	-1.1	-1.0	-1.3
8	-.7	-7.7	-3.8	-3.5\	25.9	77.8	81.8	83.2\	6.9	2.3	-.1	-1.7	-1.7	-1.5	-2.0
7	-.8	-6.6	-3.5	-3.1	-2.9\	80.9	82.6	83.4	84.1\	7.3	.7	-2.4	-2.3	-2.0	-2.8
6	-.9	-5.5	-3.1	-2.7	-2.6	1.9\	83.5	83.5	83.7	84.7\	4.2	-3.1	-2.9	-2.6	-3.7
5	-.8	-4.4	-2.6	-2.2	-2.1	-.2	4.4\	83.7	83.2	82.9	85.0\	-3.6	-3.5	-3.1	-4.7
4	-.6	-3.3	-2.0	-1.7	-1.6	-.6	1.1	4.8\	82.7	81.2	80.9	83.0\	-4.2	-3.7	-5.6
3	-.4	-2.2	-1.4	-1.2	-1.1	-.5	.3	1.3	4.2\	79.4	77.0	77.0	60.1\	-4.2	-5.8
2	-.2	-1.1	-.7	-.6	-.6	-.3	.0	.4	1.0	3.0\	73.0	64.5	41.6	-50.7\	-4.2

Table 4.3 (b)   Flow direction angle for inlet flow = 0.5 m/s (4° pleat, 3 cm high).

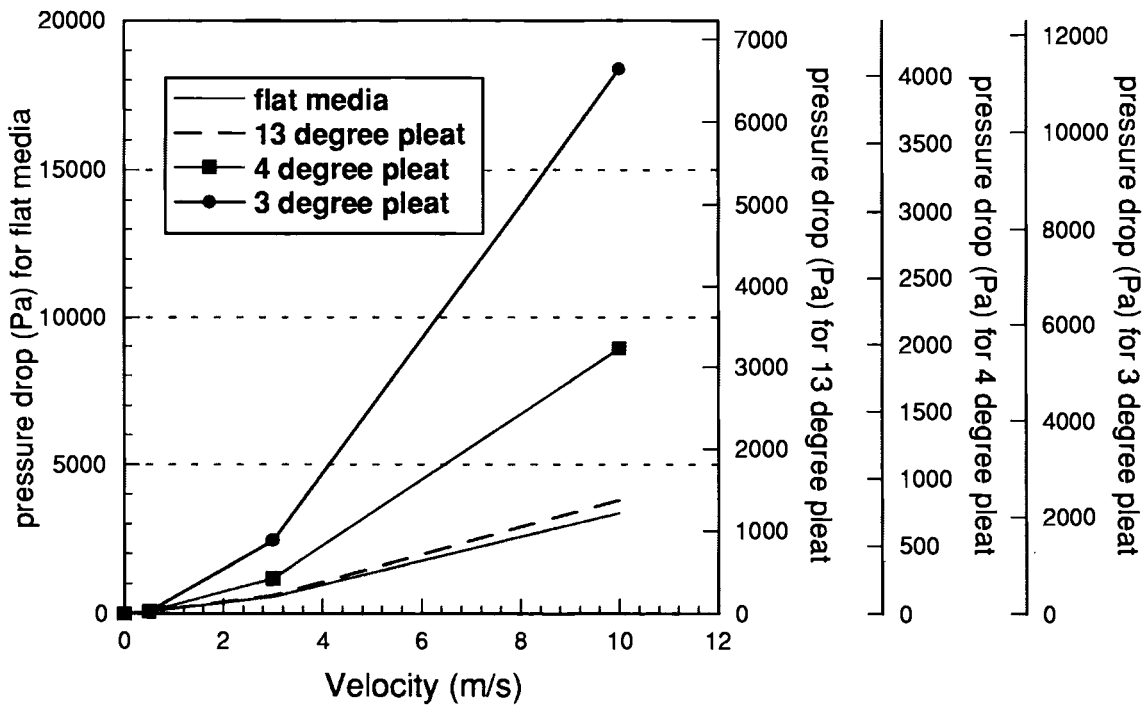## Pressure Drop vs. Inlet Velocity

Fig. 4.3   Pressure drop vs. inlet velocity for varying pleat angles.
The curves are each separately scaled versus their first datum point at V=0.5 m/s.

4.4 Pleat Angle

Flow through a flat piece of media would yield a pressure drop as a direct function of the inlet flow velocity (Eq 2.25). Angling the media through pleating allows the same flow to exit over a larger area, thus the exit flow rate is reduced by continuity. For steady incompressible flow, the flow entering a control volume must equal the flow exiting.
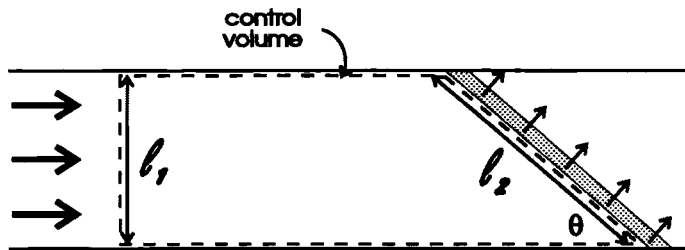
$$l_1 V_1 = l_2 V_2 \tag{4-1}$$

Fig. 4.4   Control volume for flow entering filter pleat.

For this geometry, the relation depends on the pleat angle.

$$V_2 = V_1 \sin \theta \tag{4-2}$$

Thus the smaller the angle, the slower the flow across the filter is, while continuity is always maintained. As the main component of pressure drop across the filter is directly related to velocity, this slower flow decreases the pressure drop.

However, as the angle is further reduced the area within the pleats becomes tighter and the velocity gradient gets stronger. This increases the laminar and turbulent viscous drag, thus increasing the pressure drop. This becomes quite strong at low pleat angles, and serves to increase the pressure drop. This viscous effect is clear on the left side of the graph below

(Fig. 4.5), and certainly plays a role in the higher pressure drops in the near-vertical pleats of Fig. 4.3.
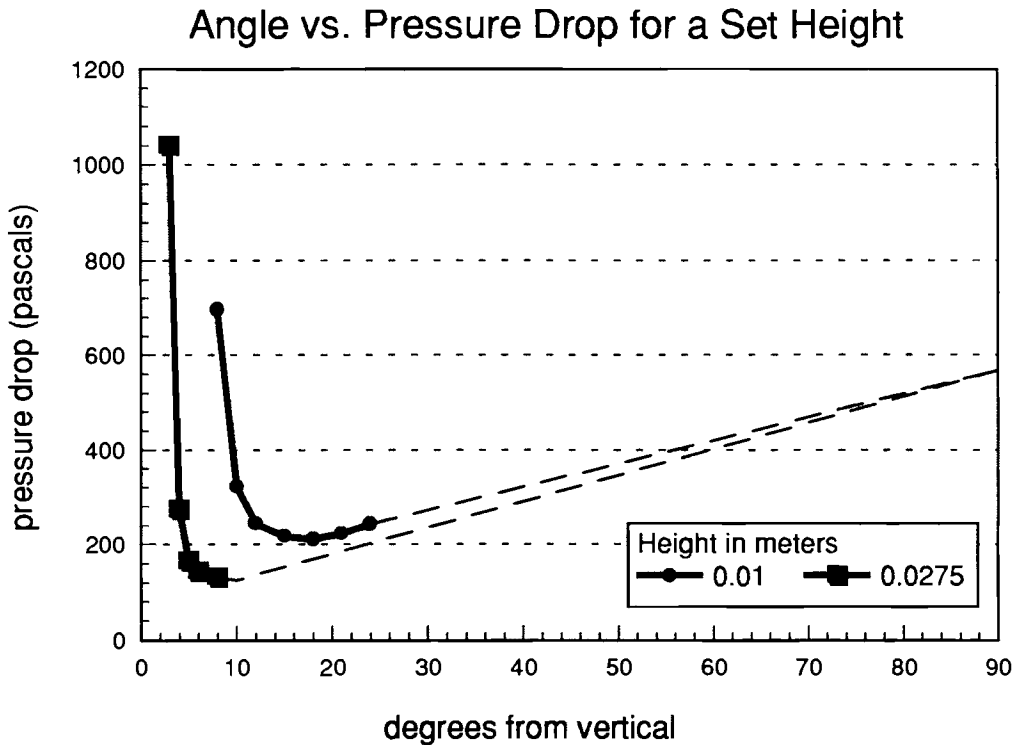
Angle vs. Pressure Drop for a Set Height

Fig. 4.5. Angle vs. pressure drop.
The value at the far right represents the analytical value of flow through a flat pleat;
it is connected linearly to the tails of the curves for demonstration only.

Part of this viscous effect is played by the turbulent stresses simulated by the model of Section 2.2. This model was developed to represent turbulent stress in the jet like flow downstream of the pleat. However, as the pleat angle shrinks, it begins to have a significant effect on the pressure drop in the crevasse of the pleat. Conversely as the pleat angle shrinks turbulence would be expected to relax, i.e. the Reynolds number at the opening of the simulated AF3192 pleat crevasse is only about 300. It would probably be preferable to model the air flow within the crevasse with the laminar equations. Because of this artificial increase in turbulent drag, the actual angle of minimum pressure drop point would be slightly lower.
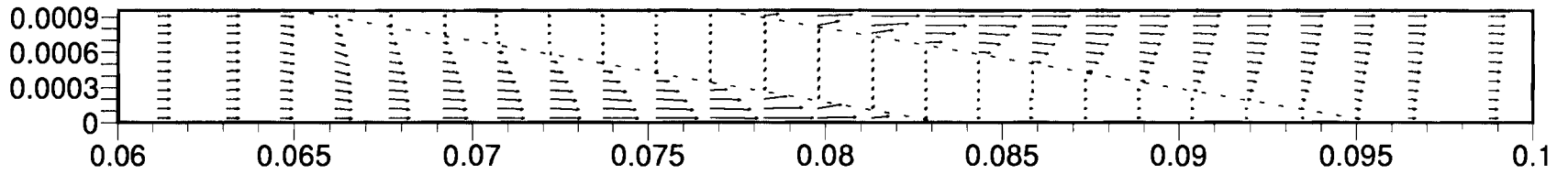
82

Fig. 4.6.(a)   3.0 ° pleat, 3 cm high [Y-Weighted 330%, Linear-scale Vectors]
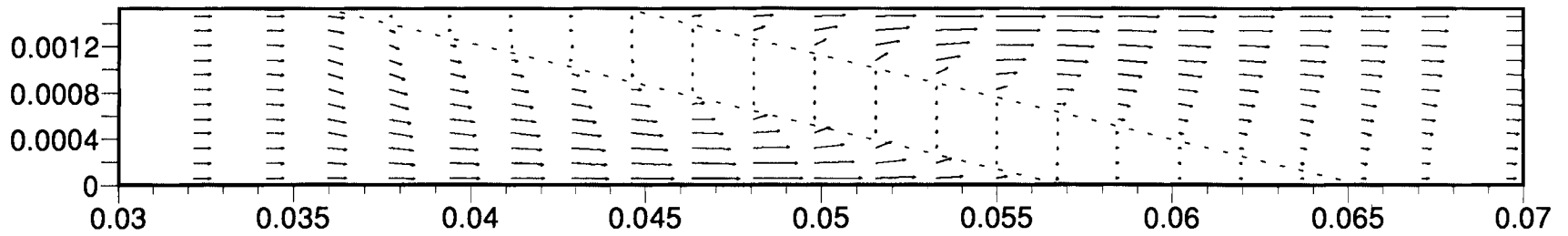

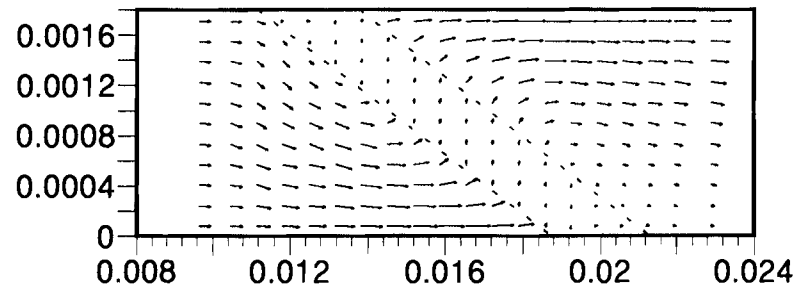*Fig. 4.6(b)   4.2 ° pleat, 3 cm high [Y-Weighted 330%, Linear-scale Vectors]*

Fig. 4.6(c)   13.6 ° pleat, 1 cm high [Y-Weighted 330%, Linear-scale Vectors]

Fig. 4.6   Comparison of flowfields for different pleat angles

4.5 Pleat Height

One of the main effects of altering the pleat height on the flowfield is in relation to the "freelength" referred to in Section 3.7. The flow characteristics through the section of the filter not directly affected by the pleat folds are essentially consistent for a tall or short pleat (Fig. 3.10). However, one measurable difference in the results of different pleat heights is the pressure drop across the filter. For a given angle, an increase in the pleat height will decrease the pressure drop across the filter. This is not due to a continuity-based velocity drop (i.e. Fig. 4.4); the continuity relation to flow velocity within the filter is related by pleat *angle* only (Eq. 4-2). Thus, the decreased pressure drop is solely a result of the reduced influence of the pleat folds. However, once some freelength is established, only diminishing returns are gained with further increases in height, as shown in Fig. 4.7.
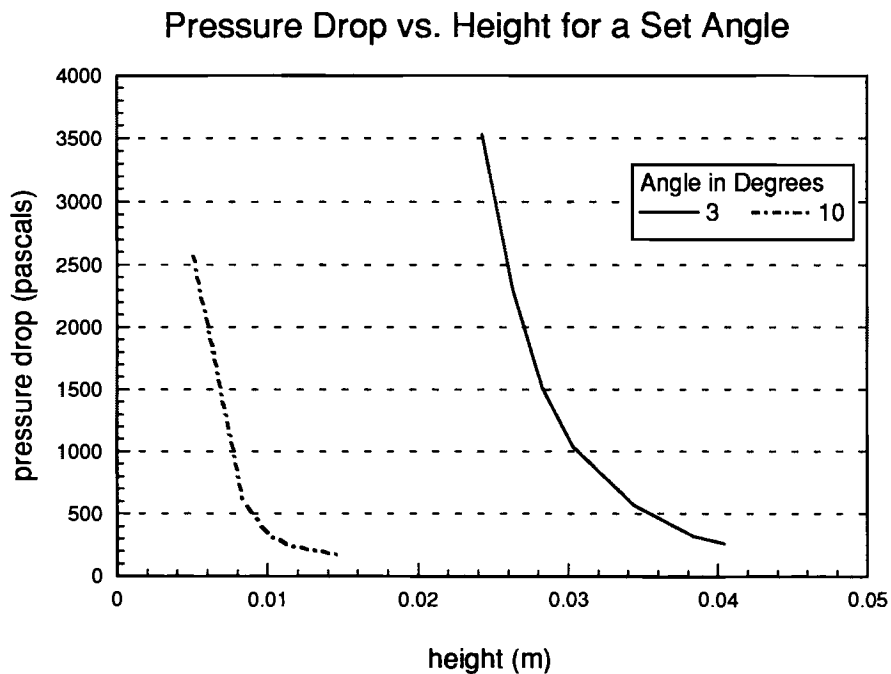

Fig. 4.7 Height vs. pressure drop for two pleat angles.

Viewing any of the simulated flowfields shows that the fold areas handle an insignificant portion of the flow (particularly noticeable with log-scaled vectors as in Fig. 4.1). In practice, this is exacerbated by the decreased permeability within the fold due to the crimping of the media and the use of glue along the fold.

4.6 Simulated Dust Loading

When the filter becomes laden with dirt, the pressure drop increases. The actual effect of dust loading is rather complicated. However, a simple simulation of dust loading can be done by altering the permeability within the filter momentum equations. The simple underlying principle is that dust reduces the permeability of the filter. However, no effort is made to estimate the effect on the inertia coefficient b, even though it certainly is affected as well, as it is a direct function of the permeability as shown in Eq. 2-21. From the $\frac{1}{\sqrt{K}}$ term in that equation, an increase in permeability is shown to lead to the curtailed influence of inertia, which would serve to only increase the effects we see below.

A simulation is done with the permeability decreased by a factor of ten. This yields an additional 350 Pa pressure drop on top of the 217 Pa already found through the "clean" filter. The clean and dirty filter flowfields are compared in Fig. 4.9.

It can be seen in the dirty filter that the inertia of the flow has less influence within the filter. The flow is more evenly spread along the filter and oriented closer to the perpendicular of the filter face. This again contributes indirectly to the pressure drop (as seen in Section 4.3). Even though pressure drop is directly related to permeability, changing the permeability by a factor of ten has a significantly less than tenfold effect (Fig. 4.8).
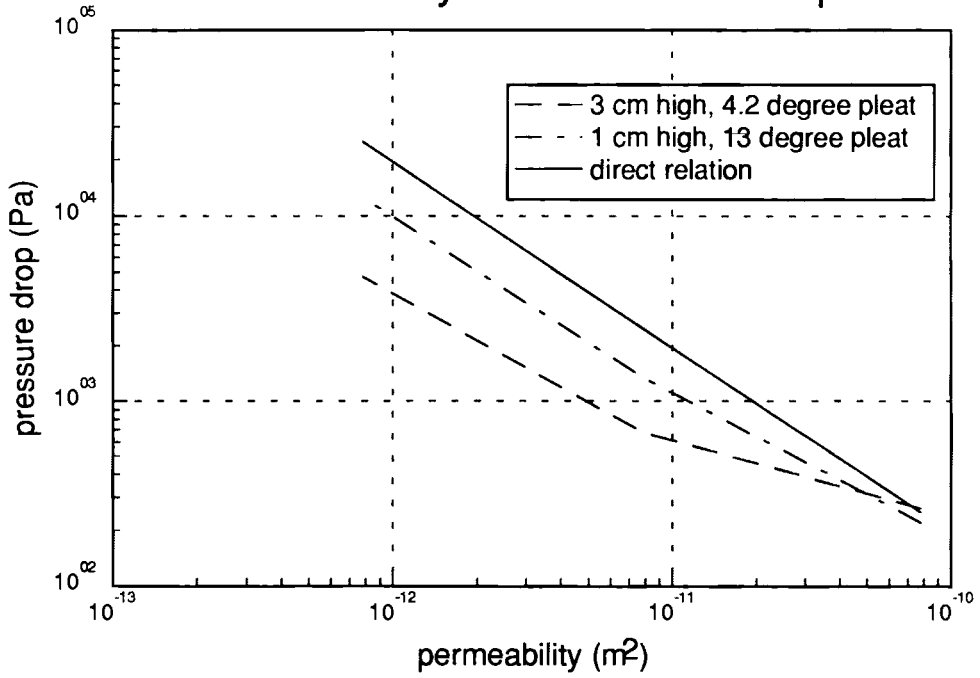
Fig. 4.8 Permeability vs. pressure drop for two pleat angles (log scale).
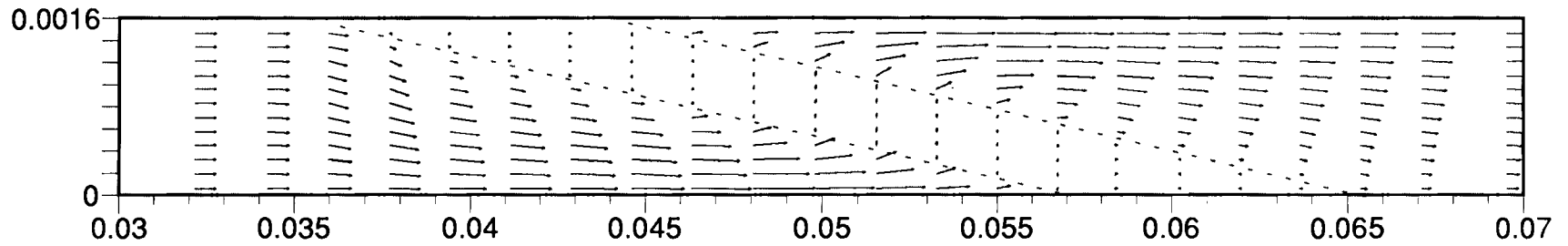
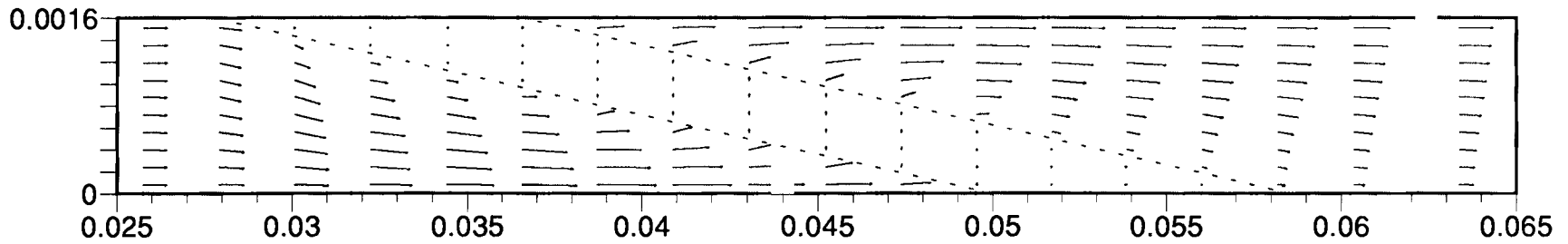*Fig. 4.9(a) Clean Filter, K=7.8e-11m ^{2} [Y-Weighted 312%, Linear-scale Vectors]*

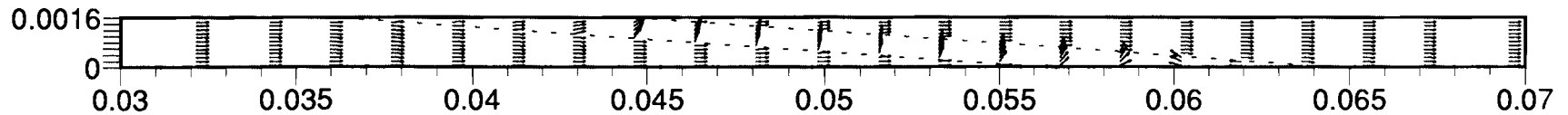*Fig. 4.9(b) Dirty Filter, K=7.8e-12m ^{2} [Y-Weighted 312%, Linear-scale Vectors]*

Fig. 4.9(c) Clean Filter, K=7.8e-11m ^{2} [Proportional, Equal-length Vectors]
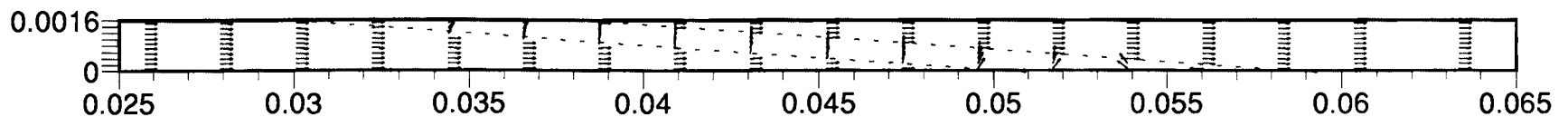

Fig. 4.9(d) Dirty Filter, K=7.8e-12m ^{2} [Proportional, Equal-length Vectors]

Figs. 4.9 Comparison of flowfield for clean and simulated dirty filter (4° pleat, 3cm high)

4.7 Flow through a Square Pleat

For the square pleat geometry (Figs. 1.5, 2.13(b)), solution convergence is more difficult to obtain. This is a result of the lack of a boundary condition to separate the fluid and filter equations, as explained in Section 3.10. Stability is sufficiently maintained in some angle formations, and these are examined below.

Recall that the relation of the angle to the pleat geometry is different for each the triangular and square geometries, $\theta_\Delta \neq \theta_\square$ (see Table 2.1). So the inputs of 3° and 10° angles using the square geometry are equivalent to 4.2° and 13.6° angles respectively with the triangular geometry (equivalent in that ht and wd are the same for both cases).
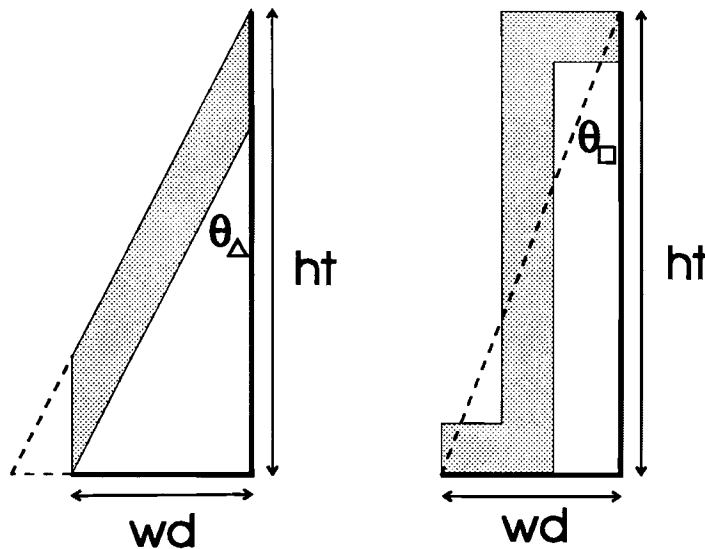

Fig. 4.10   Comparison of angles for triangular and square pleat.

Two simulations are shown in Figs. 4.12 and 4.13. The first simulation represents the

AF3192 filter, the second is a wider and shorter pleat. The input data are as follows.

```
|----------------------------------------------------------------------
|  Pleat Shape:  Square          Parameters in meters, degrees, seconds
|----------------------------------------------------------------------
|  Base Geometry Data              |  Derived Geometry Data
1) pleat height     |  ht  |.283E-01 | x) # cells in x dir | ibar |      31
2) pleat media width|  tp  |.635E-03 | x) # cells in y dir | jbar |       7
3) pleat angle      |thetad|  3.000  | x) # x-cells to filt| icell|      11
4) rel # cell upstrm|  cup |   .800  | x) # y-cells to filt| jcell|       4
5) rel # cell dnstrm| cdown|   .800  | x) x cell wdth      | delx |.318E-03
6) # of x filt cells|nfil_x|      2  | x) y cell wdth      | dely |.212E-03
7) # of y filt cells|nfil_y|      3  | x) c cell wdth      | delc |.439E-02
8) # of c filt cells|nfil_c|      6  | x) pleat width      | wd   |.148E-02
9) up expans coeff  | eta  |  1.700  | x) total flow lgth  | flgth|.335E+00
10) down expans coef| zeta |  1.900  | x) filt hts upstrm  | htup |   3.218
11) max # of iter   |jcntmx|      8  | x) filt hts dnstrm  |htdown|   7.638
12) convergence crit| epsi |.300E+01 | x) est iter runtime |estime|.400E+02
13) x inlet veloc   | uin  |  3.000  | x) est max runtime  | estot|.320E+03
|----------------------------------------------------------------------
|                          Flow Parameters
|----------------------------------------------------------------------
14) kin. visc'ty    |  nu  |.151E-04 | 17) x permeability  | K_x |.780E-10
15) upstrm flux coef| alpha|  1.000  | 18) y permeability  | K_y |.780E-10
16) turb coeff      | gamma|   .098  | 19) x inertia factor| b_x |.680E+05
|                                    | 20) y inertia factor| b_y |.680E+05
|----------------------------------------------------------------------
| Reached Convergence Criterion?       No.          Final epsi = .99E+00
| Upstream Pressure =    .70006E+03 Pa
|----------------------------------------------------------------------
```

Table 4.4 Input data for square pleat simulation (~3cm high, 3° angle).

```
|----------------------------------------------------------------------|
|  Pleat Shape:  Square          Parameters in meters, degrees, seconds |
|----------------------------------------------------------------------|
|  Base Geometry Data              |  Derived Geometry Data            |
1) pleat height     |  ht  |.108E-01 | x) # cells in x dir | ibar |      36 |
2) pleat media width|  tp  |.635E-03 | x) # cells in y dir | jbar |       6 |
3) pleat angle      |thetad| 10.000  | x) # x-cells to filt| icell|       9 |
4) rel # cell upstrm|  cup |   .500  | x) # y-cells to filt| jcell|       4 |
5) rel # cell dnstrm| cdown|   .800  | x) x cell wdth      | delx |.318E-03 |
6) # of x filt cells|nfil_x|      2  | x) y cell wdth      | dely |.318E-03 |
7) # of y filt cells|nfil_y|      2  | x) c cell wdth      | delc |.890E-03 |
8) # of c filt cells|nfil_c|     10  | x) pleat width      | wd   |.191E-02 |
9) up expans coeff  | eta  |  1.800  | x) total flow lgth  | flgth|.880E+00 |
10) down expans coef| zeta |  1.800  | x) filt hts upstrm  | htup |   4.011 |
11) max # of iter   |jcntmx|     10  | x) filt hts dnstrm  |htdown|  76.456 |
12) convergence crit| epsi |.100E-02 | x) est iter runtime |estime|.390E+02 |
13) x inlet veloc   | uin  |  3.000  | x) est max runtime  | estot|.390E+03 |
|----------------------------------------------------------------------|
|                          Flow Parameters                             |
|----------------------------------------------------------------------|
14) kin. visc'ty    |  nu  |.151E-04 | 17) x permeability  | K_x |.780E-10 |
15) upstrm flux coef| alpha|  1.000  | 18) y permeability  | K_y |.780E-10 |
16) turb coeff      | gamma|   .098  | 19) x inertia factor| b_x |.680E+05 |
|                                    | 20) y inertia factor| b_y |.680E+05 |
|----------------------------------------------------------------------|
| Reached Convergence Criterion?       No.          Final epsi =-.49E+00|
| Upstream Pressure =    .22924E+03 Pa                                  |
|----------------------------------------------------------------------|
```

Table 4.5 Input data for square pleat simulation (~1cm high, 10° angle).

89

Approaching the pleat, the majority of flow squeezes through the sudden contraction, while a considerable part of the flow does traverse the pleat head. Within the notches of the pleat the flow is flushed downstream. The flow cuts across the pleat median at a fairly brisk pace (observe log-scaled vectors). At the notch exit, the flow shoots out as a relatively strong jet. There is even a region of separation beneath the pleat bottom.

The obvious contrast between the thin and wide pleat is flow within the pleat median. In the thin pleat, these flow vectors are pointed downstream, while in the wide pleat they cut across the pleat median normal to the general flow. This agrees with the general finding of Chen et al. [1993].

The pressure drop across the square pleat is compared to that of the triangle in Fig. 4.11. Although essentially the same for large angles, the square geometry creates greater resistance at small angles. This is due to the same two indirect phenomena as pointed out before (Sections 4.4, 4.5). In the denser pleat, the flow crossing the pleat median does not take the shortest path; it is oriented more towards downstream, thus increasing overall pressure drop. Note in Fig. 4.13 that the flow in the wider pleat crosses straight through the pleat median. Additionally, the viscous drag that was shown to develop in the near-vertical triangular pleat, is exacerbated in the square geometry as the gradient is even larger for this case.

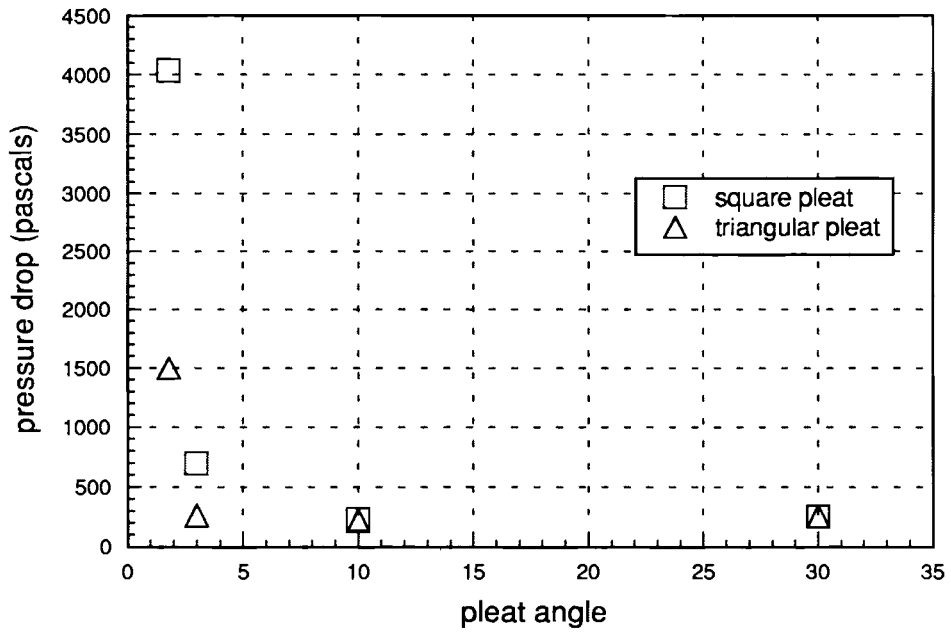**Pleat Angle vs. Pressure Drop for Different Geometries**

Fig. 4.11 Pleat angle vs. pressure drop for two geometries.
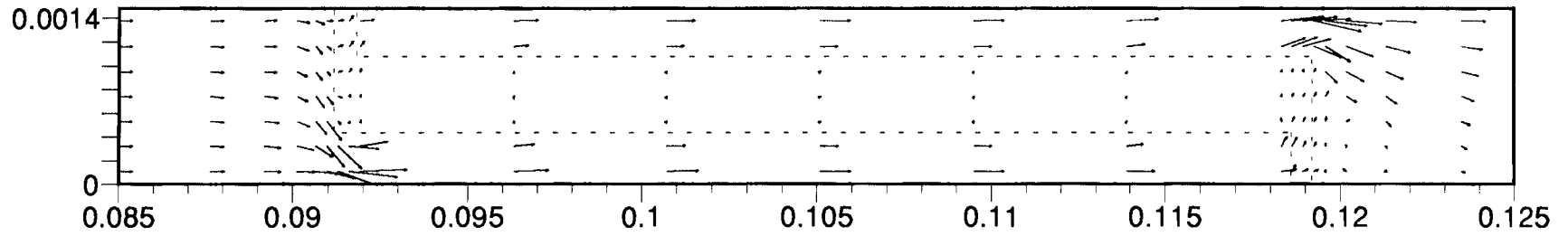*(Square pleat angle converted to triangular equivalent).*

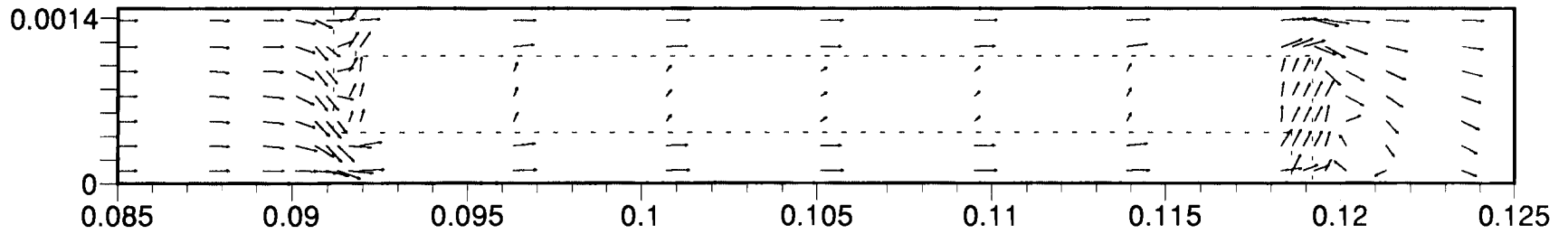*Fig. 4.12(a)   [Y-Weighted 330%, Linear-scale Vectors]*
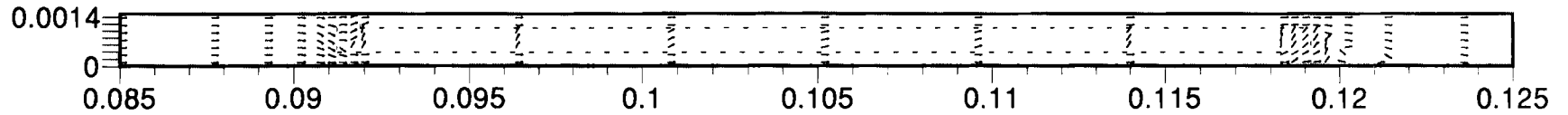

Fig. 4.12(b)   [Y-Weighted 330%, Log-scale Vectors]

Fig. 4.12(c)   [Proportional; Equal-length Vectors]

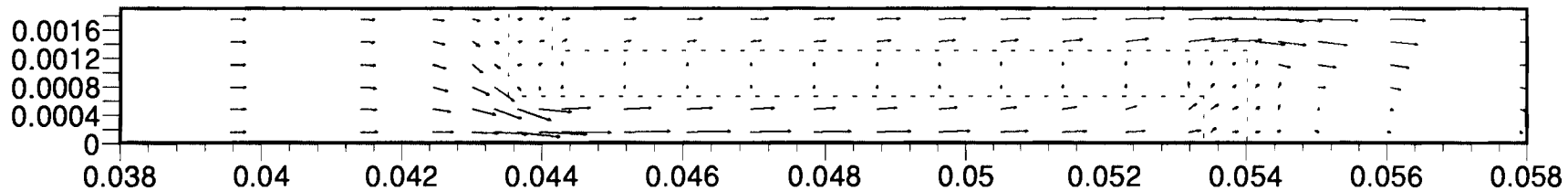*Figs. 4.12   Flow through square pleat, 4 ° angle (θ_Δ), ~ 3 cm high*

Fig. 4.13(a)   [Proportional, Linear-scaled Vectors]

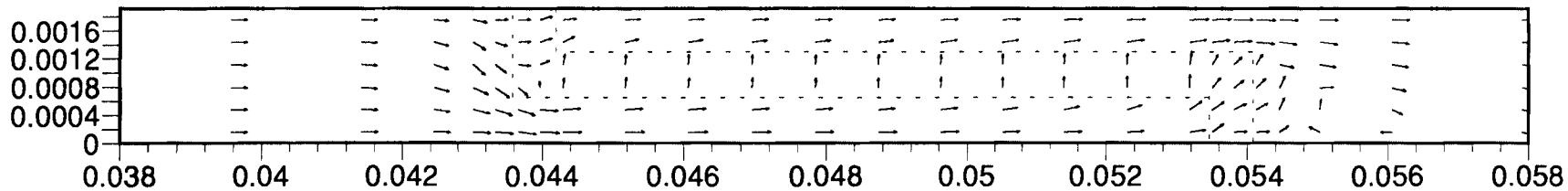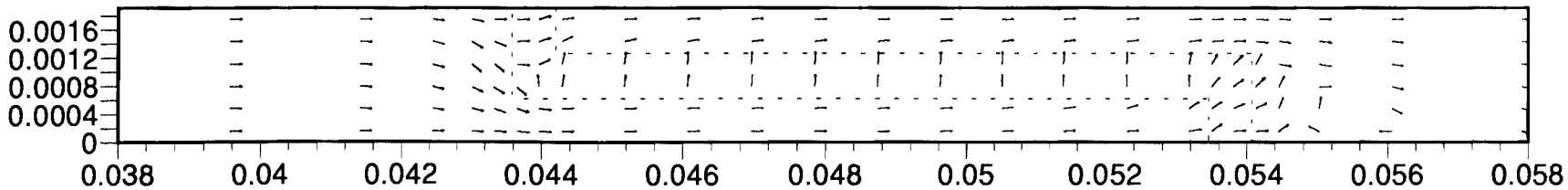Fig. 4.13(b)   Proportional, Log-scaled Vectors]

Fig. 4.13(b)   [Proportional, Equal-length Vectors]

Figs. 4.13   Flow through square pleat,   13° angle (θ_Δ), ~ 1 cm high

4.8 Discussion of Results

4.8.1 Suggested Experimental Confirmation

As mentioned earlier, experimental measurements of detailed flow through filter pleats are difficult to obtain. In practice, the pleats are very narrow, i.e. the AF3192 filter. This precludes measurement with the laser Doppler anemometer used in the OSU filtration lab. Moreover, the flowfield within the media is essentially impossible to measure directly. An experimental apparatus specifically for measuring flow entering and exiting different pleat configurations could be devised with pleats large enough to allow velocity measurements, however it might be more practical to concentrate on verifying the theory that the simulated flow is based upon.

Pressure drop, on the other hand, is fairly easy to measure. However, unless the apparatus mentioned above were devised, comparison is limited to available filters. This, too, is limited in that conventional filter test housings do not provide conditions close to the idealized conditions used in the simulation. A key consideration in comparing experimental and CFD results is determining what velocity from experiment is applicable to an equivalent simulation. The velocity profile entering the filter is far from uniform, especially for the J726 standard test housing [Newman, 1994]. Newman [1994] devised a prototype test housing for the AF3192 filter that considerably flattened the flow profile entering the filter. As shown by Newman, at 3.54 m³/s the velocities 13 mm upstream of the filter vary between 30% and 210% of the average velocity for the J726 standard filter test housing and between 60% and 130% of the average velocity for his prototype housing. An average inlet velocity can obviously be taken by dividing the flow rate by the normal area of the filter. However, choosing a true average velocity through the filter is complicated by the relative obstruction of the flow at the edges of the filter.

4.8.2 Re-examination of the Results from Cai

The CFD work of Cai [1993] was done as a part of the OSU filtration project, so its documentation and results are readily available to this researcher. The results from Cai showed a flowfield barely affected by the presence of the pleats. This was, in large part, due to the application of the same values for K and b as used by Gurumoothy. These were developed for flow through the filter as a whole, not for flow through the individual pleats. Thus, these values were off by about two orders of magnitude (compare Eq. 1-6 with Eq. 2-28). Unfortunately, application of the more accurate values of K and b make the time step required for stability even smaller, thus bringing the number of iterations needed to reach steady-state even greater than before. So Cai's program cannot be used for comparison at realistic resistance parameter values. The program would take far too long to converge.

4.8.3 Problems with the Boundary Condition at the Filter Interface

One discrepancy consistently observed in the results is negative pressure on the downstream side of the pleat (see Table 3.1). Originally it was thought that this was the result of insufficient iterations. However, it turns out to be a result of equation overlap at the exit (see Section 2.6). The filter equations force the pressure down in the region downstream of the pleat, because they extend to the first cell outside of the pleat on the downstream side (see the p terms in Eqs. 2-47 & 2-48).

This demonstrates the need of a boundary condition at the pleat interface. A boundary condition at the interface would keep variables belonging to cells of the filter region out of the equations of the non-filter region, and vice versa. However, it would still allow information to be passed between the regions.

4.8.2 Re-examination of the Results from Cai

The CFD work of Cai [1993] was done as a part of the OSU filtration project, so its documentation and results are readily available to this researcher. The results from Cai showed a flowfield barely affected by the presence of the pleats. This was, in large part, due to the application of the same values for K and b as used by Gurumoothy. These were developed for flow through the filter as a whole, not for flow through the individual pleats. Thus, these values were off by about two orders of magnitude (compare Eq. 1-6 with Eq. 2-28). Unfortunately, application of the more accurate values of K and b make the time step required for stability even smaller, thus bringing the number of iterations needed to reach steady-state even greater than before. So Cai's program cannot be used for comparison at realistic resistance parameter values. The program would take far too long to converge.

4.8.3 Problems with the Boundary Condition at the Filter Interface

One discrepancy consistently observed in the results is negative pressure on the downstream side of the pleat (see Table 3.1). Originally it was thought that this was the result of insufficient iterations. However, it turns out to be a result of equation overlap at the exit (see Section 2.6). The filter equations force the pressure down in the region downstream of the pleat, because they extend to the first cell outside of the pleat on the downstream side (see the p terms in Eqs. 2-47 & 2-48).

This demonstrates the need of a boundary condition at the pleat interface. A boundary condition at the interface would keep variables belonging to cells of the filter region out of the equations of the non-filter region, and vice versa. However, it would still allow information to be passed between the regions.

The intra-filter equations (Eqs. 2-32, 2-33) can easily adapt a boundary condition. They contain no derivatives of velocity, and the pressure derivative can be bounded by a zero pressure boundary condition on the downstream side. The terms in the Navier-Stokes equations (Eqs. 2-30, 2-31) outside of the filter could be bounded by derivative values at the filter interface. These would be set at the interface as specified by the connected pressure points of the boundary cells (see Figs. 2.12). The values at the interface could be extrapolated from the filter side, as this region's equations carry more weight and will dominate the situation at the boundary.

4.8.4 Problems with the Turbulence Model

As noticed in Section 4.4, the algebraic turbulence model that was applied seems to create an artificially high drag within the pleat crevasse when the pleat angle is small. This is especially disconcerting as turbulence probably does not even exist in such a confined area.

One simple way to address this problem would be to turn off the turbulence model in the region upstream of the pleat and within the crevasse downstream of the pleat. It is only needed for the flow downstream of the filter for which it has been specifically modeled. However, because phenomena downstream of the filter have little influence on conditions upstream due to the upwind differencing scheme used in the convection model (as seen in Section 3.5), a better model of flow and pressure drop through the filter could be obtained by just turning off the turbulence model everywhere ($\gamma = 0$). This approach would not account for the losses which result from the flow's return to uniformity downstream, an area of secondary concern, but would yield realistic results for flow in the filter region and for pressure drop across the filter without having to change the code.

Chapter 5

Conclusion and Recommendations

5.1 Conclusions from Study

A flow simulation program using computational fluid dynamics was created for predicting

flowfields and pressure drop over a pleated air filter. The method was explained in detail

in Chapter 2. Some of the controlling parameters were examined in Chapter 3, and some

flow simulations were shown in Chapter 4. The following major conclusions are drawn.

- The general flow direction through the pleat was normal to the pleat face. However,

  any significant inertia draws the flow vectors toward the downstream direction. The

  point where velocity seemed significant in this study was somewhere between 0.5 m/s

  where the flow was essentially normal to the pleat (see Fig. 4.2 and Table 4.3) and 3.0

  m/s where inertia began to play a role (Fig. 4.1 and Table 4.2). Assuming this

  boundary number to be 1.0 m/s, the permeability Reynolds number is (permeability of

  7.8e-11 m^2)

$$\text{Re}_{\sqrt{K}} \approx 0.6 \qquad (5\text{-}1)$$

and the fiber diameter-based Reynolds number is (average fiber diameter of 40 μm)

$$\text{Re}_D \approx 2.6 \qquad (5\text{-}2)$$

- Inertia plays an indirect role in the formation of pressure drop over a pleat. Inertia tends to bend the flow streamlines away from the shortest route through the high resistance media. Therefore, an additional increase in the pressure gradient arises from this "excess expense of energy."

- Viscous drag contributes significantly to pressure drop for small pleat angles. The very strong velocity gradients within the pleat crevasse amount to an increased drag on the flow, thus increasing the pressure gradient exponentially for smaller pleat angles.

- The pleat folds can negatively affect the flowfield and pressure drop if they constitute a significant portion of pleat length. Not only can the folds influence the flow through the main section of the pleat, but they essentially perform no filtration function because no flow enters due to the strong resistance. Whether they are consequential or not is a dual function of height and angle. This effect was found to be significant even in our model of geometries typical of commercially available air filters. However, the effect would ease greatly as the crease in the pleat is relaxed.

5.2 Further Refinements to Model

The following suggestions review some of the comments made within this report as to the improvement of the flow model and the numerical method.

- The turbulence model used herein presents some problems. It is not equally applicable to all geometries. It is not tailored to our model so it is quite approximate. Most importantly, it has an exaggerated effect within the pleat crevasse (Section 3.4). Even though the existence of turbulence within the pleats at small angles is questionable (Section 4.4), its effect through the present model is intensified because of the stronger velocity gradient therein (Eq. 2-17). One way to avoid this undesired effect is to turn

off the turbulence model upstream of the pleat, using just the laminar Navier-Stokes equation upstream. Another way to fix this problem would be to apply a more universal model like the k-ε model. However, this would significantly increase computation time.

- The interface of the media with the air should be treated as a boundary. Presently, the extra- and intra-filter governing equations are allowed to overlap somewhat. This seems to affect program stability with some geometries. A boundary condition should be made to segregate the regions while still allowing transfer of information between the zones.

- A better model of filter geometry could be used. A type of sine wave would probably be closer to the shape of an actual automotive air filter.

- Lastly, with regard to the numerical method, a thorough stability analysis of the equations should be done. This could determine the accuracy of the model, and optimize a stability criterion to set program parameters against.

REFERENCES

Anderson, D.A., Tannehill, J.C., and Pletcher, R.H. (1984): *Computational Fluid Mechanics and Heat Transfer,* Hemisphere Publishing.

Bejan, A. (1984): *Convection Heat Transfer,* John Wiley & Sons, New York.

Brown, R.C. (1993): *Air Filtration: An Integrated Approach to the Theory and Applications of Fibrous Filters,* Pergamon Press, Oxford.

Cai, Q. (1993): "A Study of Air Filter Flow By Computational Fluid Dynamics." M.S. Thesis, School of Mechanical & Aerospace Engineering, Oklahoma State U., Stillwater, OK.

Chambers, F.W. (1994): Turbulence Course MAE 6233, Class Notes, Dept. of Mechanical & Aerospace Engineering, Oklahoma State U., Stillwater, OK.

Chen, D.R., Pui, D.Y.H., and Liu, B.Y.H. (1993): "Numerical Study and Optimization of Pleated Gas Filters," *Proceedings of the 1993 Institute of Environmental Sciences,* pp. 414-422.

Chow, C.Y. (1979): *An Introduction to Computational Fluid Dynamics,* John Wiley & Sons, New York.

Davies, C.N. (1973): *Air Filtration,* Academic Press, London.

Gerald, C.F.& Wheatley, P.O. (1994): *Applied Numerical Analysis,* 5th Ed., Addison-Wesley, Reading, MA.

Gurumoothy, V. (1990): *Computational Fluid Dynamics Modeling of an Air Induction System,* M.S. Thesis, Dept. of Mechanical Engineering, U. of Rhode Island.

Hirt, C.W., Nichols, B.D., and Romero, N.C. (1975): "SOLA -- A Numerical Solution Algorithm for Transient Fluid Flows," Los Alamos Scientific Laboratory Report LA-5852, Los Alamos Scientific Laboratory at the U. of California, Los Alamos.

Janna, W.S. (1987): *Introduction to Fluid Mechanics,* 2nd Ed., PWS-KENT, Boston.

Jaroszczyk, T., Wake, J., and Conner, M.J. (1993): "Automotive Engine Air Filter Performance," *Filtech Conference at Karlsruhe, Germany*, Vol. 2, Filtration Society, West Sussex U.K.

Katto, Y. & Masuoka, T. (1966): "Criterion for the Onset of Convective Flow in a Fluid in a Porous Medium," *International Journal of Heat and Mass Transfer*, Vol. 10, 1967, pp. 297-309.

Lilley, D.G. (1992): *Computational Fluid Dynamics*, Dept. of Mechanical & Aerospace Engineering, Oklahoma State U., Stillwater, OK.

Liu, G. (1995): Measurements of Pressure Drop over Clean and Dirty Air Filters, Ongoing research at Oklahoma State University Filtration Research Laboratory, Stillwater, OK.

Newman, R. (1994): "Uniformity of Airflow in Automotive Air Filter Test Housings and Its Effects on the Efficiency of Fibrous Filters," M.S. Thesis, School of Mechanical & Aerospace Engineering, Oklahoma State U., Stillwater, OK.

Patankar, S.V. (1980): *Numerical Heat Transfer and Fluid Flow*, Hemisphere Publishing.

Sabnis, R.D. (1993): "Effects of Non-Uniform Airflow Through Filters on Filtration Efficiency," M.S. Thesis, School of Mechanical & Aerospace Engineering, Oklahoma State U., Stillwater, OK.

Society of Automotive Engineers (1987): "Air Cleaner Test Code", (J726).

Stenhouse, J.I.T. (1975): "Filtration of Air by Fibrous Filters," *Filtration and Separation*, Vol. 12, pp. 268-274.

Townsend, A.A. (1976): *The Structure of Turbulent Shear Flow*, 2nd Ed., Cambridge U.P., Cambridge, U.K.

Vafai, K. and Tien, C.L. (1981): "Boundary and Inertia Effects on Flow and Heat Transfer in Porous Media," *International Journal of Heat and Mass Transfer*, Vol. 24, pp. 195-203.

White, F.M. (1991): *Viscous Fluid Flow*, McGraw-Hill, Inc., New York.

Wilcox, D.C. (1993): *Turbulence Modeling for CFD*, DCW Industries, La Canada, CA.

Appendix
Experiment to Determine K and b for Specific Media

The extended Darcy equation as a function of *flow rate* is as follows:

$$\Delta p = \frac{\mu t}{KA}Q + \frac{b\rho t}{2A^2}Q^2 \qquad\qquad \text{(A-1)}$$

where

$t \equiv$ media thickness

$A \equiv$ media face area normal to flow

$Q \equiv$ flow rate

$p \equiv$ pressure

$K \equiv$ media permeability

$b \equiv$ inertial factor

This equation is of the form :

$$\Delta p = eQ + fQ^2 \qquad\qquad \text{(A-2)}$$

Experimental data are taken to find Δp versus Q across the filter media. Then e and f are determined so as to fit a second degree polynomial to the data. Then K and b are derived.
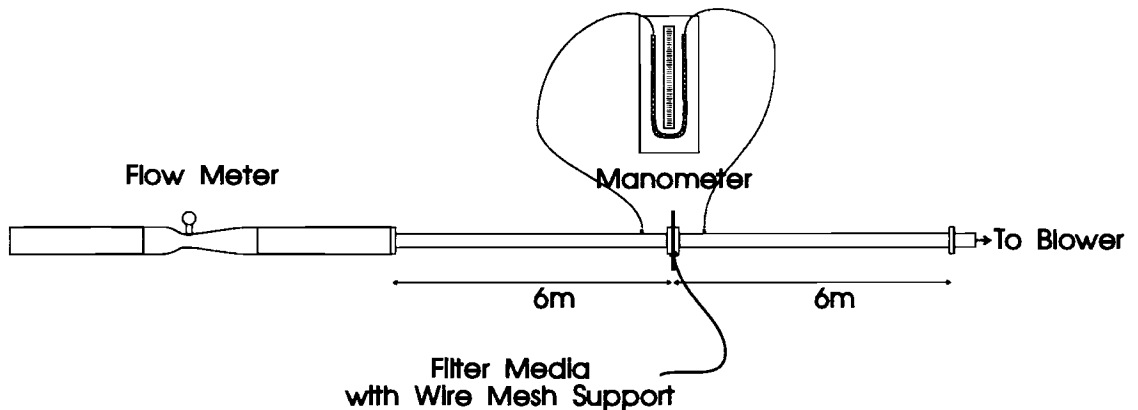
Experimental Setup

Fig. A.1   Setup for experiment to determine Darcy parameters.

The Purolator Filter Test Stand's 40 hp induction blower provided a constant flow rate.
Forty feet of 3 in. ID schedule 40 pvc pipe was added upstream of the test stand. A TSI
flow meter was attached upstream of this pipe with 10 feet of 6 in. ID pvc pipe both
before and after it.

A flat section of filter media was placed between the flanges at the halfway point of the 40
ft. pipe. The flange was sealed with cork sheeting. A section of quarter inch steel mesh
was placed in between the flanges to support the filter media. Pressure taps were located 4
inches up and downstream of the flange.

Experimental Results

Initially, pressure drop data were taken with only the wire mesh in place. Next data were
taken with the AF3192 filter media in place. The curve showing pressure drop versus flow
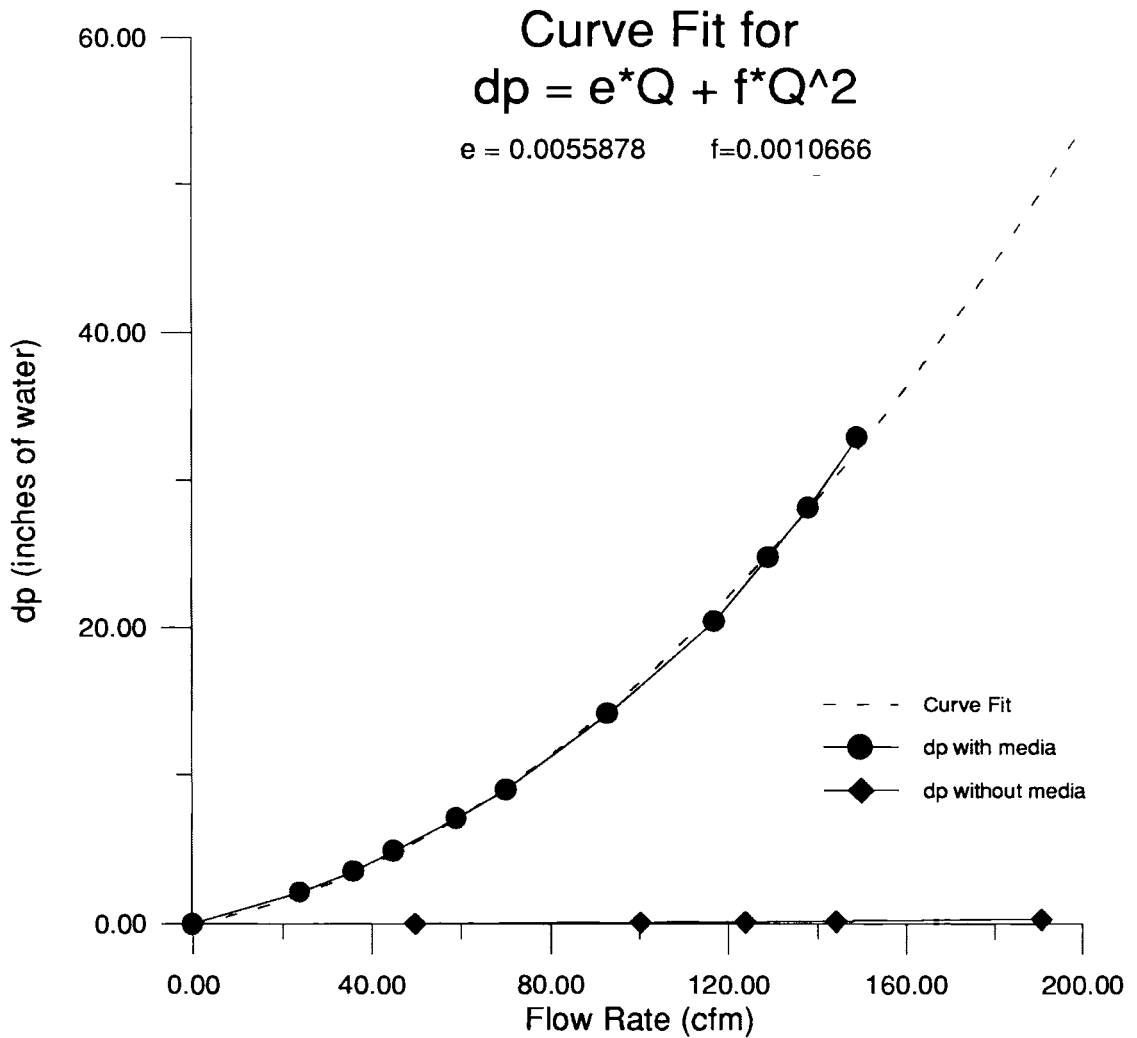rate is as follows.

Fig. A.2 Curve fit for one layer of filter media.

The pressure drop with only the wire mesh in place was insignificant. The curve fit was calculated using a 2nd degree Least Squares method modified for a constant (*c*) equal to zero.

$$ax^2 + bx + c = 0,$$
$$c = 0$$

The coefficients were found to be

$$e = 5.5878e - 2$$
$$f = 1.0666e - 3$$

K and b can be calculated as:

$$K = \frac{\mu t}{eA} \qquad b = \frac{2fA^2}{\rho t} \qquad\qquad \text{(A-1)}$$

The values for K and b for this case are:

$$K = 8.16e - 11m^2$$
$$b = 6.79e + 04m^{-1}$$

To ensure the results were not a function of filter thickness, the experiment was repeated using two layers of filter media. This yields the 2nd order equation:

$$\Delta p = 0.12321Q + 0.0021027Q^2$$

This yielded similar results for K and b.

$$K = 7.40e - 11m^2$$
$$b = 6.89e + 04m^{-1}$$

The values used for a clean filter media in this research are

$$K = 7.8e - 11m^2 \quad b = 6.8e + 04m^{-1}$$

VITA

Charles Tebbutt

Candidate for the Degree of

Master of Science

Thesis: CFD MODEL OF FLOW THROUGH AIR FILTER PLEATS

Major Field: Mechanical Engineering

Biographical:

   Personal Data: Born in Wilmette, Illinois on October 10, 1965, son of Arthur V.
      and Maryan B. Tebbutt.

   Education: Received a Bachelor of Arts degree from Columbia College,
      Columbia University, New York majoring in East Asian Studies in October
      1988. Completed the requirements for the Master of Science degree with a
      major in Mechanical Engineering at Oklahoma State University in July
      1995.

   Experience: Graduate Research Assistant, Filtration Project, Oklahoma State
      University, January 1994 to present; Teaching Assistant, Materials Science
      Class, Oklahoma State University, January to December 1993; Technical
      Writer, English Teacher, Publisher, Sales Consultant, Taipei, Taiwan 1988
      to 1992.

   Professional Membership: AIAA